

SUPPLEMENTARY INFORMATION FOR

Rational reprogramming *O*-methylation regioselectivity for combinatorial

biosynthetic tailoring of benzenediol lactone scaffolds

Xiaojing Wang^{a,b,c,1}, Chen Wang^{a,b,1}, Lixin Duan^{b,d,1}, Liwen Zhang^a, Hang Liu^{a,b}, Ya-ming Xu^b,
Qingpei Liu^{b,e}, Tonglin Mao^c, Wei Zhang^a, Ming Chen^a, Min Lin^a, A.A. Leslie Gunatilaka^b, Yuquan
Xu^{a*}, and István Molnár^{b*}

^a Biotechnology Research Institute, Chinese Academy of Agricultural Sciences, 12 Zhongguancun
South Street, Beijing 100081, P.R. China

^b Southwest Center for Natural Products Research, University of Arizona, 250 E. Valencia Rd.,
Tucson, AZ 85706, USA

^c State Key Laboratory of Plant Physiology and Biochemistry, Department of Plant Sciences,
College of Biological Sciences, China Agricultural University, Beijing 100193, P.R. China

^d Guangzhou University of Chinese Medicine, 232 Waihuan East Road, Guangzhou University
City, Panyu District, Guangzhou 510006, P.R. China

^e Key Laboratory of Environment Correlative Dietology, College of Food Science and Technology
, Huazhong Agricultural University, Wuhan 430070, P.R. China

¹ These authors contribute equally to this work.

* Corresponding authors: I. Molnár (imolnar@email.arizona.edu), Tel: +1 (520) 621-9932; and Y.
Xu (xuyuquan@caas.cn), Tel: +86 (010) 8210-9850.

Contents

1	SI Materials and Methods.....	7
1.1	Molecular biology, microbiology and bioinformatics.....	7
1.1.1	Construction of <i>Saccharomyces cerevisiae</i> expression vectors.	7
1.1.2	Total biosynthesis and biotransformation.	8
1.1.3	OMT expression in <i>E. coli</i> and protein purification.....	9
1.1.4	Protein structure modeling.	10
1.2	Isolation and characterization of <i>O</i> -methylated products.....	11
1.2.1	General methods.	11
1.2.2	Lasiodiplodin (1a).....	12
1.2.3	5- <i>O</i> -Methyl-desmethyllasiodiplodin (1b).....	13
1.2.4	3,5-Di- <i>O</i> -methyl-desmethyllasiodiplodin (1c).....	13
1.2.5	3- <i>O</i> -Methylradiplodin (2a)	14
1.2.6	5- <i>O</i> -Methylradiplodin (2b)	14
1.2.7	3,5-Di- <i>O</i> -methylradiplodin (2c).....	14
1.2.8	14,15-Dehydro-3- <i>O</i> -methylzearalenol (3a)	15
1.2.9	14,15-Dehydro-5- <i>O</i> -methylzearalenol (3b)	15
1.2.10	14,15-Dehydro-3,5-di- <i>O</i> -methylzearalenol (3c)	16
1.2.11	3- <i>O</i> -Methylzearalenol (4a)	16
1.2.12	5- <i>O</i> -Methylzearalenol (4b)	16
1.2.13	3,5-Di- <i>O</i> -methylzearalenol (4c).....	17
1.2.14	3- <i>O</i> -Methylasicicol (5a)	17
1.2.15	7- <i>O</i> -methyllasilarin (6a)	17
1.2.16	5- <i>O</i> -methyllasilarin (6b)	18
1.2.17	5,7-Di- <i>O</i> -methyllasilarin (6c)	18
1.2.18	7-[(<i>R,E</i>)-6-Hydroxyhept-1-en-1-yl]-3- <i>O</i> -methylresorcylic acid ethyl ester (7a) 18	
1.2.19	7-[(<i>R,E</i>)-6-Hydroxyhept-1-en-1-yl]-5- <i>O</i> -methylresorcylic acid ethyl ester (7b) 19	
1.2.20	7-[(<i>R,E</i>)-6-Hydroxyhept-1-en-1-yl]-3,5-di- <i>O</i> -methylresorcylic acid ethyl ester (7c) 19	
1.2.21	7-[(<i>S,E</i>)-6-Hydroxyhept-1-en-1-yl]-resorcylic acid ethyl ester (8)	20

1.2.22	7-[(<i>S,E</i>)-6-Hydroxyhept-1-en-1-yl]-3- <i>O</i> -methylresorcylic acid ethyl ester (8a)	20
1.2.23	7-[(<i>S,E</i>)-6-Hydroxyhept-1-en-1-yl]-5- <i>O</i> -methylresorcylic acid ethyl ester (8b)	21
1.2.24	7-[(<i>S,E</i>)-6-Hydroxyhept-1-en-1-yl]-3,5-di- <i>O</i> -methylresorcylic acid ethyl ester (8c)	21
1.3	Structure elucidation.....	21
2	SI Tables.....	27
	Table S1. Mutations engineered into LtOMT.....	27
	Table S2. ¹ H NMR (400 MHz) and ¹³ C NMR (100 MHz) data.....	28
	Table S2.1. Compounds 1a , 1b and 1c (in methanol- <i>d</i> ₄).....	28
	Table S2.2. Compounds 2a , 2b and 2c (in CDCl ₃).....	29
	Table S2.3. Compounds 3a , 3b and 3c (in DMSO- <i>d</i> ₆).....	30
	Table S2.4. Compounds 4a , 4b , 4c (in methanol- <i>d</i> ₄) and 5a (in CDCl ₃).....	31
	Table S2.5. Compounds 6a , 6b and 6c (in methanol- <i>d</i> ₄).....	32
	Table S2.6. Compounds 7a , 7b and 7c (in methanol- <i>d</i> ₄).....	33
	Table S2.7. Compounds 8a , 8b and 8c (in methanol- <i>d</i> ₄).....	34
	Table S3. Combinatorial methylation with LtOMT and HsOMT.....	35
	Table S4. Methylation of the model substrate DLD (1) with mutant LtOMT enzymes.....	39
	Table S5. Combinatorial methylation with selected LtOMT variants.....	41
	Table S6. Primers used in this study.....	46
3	SI Figures.....	49
	Figure S1. Compounds not accepted as substrates by LtOMT and HsOMT.....	49
	Figure S2. Influence of preexisting methylation on the activities of LtOMT and HsOMT.....	52
	Figure S3. Topology of LtOMT and HsOMT.....	54
	Figure S4. Docking models of DLD and SAM for LtOMT and HsOMT.....	55
	Figure S5. SDS-PAGE analysis of purified methyltransferases.....	56
	Figure S6. Chemical structures and key HMBC (→) and NOE (<--->) correlations of isolated compounds.....	57
	Figure S7. NMR spectra.....	58
	Figure S7.1. ¹ H NMR spectrum of compound 1a in methanol- <i>d</i> ₄	58
	Figure S7.2. ¹³ C NMR spectrum of compound 1a in methanol- <i>d</i> ₄	59

Figure S7.3.	^1H NMR spectrum of compound 1b in methanol- d_4	60
Figure S7.4.	^{13}C NMR spectrum of compound 1b in methanol- d_4	61
Figure S7.5.	HSQC spectrum of compound 1b in methanol- d_4	62
Figure S7.6.	HMBC spectrum of compound 1b in methanol- d_4	63
Figure S7.7.	1D NOESY spectrum of compound 1b in methanol- d_4	64
Figure S7.8.	^1H NMR spectrum of compound 1c in methanol- d_4	65
Figure S7.9.	^{13}C NMR spectrum of compound 1c in methanol- d_4	66
Figure S7.10.	HMBC spectrum of compound 1c in methanol- d_4	67
Figure S7.11.	^1H NMR spectrum of compound 2a in CDCl_3	68
Figure S7.12.	^{13}C NMR spectrum of compound 2a in CDCl_3	69
Figure S7.13.	HMBC spectrum of compound 2a in CDCl_3	70
Figure S7.14.	^1H NMR spectrum of compound 2b in CDCl_3	71
Figure S7.15.	^{13}C NMR spectrum of compound 2b in CDCl_3	72
Figure S7.16.	HSQC spectrum of compound 2b in CDCl_3	73
Figure S7.17.	HMBC spectrum of compound 2b in CDCl_3	74
Figure S7.18.	^1H NMR spectrum of compound 2c in CDCl_3	75
Figure S7.19.	^{13}C NMR spectrum of compound 2c in CDCl_3	76
Figure S7.20.	DEPT 135 spectrum of compound 2c in CDCl_3	77
Figure S7.21.	^1H - ^1H COSY spectrum of compound 2c in CDCl_3	78
Figure S7.22.	HSQC spectrum of compound 2c in CDCl_3	79
Figure S7.23.	HMBC spectrum of compound 2c in CDCl_3	80
Figure S7.24.	^1H NMR spectrum of compound 3a in $\text{DMSO}-d_6$	81
Figure S7.25.	^{13}C NMR spectrum of compound 3a in $\text{DMSO}-d_6$	82
Figure S7.26.	^1H - ^1H COSY spectrum of compound 3a in $\text{DMSO}-d_6$	83
Figure S7.27.	HSQC spectrum of compound 3a in $\text{DMSO}-d_6$	84
Figure S7.28.	HMBC spectrum of compound 3a in $\text{DMSO}-d_6$	85
Figure S7.29.	^1H NMR spectrum of compound 3b in $\text{DMSO}-d_6$	86
Figure S7.30.	^{13}C NMR spectrum of compound 3b in $\text{DMSO}-d_6$	87
Figure S7.31.	^1H - ^1H COSY spectrum of compound 3b in $\text{DMSO}-d_6$	88
Figure S7.32.	HSQC spectrum of compound 3b in $\text{DMSO}-d_6$	89
Figure S7.33.	HMBC spectrum of compound 3b in $\text{DMSO}-d_6$	90
Figure S7.34.	^1H NMR spectrum of compound 3c in $\text{DMSO}-d_6$	91

Figure S7.35.	^{13}C NMR spectrum of compound 3c in $\text{DMSO}-d_6$	92
Figure S7.36.	^1H - ^1H COSY spectrum of compound 3c in $\text{DMSO}-d_6$	93
Figure S7.37.	HSQC spectrum of compound 3c in $\text{DMSO}-d_6$	94
Figure S7.38.	HMBC spectrum of compound 3c in $\text{DMSO}-d_6$	95
Figure S7.39.	^1H NMR spectrum of compound 4a in methanol- d_4	96
Figure S7.40.	^{13}C NMR spectrum of compound 4a in methanol- d_4	97
Figure S7.41.	DEPT 135 spectrum of compound 4a in methanol- d_4	98
Figure S7.42.	1D NOESY spectrum of compound 4a in methanol- d_4	99
Figure S7.43.	^1H NMR spectrum of compound 4b in methanol- d_4	100
Figure S7.44.	^{13}C NMR spectrum of compound 4b in methanol- d_4	101
Figure S7.45.	1D NOESY NMR spectrum of compound 4b in methanol- d_4	102
Figure S7.46.	^1H NMR spectrum of compound 4c in methanol- d_4	103
Figure S7.47.	^{13}C NMR spectrum of compound 4c in methanol- d_4	104
Figure S7.48.	HMBC spectrum of compound 4c in methanol- d_4	105
Figure S7.49.	^1H NMR spectrum of compound 5a in CDCl_3	106
Figure S7.50.	^{13}C NMR spectrum of compound 5a in CDCl_3	107
Figure S7.51.	HMBC spectrum of compound 5a in CDCl_3	108
Figure S7.52.	^1H NMR spectrum of compound 6a in methanol- d_4	109
Figure S7.53.	^{13}C NMR spectrum of compound 6a in methanol- d_4	110
Figure S7.54.	1D NOESY spectrum of compound 6a in methanol- d_4	111
Figure S7.55.	^1H NMR spectrum of compound 6b in methanol- d_4	112
Figure S7.56.	^{13}C NMR spectrum of compound 6b in methanol- d_4	113
Figure S7.57.	HSQC spectrum of compound 6b in methanol- d_4	114
Figure S7.58.	HMBC spectrum of compound 6b in methanol- d_4	115
Figure S7.59.	^1H NMR spectrum of compound 6c in methanol- d_4	116
Figure S7.60.	^{13}C NMR spectrum of compound 6c in methanol- d_4	117
Figure S7.61.	^1H NMR spectrum of compound 7a in methanol- d_4	118
Figure S7.62.	^{13}C NMR spectrum of compound 7a in methanol- d_4	119
Figure S7.63.	HMBC spectrum of compound 7a in methanol- d_4	120
Figure S7.64.	^1H NMR spectrum of compound 7b in methanol- d_4	121
Figure S7.65.	^{13}C NMR spectrum of compound 7b in methanol- d_4	122
Figure S7.66.	HSQC spectrum of compound 7b in methanol- d_4	123

Figure S7.67.	HMBC spectrum of compound 7b in methanol- d_4	124
Figure S7.68.	^1H NMR spectrum of compound 7c in methanol- d_4	125
Figure S7.69.	^{13}C NMR spectrum of compound 7c in methanol- d_4	126
Figure S7.70.	HSQC spectrum of compound 7c in methanol- d_4	127
Figure S7.71.	HMBC spectrum of compound 7c in methanol- d_4	128
Figure S7.72.	^1H NMR spectrum of compound 8a in methanol- d_4	129
Figure S7.73.	^{13}C NMR spectrum of compound 8a in methanol- d_4	130
Figure S7.74.	HMBC NMR spectrum of compound 8a in methanol- d_4	131
Figure S7.75.	^1H NMR spectrum of compound 8b in methanol- d_4	132
Figure S7.76.	^{13}C NMR spectrum of compound 8b in methanol- d_4	133
Figure S7.77.	HMBC spectrum of compound 8b in methanol- d_4	134
Figure S7.78.	^1H NMR spectrum of compound 8c in methanol- d_4	135
Figure S7.79.	^{13}C NMR spectrum of compound 8c in methanol- d_4	136
Figure S7.80.	HMBC spectrum of compound 8c in methanol- d_4	137
Figure S8.	CD spectra of ARA7 and ARA8.	138
4	SI References.	139

1 SI Materials and Methods

1.1 Molecular biology, microbiology and bioinformatics.

1.1.1 Construction of *Saccharomyces cerevisiae* expression vectors.

The gene encoding LtOMT was cloned from *Lasioidiplodia theobromae* NBRC 31059 as described (1), and the *hpm5* gene for HsOMT (2) and the gene for the LtOMT variant M1 were commercially synthesized (Joint Genome Institute and BioBasic, respectively). Hybrid OMT genes were constructed by amplifying the appropriate fragments of the parental genes by PCR and fusing these initial PCR products during a second round of PCR. Genes encoding mutant LtOMT variants were constructed by site-directed mutagenesis using synthetic DNA primers. The primers used in this study are listed in Table S6, and mutations engineered into LtOMT are listed in Table S1. OMT genes were inserted between the *NdeI-PmeI* sites of the YEpADH2p expression vector featuring a LEU selectable marker (YEpADH2p-LEU) using the InFusion Kit (BioTool). The YEpADH2p-LEU expression vector that contained the genes for both LtOMT and HsOMT was constructed by ligating the 2,142-bp *BglII-SalI* restriction fragment of YEpADH2p-LEU_LtOMT into the *BamHI-XhoI*-digested YEpADH2p-LEU vector already containing the gene for HsOMT. Highly reducing PKS (hrPKS) genes for benzenediol lactone (BDL) biosynthesis were cloned into YEpADH2p-TRP1, while BDL nonreducing PKS (nrPKS) genes were cloned into YEpADH2p-URA3 as described in our previous studies (1, 3-8) or were custom synthesized by the Joint Genome Institute based on publicly available sequence data (2). All newly constructed plasmids were verified by DNA sequencing. *Escherichia coli* DH10B and plasmid pJET1.2 (Thermo Fisher) were used for routine DNA manipulations.

1.1.2 Total biosynthesis and biotransformation.

Saccharomyces cerevisiae BJ5464-NpgA (*MATa ura3-52 his3-Δ200 leu2-Δ1 trp1 pep4::HIS3 prb1 Δ1.6R can1 GAL*)(37) was the host for expression vectors based on YEpADH2p-TRP, YEpADH2p-URA and YEpADH2p-LEU (21-29). For total biosynthesis, expression plasmids for the appropriate hrPKS, nrPKS and OMT were transformed into cells of *Saccharomyces cerevisiae* BJ5464-NpgA (*MATa ura3-52 his3-Δ200 leu2-Δ1 trp1 pep4::HIS3 prb1 Δ1.6R can1 GAL*)(9) using the LiCl-PEG procedure (10), and the cells were plated on SC minimal dropout (-Trp, -Ura, -Leu) agar plates (Clontech). For biotransformation experiments, the expression vector for the appropriate OMT was transformed into the *Saccharomyces cerevisiae* BJ5464-NpgA host (9), and transformants were selected on SC minimal dropout (-Leu) agar plates (Clontech). Three to five independent *S. cerevisiae* transformants were tested for the production of BDL congeners or for the biotransformation of BDL substrates, and fermentations with representative isolates were repeated at least three times with three replicates each (n=9) for product identification and quantitation. Recombinant yeast cells were grown in 100-mL Erlenmeyer flasks containing 25 mL of the appropriate SC minimal dropout medium (Clontech) at 30 °C with shaking at 220 rpm until the OD₆₀₀ reached 0.6, corresponding to 0.33 ± 0.03 g of *S. cerevisiae* cells (wet weight). Then, an equal volume of YP medium (1% yeast extract, 2% peptone, 1% glucose) was added to the cultures. Polyketide substrates for biotransformations were dissolved in methanol, and supplemented to the cultures (10 µg/mL, final concentration) at the time of addition of the YP medium. The fermentations were continued at 30 °C with shaking at 220 rpm for an additional 48 hours, with the wet cell weight reaching 1.28 ± 0.18 g. No significant differences in

cell growth were noted for the *S. cerevisiae* strains expressing different variants of the OMT enzymes. Fermentations were scaled up for the isolation of polyketide compounds to two to ten liters, depending on yield.

1.1.3 OMT expression in *E. coli* and protein purification.

The gene encoding LtOMT was cloned from *Lasiodiplodia theobromae* NBRC 31059 as described (21). The *hpm5* gene for HsOMT (29) and the gene for LtOMT variant M1 were commercially synthesized (Joint Genome Institute and BioBasic, respectively). OMT-encoding genes were inserted as *NotI-EcoRI* fragments into the multiple cloning site of the pACYCDuet-1 vector (EMD Millipore) and transformed into *Escherichia coli* Arctic Express (DE3) RIL cells (Agilent Technologies). Transformed *E. coli* strains were cultivated in LB medium supplemented with chloramphenicol (17.0 µg/mL, final concentration) with shaking at 220 rpm at 37 °C until the OD₆₀₀ reached 0.6, induced with 0.1 mM isopropyl-β-D-thiogalactopyranoside (IPTG), and the incubation was continued for 24 hours with shaking at 220 rpm at 11 °C. The cells were harvested, washed, and suspended in Binding Buffer (20 mM sodium phosphate buffer (pH7.4), 500 mM NaCl) supplemented with fungal/yeast protease inhibitor cocktail (Biomake). After sonication and centrifugation at 10,000 rpm, the supernatant was loaded onto a His-Bind Ni²⁺-NTA column (Thermo) and washed with 20 bed volumes of Wash Buffer (20 mM sodium phosphate buffer (pH7.4), 500 mM NaCl, 20 mM imidazole (pH7.4)). The His tagged protein was eluted with Elution Buffer (20 mM sodium phosphate buffer (pH7.4), 500 mM NaCl, 250 mM imidazole (pH7.4)). Eluted fractions were analyzed by SDS-polyacrylamide gel electrophoresis (SDS-PAGE). Fractions demonstrating at least 95% purity for the target OMT by SDS-PAGE were concentrated and desalted by VivaSpin Turbo ultrafiltration concentrators (Sartorius, molecular weight

cutoff of 10,000) and the buffer was exchanged to Binding Buffer. Protein concentration was determined using the Bradford dye-binding assay (Thermo). Purified enzymes were stored as aliquots at -80°C after the addition of 10% (vol/vol) glycerol. Enzyme activity assays were performed in 100 µL reaction mixtures containing 50 mM Tris-HCl (pH 8.0), 10 mM MgCl₂, 0.2% Tween-20, 1 mM DLD **1** as the substrate, and 1 mM *S*-adenosyl methionine (SAM) as the methyl group donor. Reactions were initiated by adding the OMT enzyme (2 µg/100 µL for LtOMT, 20 µg/100 µL for the mutant enzymes), the mixtures were incubated at 30 °C for 1 hour for LtOMT and overnight for the mutants, and the reactions were stopped by extractions with ethyl acetate (three times 400 µL). The solvent was evaporated from the pooled ethyl acetate fractions, and the residue was dissolved in 100 µL methanol for quantitative HPLC analysis. Kinetic parameters (V_{\max} and K_m) were obtained under initial velocity conditions at 30 °C for 5 or 15 minutes (LtOMT or mutants, respectively) for substrate DLD **1** (0.125, 0.25, 0.5, 1, 2 and 4 mM, final concentrations) while the concentration of SAM was held at 1mM. Michaelis-Menten saturation curves were fitted to the equation $V=V_{\max}[S]/(K_m+[S])$ using KaleidaGraph (Synergy). Measurements were repeated three times with three replicates each (n=9).

1.1.4 Protein structure modeling.

Homology protein structure models for LtOMT and HsOMT were built with SWISS-MODEL (11) using the MmcR mitomycin 7-*O*-methyltransferase of *Streptomyces lavendulae* (PDB: 3GXO) (12) as the template. Substrates DLD **1**, DHZ **3**, and co-product SAH were modeled in Chem3D using energy minimization to a minimum root mean square (RMS) gradient of 0.010, and molecular dynamics (2.0 fs step interval, 10,000 steps, 1.0 Kcal/atoms/ps heating and cooling rate, 300 K target temperature), followed by docking with the LtOMT or the HsOMT enzymes using Autodock in a two-step approach

(first the co-product, then the methyl acceptor substrate). Protein structures were rendered in Pymol and compared using the DALI server (13). Protein topologies were illustrated with Pro-Origami (<http://munk.csse.unimelb.edu.au/pro-origami/porun.shtml>).

1.2 Isolation and characterization of *O*-methylated products.

1.2.1 General methods.

Extracts of recombinant yeast cultures were prepared and analyzed by liquid chromatography – mass spectrometry (LC-MS), and the BDL congeners were isolated from large scale fermentations (1-5 L, depending on yield) as previously described (21, 24-28). Quantitative HPLC analysis was conducted on an Agilent 1100 series HPLC instrument equipped with a reversed-phase C18 column (Kromasil 100-5-C18, 5 μ m, 4.6 mm \times 250 mm). Substrate and product amounts were determined from the area under the peak at 210 nm using a calibration curve for the analyte.

For large scale fermentations, *Saccharomyces cerevisiae* BJ5464-NpgA cultures were adjusted to pH 5.0 and extracted with equal volumes of ethyl acetate three times. The extracts were pooled, dried *in vacuo*, and reconstituted in methanol. Samples were routinely analyzed on an Agilent 1100 series HPLC instrument equipped with a C18 reversed-phase column (Kromasil 100-5-C18, 5 μ m, 4.6 mm \times 250 mm). For the isolation of *O*-methylated polyketide products, extracts were first subjected to silica gel (25 g) column chromatography and eluted with a gradient of chloroform/methanol to yield five fractions (Fraction A, v/v 100:0, 250 mL; Fraction B, v/v 99:1, 250 mL; Fraction C, v/v 98:2, 250 mL; Fraction D, v/v 95:5, 250 mL; Fraction E, v/v 90:10, 250 mL). Each of these fractions was

analyzed by LC-MS to detect the *O*-methylated products on a Thermo Scientific LXQ ESI-spray mass spectrometer coupled with an Agilent 1100 series HPLC instrument. Fractions containing the target compounds were subsequently purified by preparative HPLC on a Kromasil KR100-7-C18 reversed-phase column (5 μ m, 10 mm \times 250 mm) using a Waters Delta Prep 4000 system equipped with a PDA 996 detector. ^1H , ^{13}C , and 2D NMR spectra were recorded on a Bruker Avance III 400 spectrometer at 400 MHz for ^1H NMR and 100 MHz for ^{13}C NMR. Chemical shift values (δ) are given in parts per million (ppm), and the coupling constants (J values) are in Hz. Chemical shifts were referenced to the residual solvent peaks of methanol- d_4 , chloroform- d , and DMSO- d_6 , respectively. HPLC-HRESIMS and MS-MS spectra were acquired on an Agilent 1290 Infinity II HPLC coupled with an Agilent QTOF 6530 instrument using capillary and cone voltages of 3.6 kV and 40-150 V, respectively. The collision energy was optimized from 15 to 50 V. For accurate mass measurements the instrument was calibrated each time using a standard calibration mix (Agilent) in the range of m/z 150-1900. The HPLC was equipped with an Agilent Eclipse Plus C18 RRHD column (50 mm \times 2.1 mm id, 1.8 μ m particle size), and eluted with a linear gradient of 10-50% of acetonitrile-water over 4 min, 50-95% for 4 min, 95% acetonitrile-water for 2 min and drop down to 10% in 1 min at a flow rate of 0.5 mL/min. Unless otherwise stated, chemicals and solvents were of reagent grade and used as obtained from commercial sources.

1.2.2 Lasiodiplodin (1a)

The crude extract (1.2 g) of a 3 L fermentation broth of *S. cerevisiae* BJ5464-NpgA co-expressing LtLasS1-LtLasS2 (1) with LtOMT (1) was separated by silica gel column chromatography to yield fractions A–E. Fraction A was further purified by semi-preparative HPLC eluting with $\text{CH}_3\text{CN}/\text{H}_2\text{O}$

(85:15, v/v) to yield compound **1a** (15 mg, t_R = 14.2 min) as a colorless oil.

Compound **1a**: ^1H NMR (400 MHz, methanol- d_4) and ^{13}C NMR (100 MHz, methanol- d_4) data (Table S2.1) were in agreement with the published data (1) for lasiodiplodin (**1a**) (–)-HRESIMS m/z 291.1608 $[\text{M}-\text{H}]^-$ (calcd. for $\text{C}_{17}\text{H}_{23}\text{O}_4$, 291.1602).

1.2.3 5-*O*-Methyl-desmethyllasiodiplodin (**1b**)

The crude extract (1.5 g) of a 3 L fermentation broth of *S. cerevisiae* BJ5464-NpgA co-expressing LtLasS1-LtLasS2 (1) with HsOMT (2) was separated by silica gel column chromatography to yield fractions A–E. Fraction A was further purified by semi-preparative HPLC eluting with $\text{CH}_3\text{CN}/\text{H}_2\text{O}$ (85:15, v/v) to yield compound **1b** (20 mg, t_R = 17.5 min) as a colorless oil.

Compound **1b**: ^1H NMR (400 MHz, methanol- d_4) and ^{13}C NMR (100 MHz, methanol- d_4): Table S2.1; (–)-HRESIMS m/z 291.1603 $[\text{M}-\text{H}]^-$ (calcd. for $\text{C}_{17}\text{H}_{23}\text{O}_4$, 291.1602).

1.2.4 3,5-Di-*O*-methyl-desmethyllasiodiplodin (**1c**)

The crude extract (1.3 g) of a 3 L fermentation broth of *S. cerevisiae* BJ5464-NpgA co-expressing LtLasS1-LtLasS2 (3) with LtOMT and HsOMT was separated by silica gel column chromatography to yield fractions A–E. Fraction A was further purified by semi-preparative HPLC eluting with $\text{CH}_3\text{CN}/\text{H}_2\text{O}$ (85:15, v/v) to yield compound **1c** (12 mg, t_R = 15.2 min) as a colorless oil.

Compound **1c**: ^1H NMR (400 MHz, methanol- d_4) and ^{13}C NMR (100 MHz, methanol- d_4): Table S2.1; (+)-HRESIMS m/z 307.1904 $[\text{M}+\text{H}]^+$ (calcd. for $\text{C}_{18}\text{H}_{27}\text{O}_4$, 307.1907).

1.2.5 3-*O*-Methylradiplodin (2a)

The crude extract (1.5 g) of a 3 L fermentation broth of *S. cerevisiae* BJ5464-NpgA co-expressing CcRadS1-LtLasS2(SAT_{CcRadS2}) (5) with LtOMT was separated by silica gel column chromatography to yield fractions A–E. Fraction B was further purified by semi-preparative HPLC eluting with CH₃CN/H₂O (80:20, v/v) to yield compound **2a** (13 mg, t_R = 14.7 min) as a colorless oil.

Compound **2a**: ¹H NMR (400 MHz, CDCl₃) and ¹³C NMR (100 MHz, CDCl₃): Table S2.2; (–)-HRESIMS m/z 287.1293 [M–H][–] (calcd. for C₁₇H₁₉O₄, 287.1289).

1.2.6 5-*O*-Methylradiplodin (2b)

The crude extract (1.2 g) of a 3 L fermentation broth of *S. cerevisiae* BJ5464-NpgA co-expressing CcRadS1-LtLasS2(SAT_{CcRadS2}) (5) with LtOMT mutant M6 was separated by silica gel column chromatography to yield fractions A–E. Fraction B was further purified by semi-preparative HPLC eluting with CH₃CN/H₂O (80:20, v/v) to yield compound **2b** (13 mg, t_R = 16.2 min) as a colorless oil.

Compound **2b**: ¹H NMR (400 MHz, CDCl₃) and ¹³C NMR (100 MHz, CDCl₃): Table S2.2; (–)-HRESIMS m/z 287.1291 [M–H][–] (calcd. for C₁₇H₁₉O₄, 287.1289).

1.2.7 3,5-Di-*O*-methylradiplodin (2c)

The crude extract (1.0 g) of a 3 L fermentation broth of *S. cerevisiae* BJ5464-NpgA co-expressing CcRadS1-LtLasS2(SAT_{CcRadS2}) (5) with LtOMT and HsOMT was separated by silica gel column chromatography to yield fractions A–E. Fraction A was further purified by semi-preparative HPLC eluting with CH₃CN/H₂O (80:20, v/v) to yield compound **2c** (9.8 mg, t_R = 15.3 min) as a colorless oil.

Compound **2c**: ¹H NMR (400 MHz, CDCl₃) and ¹³C NMR (100 MHz, CDCl₃): Table S2.2; (+)-

HRESIMS m/z 303.1587 $[M+H]^+$ (calcd. for $C_{18}H_{23}O_4$, 303.1596).

1.2.8 14,15-Dehydro-3-*O*-methylzearalenol (3a)

The crude extract (1.3 g) of a 3 L fermentation broth of *S. cerevisiae* BJ5464-NpgA co-expressing the *hpm8-hpm3* genes for HsHypS1-HsHypS2 (2) with LtOMT was separated by silica gel column chromatography to yield fractions A–E. Fraction C was further purified by semi-preparative HPLC eluting with CH_3CN/H_2O (70:30, v/v) to yield compound **3a** (13.2 mg, t_R = 16.0 min) as a white solid.

Compound **3a**: 1H NMR (400 MHz, $DMSO-d_6$) and ^{13}C NMR (100 MHz, $DMSO-d_6$): Table S2.3; (–)-HRESIMS m/z 331.1554 $[M-H]^-$ (calcd. for $C_{19}H_{23}O_5$, 331.1551).

1.2.9 14,15-Dehydro-5-*O*-methylzearalenol (3b)

The crude extract (1.1 g) of a 3 L fermentation broth of *S. cerevisiae* BJ5464-NpgA co-expressing the *hpm8-hpm3* genes for HsHypS1-HsHypS2 (2) with HsOMT was separated by silica gel column chromatography to yield fractions A–E. Fraction C was further purified by semi-preparative HPLC eluting with CH_3CN/H_2O (70:30, v/v) to yield compound **3b** (12.1 mg, t_R = 18.2 min) as a white solid.

Compound **3b**: 1H NMR (400 MHz, $DMSO-d_6$) and ^{13}C NMR (100 MHz, $DMSO-d_6$): Table S2.3; (+)-HRESIMS m/z 315.1576 $[M-H_2O+H]^+$ (calcd. for $C_{19}H_{23}O_4$, 315.1596).

1.2.10 14,15-Dehydro-3,5-di-*O*-methylzearalenol (3c)

The crude extract (1.2 g) of a 4 L fermentation broth of *S. cerevisiae* BJ5464-NpgA co-expressing the *hpm8-hpm3* genes for HsHypS1-HsHypS2 (2) with LtOMT and HsOMT was separated by silica gel column chromatography to yield fractions A–E. Fraction B was further purified by semi-preparative HPLC eluting with CH_3CN/H_2O (70:30, v/v) to yield compound **3c** (10.2 mg, t_R = 17.5 min)

as a white solid.

Compound **3c**: ^1H NMR (400 MHz, DMSO- d_6) and ^{13}C NMR (100 MHz, DMSO- d_6): Table S2.3; (+)-HRESIMS m/z 329.1782 $[\text{M}-\text{H}_2\text{O}+\text{H}]^+$ (calcd. for $\text{C}_{20}\text{H}_{25}\text{O}_4$, 329.1752).

1.2.11 3-O-Methylzearalenol (4a)

The crude extract (1.2 g) of a 3 L fermentation broth of *S. cerevisiae* BJ5464-NpgA co-expressing GzZeaS1-GzZeaS2 (14, 15) with LtOMT was separated by silica gel column chromatography to yield fractions A–E. Fraction C was further purified by semi-preparative HPLC eluting with $\text{CH}_3\text{CN}/\text{H}_2\text{O}$ (70:30, v/v) to yield compound **4a** (5.3 mg, t_{R} = 15.6 min) as a white solid.

Compound **4a**: ^1H NMR (400 MHz, methanol- d_4) and ^{13}C NMR (100 MHz, methanol- d_4): Table S2.4; (–)-HRESIMS m/z 333.1713 $[\text{M}-\text{H}]^-$ (calcd. for $\text{C}_{19}\text{H}_{25}\text{O}_5$, 333.1707).

1.2.12 5-O-Methylzearalenol (4b)

The crude extract (1.4 g) of a 3 L fermentation broth of *S. cerevisiae* BJ5464-NpgA co-expressing GzZeaS1-GzZeaS2 (14, 15) with HsOMT was separated by silica gel column chromatography to yield fractions A–E. Fraction C was further purified by semi-preparative HPLC eluting with $\text{CH}_3\text{CN}/\text{H}_2\text{O}$ (70:30, v/v) to yield compound **4b** (6.5 mg, t_{R} = 17.2 min) as a white solid.

Compound **4b**: ^1H NMR (400 MHz, methanol- d_4) and ^{13}C NMR (100 MHz, methanol- d_4): Table S2.4; (–)-HRESIMS m/z 333.1705 $[\text{M}-\text{H}]^-$ (calcd. for $\text{C}_{19}\text{H}_{25}\text{O}_5$, 333.1707).

1.2.13 3,5-Di-O-methylzearalenol (4c)

Compound **4b** (4 mg) was fed to a 1 L fermentation of *S. cerevisiae* BJ5464-NpgA expressing

LtOMT. The crude extract (0.5 g) was separated by silica gel column chromatography to yield fractions A–E. Fraction D was further purified by semi-preparative HPLC eluting with CH₃CN/H₂O (75:25, v/v) to yield compound **4c** (3.0 mg, t_R = 16.2 min) as a colorless oil.

Compound **4c**: ¹H NMR (400 MHz, methanol-*d*₄) and ¹³C NMR (100 MHz, methanol-*d*₄): Table S2.4; (+)-HRESIMS m/z 331.1910 [M–H₂O+H]⁺ (calcd. for C₂₀H₂₇O₄, 331.1909).

1.2.14 3-*O*-Methyllasicicol (**5a**)

The crude extract (1.3 g) of a 3 L fermentation broth of *S. cerevisiae* BJ5464-NpgA co-expressing LtLasS1-CcRadS2 (5) with LtOMT was separated by silica gel column chromatography to yield fractions A–E. Fraction B was further purified by semi-preparative HPLC eluting with CH₃CN/H₂O (75:25, v/v) to yield compound **5a** (8.2 mg, t_R = 18.3 min) as a white solid.

Compound **5a**: ¹H NMR (400 MHz, CDCl₃) and ¹³C NMR (100 MHz, CDCl₃): Table S2.4; (–)-HRESIMS m/z 333.1708 [M–H][–] (calcd. for C₁₉H₂₅O₅, 333.1707).

1.2.15 7-*O*-methyllasilarin (**6a**)

The crude extract (1.7 g) of a 3 L fermentation broth of *S. cerevisiae* BJ5464-NpgA co-expressing LtLasS1-AtCurS2 (5) with LtOMT was separated by silica gel column chromatography to yield fractions A–E. Fraction B was further purified by semi-preparative HPLC eluting with CH₃CN/H₂O (75:35, v/v) to yield compound **6a** (13.2 mg, t_R = 15.5 min) as a white solid.

Compound **6a**: ¹H NMR (400 MHz, methanol-*d*₄) and ¹³C NMR (100 MHz, methanol-*d*₄): Table S2.5; (–)-HRESIMS m/z 333.1701 [M–H][–] (calcd. for C₁₉H₂₅O₅, 333.1707).

1.2.16 5-*O*-methyllasilarin (**6b**)

The crude extract (1.6 g) of a 3 L fermentation broth of *S. cerevisiae* BJ5464-NpgA co-expressing LtLasS1-AtCurS2 (5) with HsOMT was separated by silica gel column chromatography to yield fractions A–E. Fraction B was further purified by semi-preparative HPLC eluting with CH₃CN/H₂O (75:35, v/v) to yield compound **6b** (12.2 mg, t_R = 17.5 min) as a white solid.

Compound **6b**: ¹H NMR (400 MHz, methanol-*d*₄) and ¹³C NMR (100 MHz, methanol-*d*₄): Table S2.5; (–)-HRESIMS m/z 333.1701 [M–H][–] (calcd. for C₁₉H₂₅O₅, 333.1707).

1.2.17 5,7-Di-*O*-methyllasilarin (**6c**)

The crude extract (1.4 g) of a 3 L fermentation broth of *S. cerevisiae* BJ5464-NpgA co-expressing LtLasS1-AtCurS2 (5) with LtOMT and HsOMT was separated by silica gel column chromatography to yield fractions A–E. Fraction B was further purified by semi-preparative HPLC eluting with CH₃CN/H₂O (75:35, v/v) to yield compound **6c** (3.2 mg, t_R = 16.3 min) as a white solid.

Compound **6c**: ¹H NMR (400 MHz, methanol-*d*₄) and ¹³C NMR (100 MHz, methanol-*d*₄): Table S2.5; (–)-HRESIMS m/z 347.1874 [M–H][–] (calcd. for C₂₀H₂₇O₅, 347.1864).

1.2.18 7-[(*R,E*)-6-Hydroxyhept-1-en-1-yl]-3-*O*-methylresorcylic acid ethyl ester (**7a**)

The crude extract (1.5 g) of a 3 L fermentation broth of *S. cerevisiae* BJ5464-NpgA co-expressing AzResS1-LtLasS2(SAT_{AzResS2}) (5) with LtOMT was separated by silica gel column chromatography to yield fractions A–E. Fraction C was further purified by semi-preparative HPLC eluting with CH₃CN/H₂O (70:30, v/v) to yield compound **7a** (15.3 mg, t_R = 13.4 min) as a white solid.

Compound **7a**: ¹H NMR (400 MHz, methanol-*d*₄) and ¹³C NMR (100 MHz, methanol-*d*₄): Table

S2.6; (-)-HRESIMS m/z 307.1561 $[M-H]^-$ (calcd. for $C_{17}H_{23}O_5$, 307.1551).

1.2.19 7-[(*R,E*)-6-Hydroxyhept-1-en-1-yl]-5-*O*-methylresorcylic acid ethyl ester (**7b**)

The crude extract (1.2 g) of a 3 L fermentation broth of *S. cerevisiae* BJ5464-NpgA co-expressing AzResS1-LtLasS2(SAT_{AzResS2}) (5) with HsOMT was separated by silica gel column chromatography to yield fractions A–E. Fraction C was further purified by semi-preparative HPLC eluting with CH_3CN/H_2O (70:30, v/v) to yield compound **7b** (11.2 mg, t_R = 15.4 min) as a white solid.

Compound **7b**: 1H NMR (400 MHz, methanol- d_4) and ^{13}C NMR (100 MHz, methanol- d_4): Table S2.6; (-)-HRESIMS m/z 307.1543 $[M-H]^-$ (calcd. for $C_{17}H_{23}O_5$, 307.1551).

1.2.20 7-[(*R,E*)-6-Hydroxyhept-1-en-1-yl]-3,5-di-*O*-methylresorcylic acid ethyl ester (**7c**)

The crude extract (1.5 g) of a 3 L fermentation broth of *S. cerevisiae* BJ5464-NpgA co-expressing AzResS1-LtLasS2(SAT_{AzResS2}) (5) with LtOMT and HsOMT was separated by silica gel column chromatography to yield fractions A–E. Fraction C was further purified by semi-preparative HPLC eluting with CH_3CN/H_2O (70:30, v/v) to yield compound **7c** (8.9 mg, t_R = 14.4 min) as a white solid.

Compound **7c**: 1H NMR (400 MHz, methanol- d_4) and ^{13}C NMR (100 MHz, methanol- d_4): Table S2.6; (-)-HRESIMS m/z 321.1701 $[M-H]^-$ (calcd. for $C_{18}H_{25}O_5$, 321.1707).

1.2.21 7-[(*S,E*)-6-Hydroxyhept-1-en-1-yl]-resorcylic acid ethyl ester (**8**)

The crude extract (1.2 g) of a 3 L fermentation broth of *S. cerevisiae* BJ5464-NpgA co-expressing AtCurS1-LtLasS2(SAT_{AtCurS2}) was separated by silica gel column chromatography to yield fractions A–E. Fraction C was further purified by semi-preparative HPLC eluting with CH_3CN/H_2O (70:30,

v/v) to yield compound **8** (10.2 mg, t_R = 14.0 min) as a colorless oil.

Compound **8**: ^1H NMR (400 MHz, methanol- d_4): δ_{H} 6.92 (1H, d, J = 15.5 Hz, H-8), 6.37 (1H, d, J = 2.4 Hz, H-6), 6.21 (1H, d, J = 2.4 Hz, H-4), 5.90 (1H, dt, J = 15.5, 6.8 Hz, H-9), 4.36 (2H, q, J = 7.1 Hz, H-15), 3.75 (1H, m, H-13), 2.22 (2H, m, H-10), 1.61 (2H, m, H-12), 1.44 (2H, m, H-11), 1.39 (3H, t, J = 7.1 Hz, H-16), 1.17 (3H, d, J = 6.2 Hz, H-14); ^{13}C NMR (100 MHz, methanol- d_4): 172.7 (C-1), 165.4 (C-3), 163.8 (C-5), 145.1 (C-7), 133.4 (C-9), 132.6 (C-8), 109.2 (C-6), 105.2 (C-2), 102.8 (C-4), 68.7 (C-13), 62.4 (C-15), 39.9 (C-12), 34.2 (C-10), 26.7 (C-11), 23.7 (C-14), 14.8 (C-16); (–)-HRESIMS m/z 293.1400 $[\text{M}-\text{H}]^-$ (calcd. for $\text{C}_{16}\text{H}_{21}\text{O}_5$, 293.1389).

1.2.22 7-[(*S,E*)-6-Hydroxyhept-1-en-1-yl]-3-*O*-methylresorcylic acid ethyl ester (**8a**)

The crude extract (1.3 g) of a 3 L fermentation broth of *S. cerevisiae* BJ5464-NpgA co-expressing AtCurS1-LtLasS2(SAT_{AtCurS2}) (5) with LtOMT was separated by silica gel column chromatography to yield fractions A–E. Fraction C was further purified by semi-preparative HPLC eluting with $\text{CH}_3\text{CN}/\text{H}_2\text{O}$ (70:30, v/v) to yield compound **8a** (3.2 mg, t_R = 13.5 min) as a white solid.

Compound **8a**: ^1H NMR (400 MHz, methanol- d_4) and ^{13}C NMR (100 MHz, methanol- d_4): Table S2.7; (–)-HRESIMS m/z 307.1549 $[\text{M}-\text{H}]^-$ (calcd. for $\text{C}_{17}\text{H}_{23}\text{O}_5$, 307.1551).

1.2.23 7-[(*S,E*)-6-Hydroxyhept-1-en-1-yl]-5-*O*-methylresorcylic acid ethyl ester (**8b**)

The crude extract (1.4 g) of a 3 L fermentation broth of *S. cerevisiae* BJ5464-NpgA co-expressing AtCurS1-LtLasS2(SAT_{AtCurS2}) (5) with HsOMT was separated by silica gel column chromatography to yield fractions A–E. Fraction C was further purified by semi-preparative HPLC eluting with $\text{CH}_3\text{CN}/\text{H}_2\text{O}$ (70:30, v/v) to yield compound **8b** (1.8 mg, t_R = 15.3 min) as a white solid.

Compound **8b**: ^1H NMR (400 MHz, methanol- d_4) and ^{13}C NMR (100 MHz, methanol- d_4): Table S2.7; (–)-HRESIMS m/z 307.1544 $[\text{M}-\text{H}]^-$ (calcd. for $\text{C}_{17}\text{H}_{23}\text{O}_5$, 307.1551).

1.2.24 7-[(*S,E*)-6-Hydroxyhept-1-en-1-yl]-3,5-di-*O*-methylresorcylic acid ethyl ester (**8c**)

The crude extract (1.4 g) of a 3 L fermentation broth of *S. cerevisiae* BJ5464-NpgA co-expressing AtCurS1-LtLasS2(SAT_{AtCurS2}) (5) with LtOMT and HsOMT was separated by silica gel column chromatography to yield fractions A–E. Fraction C was further purified by semi-preparative HPLC eluting with $\text{CH}_3\text{CN}/\text{H}_2\text{O}$ (70:30, v/v) to yield compound **8c** (3.2 mg, t_R = 14.3 min) as a colorless oil.

Compound **8c**: ^1H NMR (400 MHz, methanol- d_4) and ^{13}C NMR (100 MHz, methanol- d_4): Table S2.7; (–)-HRESIMS m/z 321.1699 $[\text{M}-\text{H}]^-$ (calcd. for $\text{C}_{18}\text{H}_{25}\text{O}_5$, 321.1707).

1.3 Structure elucidation.

The HRESIMS-determined molecular formula of compound **1b**, $\text{C}_{17}\text{H}_{24}\text{O}_4$, was identical to that of **1a**. The ^1H and ^{13}C NMR spectra of **1b** displayed resonances corresponding to a desmethyl-lasiiodiplodin core and an *O*-methyl functionality, and were highly similar to those of **1a**. However, discrepancies in the ^1H and ^{13}C chemical shifts were observed (Table S2.1), indicating that these two compounds were regioisomers which only differed in the position of the *O*-methylation. Next, HSQC, HMBC and 1D NOESY experiments were carried out to identify the position to which the *O*-methyl functionality was attached in **1b**. The HMBC correlations of the aromatic protons (δ_{H} 6.29, d, J = 2.8 Hz; δ_{H} 6.31, d, J = 2.8 Hz) and the *O*-methyl protons (δ_{H} 3.78, s) with the aromatic carbon at δ_{C} 165.1

suggested that the *O*-methyl functionality was attached to C-5 (Figure S6). This was further supported by the fact that both aromatic protons had NOE correlations with the *O*-methyl protons (Figure S6). Based on the above-described evidence, the structure of **1b** was established as 5-*O*-methyl-desmethyllasiodiplodin.

The HRESIMS-determined molecular weight of **1c** was 14 amu higher than that of **1a** and **1b**. The ¹H and ¹³C NMR spectra of **1c** were similar to those of **1a** and **1b** (Table S2.1), except for the presence of resonances corresponding to two *O*-methyl functionalities (δ_{H} 3.80, s, δ_{C} 55.8; δ_{H} 3.79, s, δ_{C} 56.4) instead of one. Extensive analysis of the HMBC spectrum confirmed that **1c** was the 3,5-di-*O*-methylated derivative of desmethyllasiodiplodin **1** (Figure S6).

The HRESIMS-determined molecular weight of compounds **2a** and **2b** were 14 amu higher than that of radiplodin. The ¹H and ¹³C NMR spectra of **2a** and **2b** were quite similar, and both showed resonances corresponding to an extra *O*-methyl substituent (**2a**: δ_{H} 3.69, s; δ_{C} 56.0; **2b**: δ_{H} 3.79, s; δ_{C} 55.4) when compared to those of radiplodin (Table S2.2). The determination of *O*-methylation positions and the assignments of ¹H and ¹³C NMR data were achieved by analyzing the 2D NMR spectra. In the HMBC spectra, the *O*-methyl protons of **2a** showed correlations with C-3 (δ_{C} 158.0), while the *O*-methyl protons of **2b** had correlations with C-5 (δ_{C} 163.8), which suggested **2a** and **2b** as the 3-*O*-methylated and 5-*O*-methylated products of radiplodin, respectively (Figure S6).

Based on the HRESIMS-determined molecular weight and the 1D NMR spectra (Table S2.2), **2c** was elucidated as the 3,5-di-*O*-methylated product of radiplodin, and this hypothesis was verified by HSQC and HMBC experiments (Figure S6).

The molecular formula of compounds **3a** and **3b** were determined as C₁₉H₂₄O₅ by the HRESIMS. The initial interpretation of the ¹H and ¹³C NMR data (Table S2.3) established their structures as mono-*O*-methyl substituted 14,15-dehydrozearalenol. Next, HSQC and HMBC experiments were carried out to determine the *O*-methylation position. In the HMBC spectrum of **3a**, the aromatic proton at δ_{H} 6.31 (d, J = 2.0 Hz, H-4) and the *O*-methyl protons (δ_{H} 3.68, s) had a cross peak with the aromatic carbon at δ_{C} 157.2 (C-3), indicating that **3a** was the 3-*O*-methylated product of 14,15-dehydrozearalenol (Figure S6). By contrast, both aromatic protons (δ_{H} 6.30, d, J = 2.4 Hz, H-4; δ_{H} 6.56, d, J = 2.4 Hz, H-6) and the *O*-methyl protons (δ_{H} 3.73, s) of **3b** had HMBC correlations with the aromatic carbon at δ_{C} 160.9 (C-5), defining the structure of **3b** as 14,15-dehydro-3-*O*-methylzearalenol (Figure S6).

The HRESIMS-determined molecular weight of compound **3c** was 14 amu higher than those of **3a** and **3b**, indicating the presence of an extra methyl functional group. After the comprehensive analysis of 1D and 2D NMR data (Table S2.3 and Figure S6), the structure of **3c** was elucidated as 14,15-dehydro-3,5-di-*O*-methylzearalenol.

The HRESIMS-determined molecular formula, C₁₉H₂₆O₅, as well as the ¹H and ¹³C NMR data of compounds **4a** and **4b** (Table S2.4) indicated that they were both mono-*O*-methylated products of zearalenol. The 1D NOESY spectrum of **4a** showed that the *O*-methyl protons (δ_{H} 3.76, s) correlated with only one aromatic proton (δ_{H} 6.55, d, J = 2.0 Hz). On the other hand, the *O*-methyl protons of **4b** (δ_{H} 3.80, s) had NOE correlations with not only one, but both aromatic protons (δ_{H} 6.56, d, J = 2.0 Hz; δ_{H} 6.34, d, J = 2.0 Hz) (Figure S6). These evidences strongly indicated that **4a** and **4b** were 3-*O*-methylzearalenol and 5-*O*-methylzearalenol, respectively.

The HRESIMS-determined molecular weight of compound **4c** was 14 amu higher than those of **4a**

and **4b**, indicating the presence of an additional methyl group. The ^1H and ^{13}C NMR data (Table S2.4) further supported **4c** as the di-*O*-methylated product of zearalenol. Based on the HMBC correlations of one set of methoxy protons (δ_{H} 3.83, s) with the aromatic carbon at δ_{C} 162.9, and the other set of methoxy protons (δ_{H} 3.79, s) with the aromatic carbon at δ_{C} 159.0 (Figure S6), the structure of **4c** was confirmed as 3,5-di-*O*-methylzearalenol.

The HRESIMS-determined molecular formula and the 1D NMR data (Table S2.4) of compound **5a** suggested that it was an *O*-methylated product of lasicol. The HMBC correlations of one aromatic proton (δ_{H} 6.21, d, $J = 2.0$ Hz) and the *O*-methyl protons (δ_{H} 3.71, s) with the aromatic carbon at δ_{C} 159.1 confirmed that the OH at C-3 of lasicol was *O*-methylated in **5a** (Figure S6).

The HRESIMS-determined molecular weight of compounds **6a** and **6b** were both 14 amu higher than that of lasilarin. Their ^1H and ^{13}C NMR spectra were very similar, both showing resonances corresponding to a lasilarin core and an *O*-methyl functionality, but not superimposable with each other (Table S2.5). These evidences suggested that **6a** and **6b** were regioisomeric mono-*O*-methylated products of lasilarin. The 1D NOESY spectrum of **6a** showed that the *O*-methyl protons (δ_{H} 3.80, s) correlated with only one aromatic proton (δ_{H} 6.41, d, $J = 2.2$ Hz), indicating the *O*-methyl group was attached to C-7 in **6a** (Figure S6). By contrast, HMBC correlations of both aromatic protons (δ_{H} 6.34, d, $J = 2.2$ Hz; δ_{H} 6.36, d, $J = 2.2$ Hz) and the *O*-methyl protons (δ_{H} 3.77, s) with the aromatic carbon at δ_{C} 163.0 suggested that the *O*-methyl group in **6b** was attached to C-5 (Figure S6). Based on the above-described evidence, the structures of **6a** and **6b** were elucidated as 7-*O*-methyllasilarin and 5-*O*-methyllasilarin, respectively.

The HRESIMS-determined molecular formula, $\text{C}_{20}\text{H}_{28}\text{O}_5$, and the 1D NMR data of **6c** were

consistent with those of a di-*O*-methylated product of lasilarin (Table S2.5). Since lasilarin had only two positions suitable for *O*-methylation, the structure of **6c** was elucidated as 5,7-di-*O*-methyllasilarin.

The molecular formula of compounds **7a** and **7b** were established as C₁₇H₂₅O₅ by HRESIMS. The ¹H and ¹³C NMR data of **7a** and **7b** (Table S2.6) suggested that they were regioisomeric mono-*O*-methylated products of ARA7 (**7**). In the HMBC spectrum of **7a**, the *O*-methyl protons (δ_{H} 3.76, s) and one aromatic proton (δ_{H} 6.35, d, $J = 2.0$ Hz) had correlations with the aromatic carbon at δ_{C} 159.6 (C-3). However, in the case of **7b** the *O*-methyl protons (δ_{H} 3.81, s) and both aromatic protons (δ_{H} 6.36, d, $J = 2.4$ Hz; δ_{H} 6.47, d, $J = 2.4$ Hz) correlated with the aromatic carbon at δ_{C} 164.9 (C-5) (Figure S6). Based on these, the structures of **7a** and **7b** were established as 7-[(*R,E*)-6-Hydroxyhept-1-en-1-yl]-3-*O*-methylresorcylic acid ethyl ester and 7-[(*R,E*)-6-Hydroxyhept-1-en-1-yl]-5-*O*-methylresorcylic acid ethyl ester, respectively.

The HRESIMS-determined molecular weight of **7c** was 14 amu higher than those of **7a** and **7b**, suggesting that **7c** was the di-*O*-methylated derivative of **7**. After careful examination of the 1D and 2D NMR data (Table S2.6 and Figure S6), the structure of **7c** was elucidated as 7-[(*R,E*)-6-Hydroxyhept-1-en-1-yl]-3,5-di-*O*-methylresorcylic acid ethyl ester.

The ¹H and ¹³C NMR data of ARA8 (**8**) (see section 1.2.21) were identical to those of ARA7 (**7**) (**5**), while the circular dichroism (CD) spectra (Figure S8) indicated that **8** was the enantiomer of **7** whereby C-13 of **8** displays an *S*-configuration. The HRESIMS-determined molecular weight and the 1D NMR spectra of **8a** and **8b** (Table S2.7) were identical to those of **7a** and **7b**, respectively, suggesting that **8a** is the 3-*O*-methylated derivative of **8**, while **8b** is the 5-*O*-methylated product. Further examination of the HMBC correlations supported this hypothesis (Figure S6). Thus, the structures of

8a and **8b** were elucidated as 7-[(*S,E*)-6-Hydroxyhept-1-en-1-yl]-3-*O*-methylresorcylic acid ethyl ester and 7-[(*S,E*)-6-Hydroxyhept-1-en-1-yl]-5-*O*-methylresorcylic acid ethyl ester, respectively.

Similarly, the HRESIMS determined molecular weight and the 1D NMR spectra of **8c** (Table S2.7) were identical to those of **7c**. Interpretation of the HMBC spectrum confirmed that **8c** was 7-[(*S,E*)-6-Hydroxyhept-1-en-1-yl]-3,5-di-*O*-methylresorcylic acid ethyl ester (Figure S6).

2 SI Tables

Table S1. Mutations engineered into LtOMT.

LtOMT			Mutations	
Sites	Amino acid	Codon	Amino acid	Codon
330	F	TTC	V	GTC
356	T	ACT	M	ATG
384	Q	CAA	K	AAG
386	G	GGT	R	AGA
387	W	TGG	H	CAT
388	Q	CAA	H	CAT

Table S2. ^1H NMR (400 MHz) and ^{13}C NMR (100 MHz) data.**Table S2.1. Compounds 1a, 1b and 1c (in methanol- d_4).**

no.	1a		1b		1c	
	δ_{C} , type	δ_{H} , mult. (J in Hz)	δ_{C} , type	δ_{H} , mult. (J in Hz)	δ_{C} , type	δ_{H} , mult. (J in Hz)
1	170.9, C		172.9, C		170.6, C	
2	109.2, C		107.3, C		118.9, C	
3	159.4, C		165.6, C		159.3, C	
4	97.9, CH	6.25, d (2.8)	99.9, CH	6.29, d (2.8)	97.2, CH	6.41, d (2.0)
5	160.8, C		165.1, C		163.0, C	
6	117.6, CH	6.29, d (2.8)	110.9, CH	6.31, d (2.8)	107.1, CH	6.39, d (2.0)
7	143.8, C		149.2, C		143.8, C	
8	31.3, CH ₂	2.64, m	32.2, CH ₂	3.25, m	31.4, CH ₂	2.69, dt (15.6, 8.0)
		2.48, m		2.53, m		2.55, dt (15.6, 8.0)
9	31.1, CH ₂	1.37–1.71, m	32.0, CH ₂	1.40–1.73, m	31.3, CH ₂	1.20–1.72, m
10	25.6, CH ₂	1.37–1.71, m	25.5, CH ₂	1.40–1.73, m	25.6, CH ₂	1.20–1.72, m
11	27.7, CH ₂	1.37–1.71, m	28.1, CH ₂	1.40–1.73, m	27.7, CH ₂	1.20–1.72, m
12	26.3, CH ₂	1.37–1.71, m	25.5, CH ₂	1.40–1.73, m	26.3, CH ₂	1.20–1.72, m
13	22.4, CH ₂	1.37–1.71, m	22.6, CH ₂	1.40–1.73, m	22.3, CH ₂	1.20–1.72, m
14	33.6, CH ₂	1.92, m	34.2, CH ₂	1.92, m	33.6, CH ₂	1.93, m
		1.58–1.71, m		1.82, m		1.58–1.72, m
15	73.4, CH	5.17, m	76.0, CH	5.16, m	73.5, CH	5.17, m
16	19.9, CH ₃	1.30, d (6.4)	20.4, CH ₃	1.35, d (6.2)	19.9, CH ₃	1.31, d (6.4)
3-OCH ₃	56.3, CH ₃	3.75, s			56.4, CH ₃	3.79, s
5-OCH ₃			55.7, CH ₃	3.78, s	55.8, CH ₃	3.80, s

Table S2.2. Compounds 2a, 2b and 2c (in CDCl₃).

no.	2a		2b		2c	
	δ_C , type	δ_H , mult. (<i>J</i> in Hz)	δ_C , type	δ_H , mult. (<i>J</i> in Hz)	δ_C , type	δ_H , mult. (<i>J</i> in Hz)
1	168.9, C		171.4, C		167.9, C	
2	115.7, C		104.8, C		116.4, C	
3	158.0, C		164.6, C		157.5, C	
4	97.9, CH	6.25, d (2.4)	99.6, CH	6.35, d (2.8)	97.2, CH	6.32, d (2.4)
5	157.9, C		163.8, C		161.1, C	
6	105.0, CH	6.31, d (2.4)	108.0, CH	6.34, d (2.8)	102.1, CH	6.40, d (2.4)
7	138.6, C		144.0, C		138.1, C	
8	130.5, CH	6.23, d (15.1)	136.0, CH	6.69, d (15.6)	130.6, CH	6.29, d (16.0)
9	133.0, CH	5.77, dt (15.1, 6.0)	128.9, CH	5.70, m	132.6, CH	5.85, dt (16.0, 6.0)
10	30.7, CH ₂	2.20, m	31.0, CH ₂	2.16, m	30.7, CH ₂	2.28, m
		2.31, m		2.31, m		
11	30.0, CH ₂	2.23, m	30.9, CH ₂	2.16, m	29.8, CH ₂	2.24, m
		2.31, m		2.31, m		2.30, m
12	132.5, CH	5.28, m	134.3, CH	5.36, m	132.5, CH	5.23, m
13	128.6, CH	5.39, m	126.6, CH	5.36, m	128.6, CH	5.40, ddd (4.4, 9.6, 15.2)
14	40.2, CH ₂	2.31, m	39.1, CH ₂	2.31, m	40.1, CH ₂	2.24, m
		2.41, brd (14.1)		2.51, dt (15.2, 4.4)		2.40, brd (14.0)
15	71.9, CH	5.28, m	72.0, CH	5.13, m	71.3, CH	5.30, m
16	20.9, CH ₃	1.34, d (6.4)	20.1, CH ₃	1.41, d (6.4)	20.8, CH ₃	1.33, d (6.4)
3-OCH ₃	56.0, CH ₃	3.69, s			55.9, CH ₃	3.77, s
5-OCH ₃			55.4, CH ₃	3.79, s	55.4, CH ₃	3.78, s
3-OH				11.60, s		

Table S2.3. Compounds 3a, 3b and 3c (in DMSO-*d*₆).

no.	3a		3b		3c	
	δ_{C} , type	δ_{H} , mult. (<i>J</i> in Hz)	δ_{C} , type	δ_{H} , mult. (<i>J</i> in Hz)	δ_{C} , type	δ_{H} , mult. (<i>J</i> in Hz)
1	167.4, C		168.2, C		167.2, C	
2	114.9, C		113.5, C		116.4, C	
3	157.2, C		156.9, C		157.1, C	
4	97.9, CH	6.31, d (2.0)	100.0, CH	6.30, d (2.4)	97.49, CH	6.47, d (2.0)
5	159.0, C		160.9, C		160.8, C	
6	102.3, CH	6.50, d (2.0)	100.7, CH	6.56, d (2.4)	100.2, CH	6.69, d (2.0)
7	135.6, C		137.2, C		135.7, C	
8	125.6, CH	6.15, brs	126.6, CH	6.34, d (16.0)	125.6, CH	6.17, d (16.0)
9	131.8, CH	6.15, brs	132.1, CH	6.24, dt (16.0, 5.6)	132.5, CH	6.35, dt (16.0, 5.2)
10	29.1, CH ₂	2.13–2.23, m	29.4, CH ₂	2.13–2.24, m	29.1, CH ₂	2.19–2.25, m
11	21.5, CH ₂	1.47–1.51, m	21.4, CH ₂	1.47–1.52, m	21.5, CH ₂	1.39–1.51, m
12	35.1, CH ₂	1.37–1.47, m	34.9, CH ₂	1.43–1.45, m	35.2, CH ₂	1.37–1.48, m
13	70.6, CH	3.68, brs	70.5, CH	3.91, brs	70.6, CH	3.84, m
14	136.7, CH	5.44–5.50, m	136.9, CH	5.44–5.58, m	136.8, CH	5.41–5.55, m
15	125.7, CH	5.44–5.50, m	125.3, CH	5.44–5.58, m	125.5, CH	5.41–5.55, m
16	38.4, CH ₂	2.22–2.49, m	38.2, CH ₂	2.24–2.43, m	38.4, CH ₂	2.22–2.41, m
17	70.6, CH	5.11, m	70.9, CH	5.14, m	70.7, CH	5.13, m
18	20.6, CH ₃	1.26, d (6.0)	20.3, CH ₃	2.56, d (6.4)	20.6, CH ₃	1.26, d (6.4)
3-OCH ₃	55.7, CH ₃	3.68, s			56.0, CH ₃	3.73, s
5-OCH ₃			55.2, CH ₃	3.73, s	55.4, CH ₃	3.79, s
13-OH		4.62, brs		4.63, d (4.0)		4.62, d (4.4)
3-OH				10.09, brs		
5-OH		9.74, brs				

Table S2.4. Compounds 4a, 4b, 4c (in methanol-*d*₄) and 5a (in CDCl₃).

no.	4a		4b		4c		5a	
	δ_{C} , type	δ_{H} , mult. (<i>J</i> in Hz)	δ_{C} , type	δ_{H} , mult. (<i>J</i> in Hz)	δ_{C} , type	δ_{H} , mult. (<i>J</i> in Hz)	δ_{C} , type	δ_{H} , mult. (<i>J</i> in Hz)
1	170.3, C		171.9, C		170.0, C		168.7, C	
2	116.4, C		109.6, C		117.7, C		116.2, C	
3	160.6, C		164.4, C		159.0, C		159.1, C	
4	104.4, CH	6.55, d (2.0)	106.2, CH	6.56, d (2.0)	98.4, CH	6.47, d (2.1)	98.7, CH	6.21, d (2.0)
5	159.1, C		162.5, C		162.9, C		158.7, C	
6	98.9, CH	6.31, d (2.0)	100.8, CH	6.34, d (2.0)	102.4, CH	6.68, d (2.1)	110.4, CH	6.18, d (2.0)
7	138.1, C		140.1, C		138.0, C		133.9, C	
8	129.0, CH	6.31, d (15.8)	131.8, CH	6.69, dt (15.8, 1.5)	128.8, CH	6.35, d (15.8)	46.3, CH ₂	4.28, d (17.6) 3.48, d (17.6)
9	134.2, CH	6.08, ddd (15.8, 8.6, 5.1)	133.7, CH	6.03, ddd (15.8, 8.6, 5.1)	134.7, CH	6.17, ddd (15.8, 8.5, 5.1)	211.0, C	
10	31.3, CH ₂	2.26, m	31.9, CH ₂	2.30, m	31.3, CH ₂	2.28, m	41.8, CH ₂	2.56, m 2.33, m
11	23.9, CH ₂	1.15–1.85, m	23.7, CH ₂	1.25–1.93, m	23.8, CH ₂	1.21–1.88, m	22.5, CH ₂	1.16–1.70, m
12	33.2, CH ₂	1.15–1.85, m	32.7, CH ₂	1.25–1.93, m	33.3, CH ₂	1.21–1.88, m	25.6, CH ₂	1.16–1.70, m
13	69.5, CH	3.62, m	69.4, CH	3.71, m	69.5, CH	3.62, m	25.5, CH ₂	1.16–1.70, m
14	37.5, CH ₂	1.15–1.85, m	37.2, CH ₂	1.25–1.93, m	37.5, CH ₂	1.21–1.88, m	26.4, CH ₂	1.16–1.70, m
15	20.5, CH ₂	1.15–1.85, m	20.4, CH ₂	1.25–1.93, m	20.5, CH ₂	1.21–1.88, m	23.3, CH ₂	1.16–1.70, m
16	35.9, CH ₂	1.15–1.85, m	35.6, CH ₂	1.25–1.93, m	35.9, CH ₂	1.21–1.88, m	35.0, CH ₂	1.16–1.70, m
17	72.3, CH	5.28, m	74.1, CH	5.17, m	72.4, CH	5.29, m	71.0, CH	5.23, m
18	19.6, CH ₃	1.28, d (6.5)	19.1, CH ₃	1.34, d (6.5)	19.6, CH ₃	1.28, d (6.5)	20.5, CH ₃	1.31, d (6.3)
3-OCH ₃	56.3, CH ₃	3.76, s			56.5, CH ₃	3.79, s	55.8, CH ₃	3.71, s
5-OCH ₃			55.8, CH ₃	3.80, s	55.9, CH ₃	3.83, s		

Table S2.5. Compounds 6a, 6b and 6c (in methanol-*d*₄).

no.	6a		6b		6c	
	δ_{C} , type	δ_{H} , mult. (<i>J</i> in Hz)	δ_{C} , type	δ_{H} , mult. (<i>J</i> in Hz)	δ_{C} , type	δ_{H} , mult. (<i>J</i> in Hz)
1	173.2, C		173.4, C		173.1, C	
2	38.7, CH ₂	3.87, d (17.0) 3.49, d (17.0)	39.3, CH ₂	3.99, d (17.0) 3.56, d (17.0)	38.7, CH ₂	3.91, d (17.0) 3.56, d (17.0)
3	135.7, C		136.3, C		135.5, C	
4	112.0, CH	6.32, d (2.2)	110.6, CH	6.36, d (2.2)	110.0, CH	6.54, d (2.2)
5	160.6, C		163.0, C		163.0, C	
6	98.9, CH	6.41, d (2.2)	101.1, CH	6.34, d (2.2)	98.3, CH	6.47, d (2.2)
7	161.1, C		159.2, C		160.2, C	
8	123.9, C		122.9, C		125.3, C	
9	209.8, C		209.8, C		209.6, C	
10	44.4, CH ₂	2.91, ddd (16.6, 8.6, 3.7) 2.76, ddd (16.6, 7.8, 3.9)	44.3, CH ₂	3.01, ddd (16.6, 8.6, 3.7) 2.84, ddd (16.6, 7.8, 3.9)	44.4, CH ₂	2.91, ddd (16.6, 8.6, 3.7) 2.77, ddd (16.6, 7.8, 3.9)
11	28.1, CH ₂	1.20–1.44, m	28.0, CH ₂	1.20–1.44, m	28.1, CH ₂	1.20–1.44, m
12	24.5, CH ₂	1.58, m 1.50, m	24.6, CH ₂	1.58, m 1.50, m	24.4, CH ₂	1.58, m 1.50, m
13	27.5, CH ₂	1.20–1.44, m	27.6, CH ₂	1.20–1.44, m	27.6, CH ₂	1.20–1.44, m
14	27.1, CH ₂	1.20–1.44, m	27.0, CH ₂	1.20–1.44, m	27.1, CH ₂	1.20–1.44, m
15	22.6, CH ₂	1.41, m 1.27, m	22.6, CH ₂	1.41, m 1.27, m	22.6, CH ₂	1.41, m 1.27, m
16	34.9, CH ₂	1.54, m	35.0, CH ₂	1.54, m	34.9, CH ₂	1.54, m
17	71.9, CH	4.95, m	71.9, CH	4.97, m	72.0, CH	4.98, m
18	20.4, CH ₃	1.18, d (6.3)	20.5, CH ₃	1.19, d (6.3)	20.4, CH ₃	1.19, d (6.3)
5-OCH ₃			55.7, CH ₃	3.77, s	55.9, CH ₃	3.83, s
7-OCH ₃	56.1, CH ₃	3.80, s			56.2, CH ₃	3.84, s

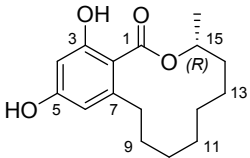
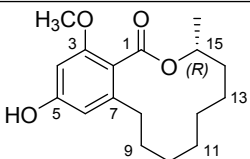
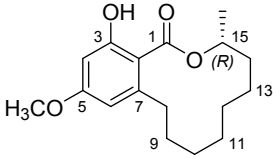
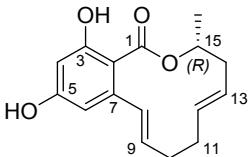
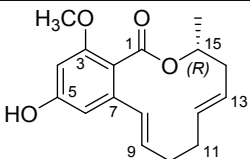
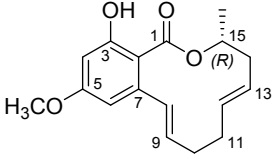
Table S2.6. Compounds 7a, 7b and 7c (in methanol-*d*₄).

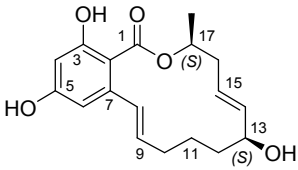
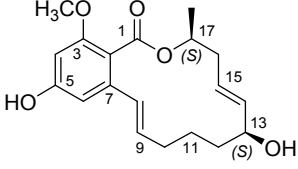
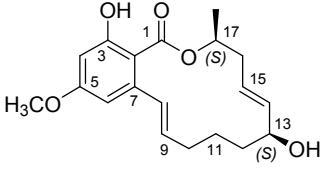
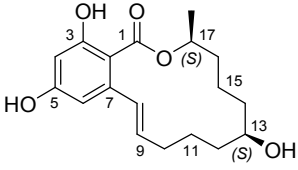
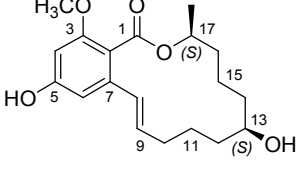
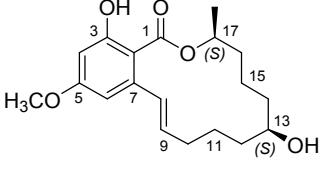
no.	7a		7b		7c	
	δ_{C} , type	δ_{H} , mult. (<i>J</i> in Hz)	δ_{C} , type	δ_{H} , mult. (<i>J</i> in Hz)	δ_{C} , type	δ_{H} , mult. (<i>J</i> in Hz)
1	170.5, C		172.4, C		170.3, C	
2	115.4, C		106.2, C		116.8, C	
3	159.6, C		165.2, C		159.4, C	
4	98.8, CH	6.35, d (2.0)	100.6, CH	6.36, d (2.4)	98.2, CH	6.46, d (2.0)
5	160.8, C		164.9, C		163.0, C	
6	104.9, CH	6.55, d (2.0)	108.0, CH	6.47, d (2.4)	102.7, CH	6.65, d (2.0)
7	139.0, C		144.3, C		138.9, C	
8	128.0, CH	6.33, brd (15.0)	132.1, CH	6.91, dt (15.6, 1.5)	127.9, CH	6.34, dt (16.0, 1.5)
9	134.7, CH	6.17, dt (15.0, 6.7)	133.6, CH	5.95, dt (15.6, 6.8)	135.2, CH	6.24, dt (16.0, 6.4)
10	34.1, CH ₂	2.20, m	34.1, CH ₂	2.22, m	34.1, CH ₂	2.20, m
11	26.4, CH ₂	1.41–1.65, m	26.6, CH ₂	1.45–1.62, m	26.4, CH ₂	1.52–1.65, m
12	39.6, CH ₂	1.41–1.65, m	39.8, CH ₂	1.48–1.55, m	39.6, CH ₂	1.40–1.52, m
13	68.4, CH	3.74, m	68.4, CH	3.75, m	68.4, CH	3.74, m
14	23.5, CH ₃	1.17, d (6.1)	23.6, CH ₃	1.17, d (6.2)	23.6, CH ₃	1.16, d (6.4)
15	62.2, CH ₂	4.32, q (7.0)	62.4, CH ₂	4.37, q (7.2)	62.3, CH ₂	4.32, q (7.2)
16	14.6, CH ₃	1.35, t (7.0)	14.7, CH ₃	1.40, t (7.2)	14.6, CH ₃	1.34, t (7.2)
3-OCH ₃	56.3, CH ₃	3.76, s			56.4, CH ₃	3.79, s
5-OCH ₃			55.9, CH ₃	3.81, s	55.9, CH ₃	3.83, s

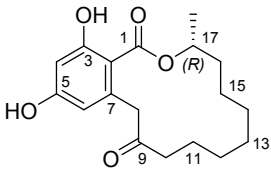
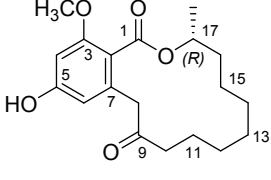
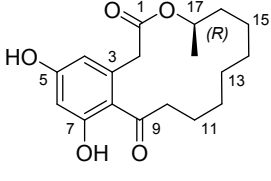
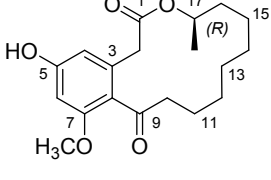
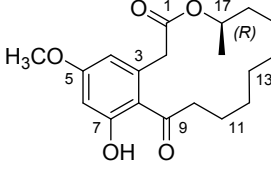
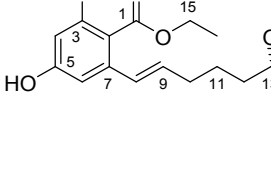
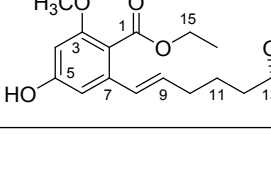
Table S2.7. Compounds 8a, 8b and 8c (in methanol-*d*₄).

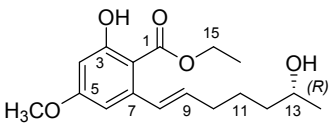
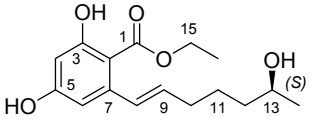
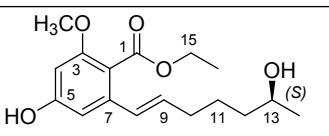
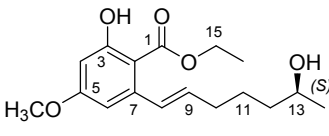
no.	8a		8b		8c	
	δ_{C} , type	δ_{H} , mult. (<i>J</i> in Hz)	δ_{C} , type	δ_{H} , mult. (<i>J</i> in Hz)	δ_{C} , type	δ_{H} , mult. (<i>J</i> in Hz)
1	170.5, C		172.3, C		170.3, C	
2	115.4, C		106.3, C		116.8, C	
3	159.6, C		165.2, C		159.4, C	
4	98.8, CH	6.34, d (2.0)	100.7, CH	6.36, d (2.4)	98.2, CH	6.46, d (2.0)
5	160.8, C		164.9, C		163.0, C	
6	104.9, CH	6.53, d (2.0)	108.0, CH	6.47, d (2.4)	102.7, CH	6.65, d (2.0)
7	139.0, C		144.4, C		138.9, C	
8	128.0, CH	6.32, dt (15.6, 1.4)	132.1, CH	6.91, dt (15.6, 1.5)	127.9, CH	6.34, dt (16.0, 1.5)
9	134.7, CH	6.16, dt (15.6, 6.8)	133.6, CH	5.95, dt (15.6, 6.8)	135.2, CH	6.24, dt (16.0, 6.4)
10	34.1, CH ₂	2.20, m	34.1, CH ₂	2.22, m	34.1, CH ₂	2.20, m
11	26.5, CH ₂	1.41–1.65, m	26.5, CH ₂	1.45–1.62, m	26.4, CH ₂	1.52–1.65, m
12	39.6, CH ₂	1.41–1.65, m	39.8, CH ₂	1.48–1.55, m	39.6, CH ₂	1.40–1.52, m
13	68.4, CH	3.74, m	68.5, CH	3.75, m	68.4, CH	3.74, m
14	23.6, CH ₃	1.16, d (6.2)	23.5, CH ₃	1.17, d (6.2)	23.6, CH ₃	1.16, d (6.4)
15	62.2, CH ₂	4.30, q (7.0)	62.4, CH ₂	4.37, q (7.2)	62.3, CH ₂	4.32, q (7.2)
16	14.6, CH ₃	1.34, t (7.0)	14.7, CH ₃	1.40, t (7.2)	14.6, CH ₃	1.34, t (7.2)
3-OCH ₃	56.3, CH ₃	3.76, s			56.4, CH ₃	3.79, s
5-OCH ₃			55.9, CH ₃	3.80, s	55.9, CH ₃	3.83, s

Table S3. Combinatorial methylation with LtOMT and HsOMT.

Substrate	Chemical structure	OMT enzyme	Total conversion [%]	<i>o</i> -Methoxy product [%]	<i>p</i> -Methoxy product [%]	<i>o,p</i> -Dimethoxy product [%]
DLD 1		LtOMT	95.9 ± 1.9	100	0	0
		HsOMT	41.6 ± 1.2	0	100	0
		LtOMT + HsOMT	96.5 ± 0.7	62.0 ± 2.6	2.7 ± 0.5	35.3 ± 2.9
1a		HsOMT	39.7 ± 0.1	NA	NA	100
1b		LtOMT	97.0 ± 1.8	NA	NA	100
RDN 2		LtOMT	96.7 ± 2.7	100	0	0
		HsOMT	0	NA	NA	NA
		LtOMT + HsOMT	98.6 ± 0.1	94.7 ± 0.4	0	5.3 ± 0.4
2a		HsOMT	7.7 ± 0.3	NA	NA	100
2b		LtOMT	97.1 ± 1.3	NA	NA	100

DHZ 3		LtOMT	99.5 ± 0.6	100	0	0
		HsOMT	98.2 ± 0.6	0	100	0
		LtOMT + HsOMT	99.8 ± 0.1	70.9 ± 4.9	1.0 ± 0.1	28.1 ± 4.8
3a		HsOMT	0	NA	NA	NA
3b		LtOMT	98.3 ± 0.6	NA	NA	100
ZEA 4		LtOMT	100	100	0	0
		HsOMT	72.4 ± 2.0	0	100	0
		LtOMT + HsOMT	92.9 ± 1.6	96.0 ± 0.6	0	4.0 ± 0.6
4a		HsOMT	0	NA	NA	NA
4b		LtOMT	95.4 ± 0.8	NA	NA	100

LCL 5		LtOMT	94.6 ± 0.5	100	0	0
		HsOMT	0	NA	NA	NA
		LtOMT + HsOMT	98.1 ± 0.1	100	0	0
5a		HsOMT	0	NA	NA	NA
LLN 6		LtOMT	37.7 ± 1.4	100	0	0
		HsOMT	30.7 ± 3.1	0	100	0
		LtOMT + HsOMT	24.9 ± 1.9	25.7 ± 3.1	72.8 ± 3.6	1.5 ± 0.5
6a		HsOMT	8.3 ± 0.5	NA	NA	100
6b		LtOMT	7.0 ± 1.1	NA	NA	100
ARA 7 7		LtOMT	97.4 ± 0.1	100	0	0
		HsOMT	82.2 ± 1.6	0	100	0
		LtOMT + HsOMT	79.3 ± 1.5	94.0 ± 0.7	0.9 ± 0.2	5.2 ± 0.5
7a		HsOMT	0	NA	NA	NA

7b		LtOMT	96.8 ± 0.3	NA	NA	100
ARA8 8		LtOMT	89.1 ± 1.1	100	0	0
		HsOMT	95.7 ± 1.2	0	100	0
		LtOMT + HsOMT	82.7 ± 1.3	93.8 ± 0.5	1.0 ± 0.1	5.2 ± 0.4
8a		HsOMT	0	NA	NA	NA
8b		LtOMT	96.2 ± 0.2	NA	NA	100

Total conversion: Numbers show the overall conversion percentage of the indicated substrate into all corresponding methylated products. *Individual products* are shown as their proportion amongst all three *O*-methylated product congeners (Yield of the individual product divided by the total yield of all products, multiplied by 100). Values represent the mean ± SD from three independent experiments of three replicates each (n=9). NA, not applicable. Compound **5b** (5-*O*-methyl LCL) is not produced by the LtOMT or HsOMT enzymes, thus it was not included as a substrate in these experiments.

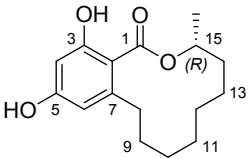
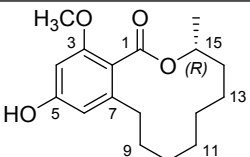
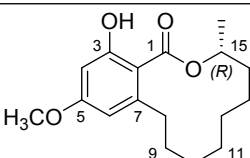
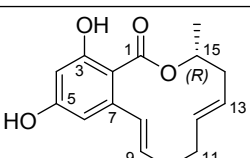
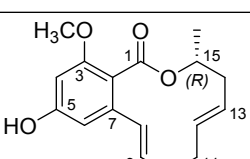
Table S4. Methylation of the model substrate DLD (1) with mutant LtOMT enzymes.

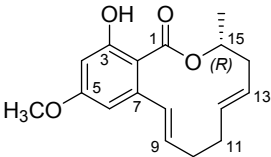
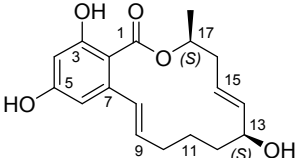
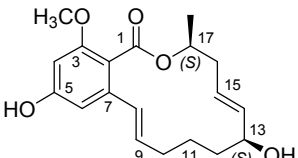
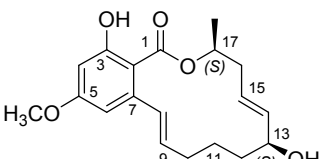
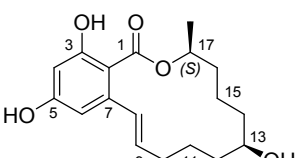
Mutant LtOMT enzyme	Mutation and/or replacement	Total conversion [%]	<i>o</i> -Methoxy product [%]	<i>p</i> -Methoxy product [%]	<i>o,p</i> -Dimethoxy product [%]
H1	1-329: HsOMT	3.8 ± 1.1	100	0	0
H2	330-398: HsOMT	26.1 ± 3.0	0	100	0
H3	366-398: HsOMT	34.5 ± 0.8	76.3 ± 0.9	23.7 ± 0.9	0
M1	Q384K, G386R, W387H, Q388H	90.0 ± 2.9	82.9 ± 0.8	3.7 ± 0.8	13.4 ± 1.5
M2	Q384K, W387H, Q388H	87.0 ± 1.1	65.1 ± 7.5	17.1 ± 5.8	17.8 ± 1.7
M3	W387H, Q388H	88.6 ± 5.6	69.8 ± 1.2	14.6 ± 0.9	15.7 ± 0.3
M4	W387H	76.6 ± 20.2	92.3 ± 0.3	0	7.7 ± 0.3
HM1	330-366: HsOMT, Q384K, G386R, W387H, Q388H	58.3 ± 11.4	0	100	0
M5	F330V, Q384K, G386R, W387H, Q388H	88.0 ± 14.0	70.9 ± 5.6	13.3 ± 5.6	15.8 ± 8.5
M6	T356M, Q384K, G386R, W387H, Q388H	70.1 ± 5.8	10.0 ± 1.9	74.3 ± 4.2	15.7 ± 3.1
M7	F330V, T356M, Q384K, G386R, W387H, Q388H	93.7 ± 1.1	2.9 ± 1.9	94.1 ± 1.0	3.0 ± 1.2
M8	T356M	80.1 ± 10.2	34.4 ± 6.3	31.3 ± 2.3	34.3 ± 8.5
M9	T356M, W387H	96.4 ± 0.7	7.0 ± 0.8	1.0 ± 0.1	92.0 ± 0.9
M10	G386R, W387H, Q388H	82.9 ± 8.0	80.7 ± 1.5	5.8 ± 0.3	13.5 ± 1.8
M11	Q384K, G386R, Q388H	90.0 ± 4.2	90.7 ± 0.2	0	9.3 ± 0.2
M12	Q384K, G386R,	74.7 ± 11.9	82.0 ± 2.4	2.7 ± 1.5	15.3 ± 1.0

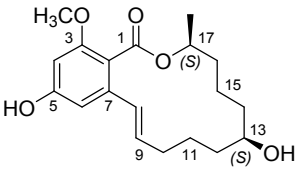
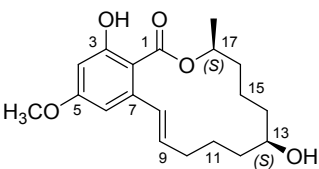
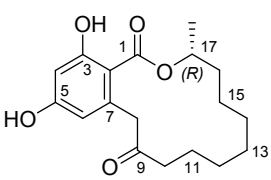
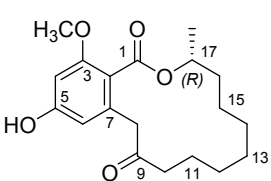
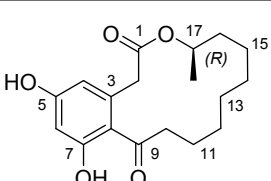
W387H					
M13	Q384K, G386R	81.2 ± 0.7	100	0	0
M14	Q384K, W387H	89.0 ± 0.1	92.2 ± 0.1	0	7.8 ± 0.1
M15	Q384K, Q388H	96.2 ± 0.1	100	0	0
M16	G386R, W387H	78.6 ± 12.7	84.7 ± 0.7	2.7 ± 0.6	12.6 ± 0.2
M17	G386R, Q388H	89.9 ± 2.0	89.8 ± 1.6	0	10.2 ± 1.6
M18	Q384K	92.7 ± 0.5	100	0	0
M19	G386R	93.0 ± 0.5	100	0	0
M20	Q388H	98.1 ± 0.1	100	0	0

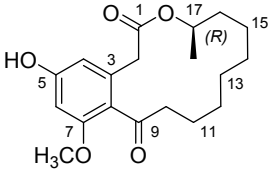
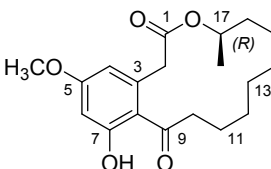
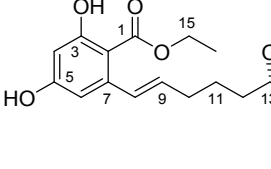
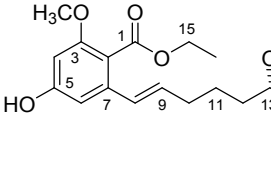
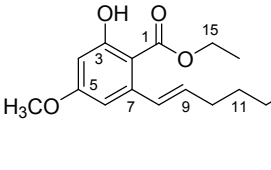
Total conversion: Numbers show the overall conversion percentage of the indicated substrate into all corresponding methylated products. *Individual products* are shown as their proportion amongst all three *O*-methylated product congeners (Yield of the individual product divided by the total yield of all products, multiplied by 100). Values represent the mean ± SD from three independent experiments of three replicates each (n=9).

Table S5. Combinatorial methylation with selected LtOMT variants.

Substrate	Chemical structure	Mutant OMT enzyme	Total conversion [%]	<i>o</i> -Methoxy product [%]	<i>p</i> -Methoxyproduct [%]	<i>o,p</i> -Dimethoxy product [%]
DLD 1		M1	90.0 ± 2.9	82.9 ± 0.8	3.7 ± 0.8	13.4 ± 1.5
		M6	70.1 ± 5.8	10.0 ± 1.9	74.3 ± 4.2	15.7 ± 3.1
		M7	93.7 ± 1.1	2.9 ± 1.9	94.1 ± 1.0	3.0 ± 1.2
		M8	80.1 ± 10.2	34.4 ± 6.3	31.3 ± 2.3	34.3 ± 8.5
		M9	96.4 ± 0.7	7.0 ± 0.8	1.0 ± 0.1	92.0 ± 0.9
1a		M1	0	NA	NA	NA
		M6	14.9 ± 0.7	NA	NA	100
		M7	15.0 ± 1.2	NA	NA	100
		M8	15.4 ± 2.7	NA	NA	100
		M9	74.7 ± 2.1	NA	NA	100
1b		M1	84.5 ± 2.4	NA	NA	100
		M6	19.7 ± 1.4	NA	NA	100
		M7	20.0 ± 1.1	NA	NA	100
		M8	69.6 ± 3.6	NA	NA	100
		M9	84.9 ± 3.2	NA	NA	100
RDN 2		M1	97.3 ± 1.0	94.5 ± 0.7	0	5.5 ± 0.7
		M6	93.9 ± 3.5	18.1 ± 3.6	15.7 ± 1.1	66.2 ± 3.3
		M7	94.2 ± 1.6	17.9 ± 1.8	21.1 ± 3.3	61.0 ± 1.5
		M8	96.6 ± 0.1	16.9 ± 2.3	0	83.1 ± 2.2
		M9	99.4 ± 0.1	5.1 ± 0.3	0	94.9 ± 0.3
2a		M1	0	NA	NA	NA
		M6	7.5 ± 0.6	NA	NA	100
		M7	7.2 ± 0.9	NA	NA	100
		M8	18.5 ± 1.1	NA	NA	100
		M9	48.0 ± 1.8	NA	NA	100

2b		M1	88.3 ± 0.9	NA	NA	100
		M6	71.8 ± 1.9	NA	NA	100
		M7	72.2 ± 4.5	NA	NA	100
		M8	83.2 ± 1.1	NA	NA	100
		M9	97.4 ± 0.3	NA	NA	100
DHZ 3		M1	92.1 ± 1.2	97.6 ± 0.1	1.3 ± 0.1	1.1 ± 0.1
		M6	54.0 ± 2.0	77.2 ± 0.9	4.7 ± 0.8	18.1 ± 0.7
		M7	63.8 ± 4.3	76.2 ± 3.0	4.3 ± 0.7	19.5 ± 2.4
		M8	80.5 ± 5.0	69.9 ± 1.5	1.5 ± 0.2	28.6 ± 1.5
		M9	99.7 ± 0.1	73.4 ± 0.6	0.5 ± 0.1	26.1 ± 0.7
3a		M1	0	NA	NA	NA
		M6	0	NA	NA	NA
		M7	0	NA	NA	NA
		M8	0	NA	NA	NA
		M9	0	NA	NA	NA
3b		M1	100	NA	NA	100
		M6	100	NA	NA	100
		M7	100	NA	NA	100
		M8	100	NA	NA	100
		M9	100	NA	NA	100
ZEA 4		M1	91.4 ± 0.7	94.6 ± 0.8	2.5 ± 0.4	2.9 ± 0.5
		M6	64.3 ± 0.5	90.6 ± 1.6	4.9 ± 0.8	4.5 ± 0.8
		M7	74.3 ± 1.4	91.5 ± 1.1	5.2 ± 0.8	3.3 ± 0.4
		M8	69.4 ± 0.7	92.6 ± 0.3	4.4 ± 0.3	3.0 ± 0.1
		M9	88.0 ± 1.7	93.1 ± 0.5	1.2 ± 0.1	5.7 ± 0.5

4a		M1	0	NA	NA	NA
		M6	0	NA	NA	NA
		M7	0	NA	NA	NA
		M8	0	NA	NA	NA
		M9	0	NA	NA	NA
4b		M1	94.7 ± 0.5	NA	NA	100
		M6	92.0 ± 0.1	NA	NA	100
		M7	92.7 ± 0.4	NA	NA	100
		M8	92.0 ± 0.3	NA	NA	100
		M9	95.7 ± 1.4	NA	NA	100
LCL 5		M1	12.8 ± 0.9	100	0	0
		M6	11.7 ± 0.5	100	0	0
		M7	11.5 ± 0.6	100	0	0
		M8	29.3 ± 2.8	100	0	0
		M9	59.9 ± 8.7	100	0	0
5a		M1	0	NA	NA	NA
		M6	0	NA	NA	NA
		M7	0	NA	NA	NA
		M8	0	NA	NA	NA
		M9	0	NA	NA	NA
LLN 6		M1	4.8 ± 0.5	74.3 ± 5.9	5.5 ± 5.7	20.2 ± 1.0
		M6	2.6 ± 1.0	55.2 ± 10.6	13.3 ± 11.6	31.5 ± 3.4
		M7	4.0 ± 0.6	51.2 ± 6.5	19.9 ± 4.1	28.9 ± 4.2
		M8	4.3 ± 0.4	36.3 ± 4.4	30.9 ± 6.2	32.8 ± 2.5
		M9	15.8 ± 1.4	61.5 ± 4.2	8.5 ± 1.0	30.0 ± 4.0

6a		M1	0	NA	NA	NA
		M6	4.1 ± 0.4	NA	NA	100
		M7	4.1 ± 0.2	NA	NA	100
		M8	3.5 ± 0.7	NA	NA	100
		M9	4.8 ± 0.3	NA	NA	100
6b		M1	5.9 ± 0.7	NA	NA	100
		M6	4.2 ± 0.5	NA	NA	100
		M7	4.0 ± 0.2	NA	NA	100
		M8	4.5 ± 0.6	NA	NA	100
		M9	5.0 ± 0.1	NA	NA	100
ARA7 7		M1	69.4 ± 1.2	93.7 ± 0.7	3.3 ± 0.6	3.0 ± 0.1
		M6	47.0 ± 1.3	14.1 ± 4.0	65.8 ± 5.2	20.1 ± 2.2
		M7	50.0 ± 0.8	11.3 ± 3.5	70.1 ± 6.9	18.7 ± 3.8
		M8	59.5 ± 2.6	23.9 ± 0.8	57.6 ± 1.1	18.4 ± 0.8
		M9	89.0 ± 2.8	82.1 ± 1.9	0.8 ± 0.2	17.2 ± 1.8
7a		M1	0	NA	NA	NA
		M6	0	NA	NA	NA
		M7	0	NA	NA	NA
		M8	0	NA	NA	NA
		M9	0	NA	NA	NA
7b		M1	81.8 ± 2.7	NA	NA	100
		M6	38.4 ± 4.0	NA	NA	100
		M7	55.5 ± 2.1	NA	NA	100
		M8	59.1 ± 4.1	NA	NA	100
		M9	93.4 ± 3.0	NA	NA	100

ARA8 8		M1	65.7 ± 2.7	92.4 ± 1.1	4.0 ± 0.8	3.6 ± 0.3
		M6	23.5 ± 0.9	2.4 ± 0.2	78.0 ± 1.3	19.6 ± 1.1
		M7	25.4 ± 0.8	2.9 ± 0.4	81.3 ± 2.9	15.9 ± 3.2
		M8	48.2 ± 0.7	13.2 ± 0.8	63.9 ± 3.1	23.0 ± 2.5
		M9	83.3 ± 0.9	73.8 ± 1.1	7.5 ± 0.6	18.7 ± 1.3
8a		M1	0	NA	NA	NA
		M6	0	NA	NA	NA
		M7	0	NA	NA	NA
		M8	0	NA	NA	NA
		M9	0	NA	NA	NA
8b		M1	94.8 ± 0.3	NA	NA	100
		M6	50.1 ± 1.0	NA	NA	100
		M7	51.7 ± 0.7	NA	NA	100
		M8	56.4 ± 1.3	NA	NA	100
		M9	95.8 ± 0.5	NA	NA	100

Total conversion: Numbers show the overall conversion percentage of the indicated substrate into all corresponding methylated products. *Individual products* are shown as their proportion amongst all three *O*-methylated product congeners (Yield of the individual product divided by the total yield of all products, multiplied by 100). Values represent the mean ± SD from three independent experiments of three replicates each (n=9). NA, not applicable. Compound **5b** (5-*O*-methyl LCL) is not produced by the LtOMT or HsOMT enzymes, thus it was not included as a substrate in these experiments.

Table S6. Primers used in this study.

Primer Name	Primer sequence (5'-3')	PCR Product (Size in bp)
pACYC- LtOMT_F	CGGAATTCGATGAGATCCTACTCATTGGA	LtOMT-EcoRI/NotI (1,216 bp)
pACYC- LtOMT_R	TAGCGGCCGCTTAACCTCTTTTCAATCTTG	
pACYC- HsOMT_F	CGGAATTCGATGTCTGCTTCTAATGGTGA	HsOMT- EcoRI/NotI (1,216 bp)
pACYC- HsOMT_R	TAGCGGCCGCTTAAGCTCTTTTAAATCTTG	
H1-1_F	AAGCTTCATATGTCTGCTTCTAATGGTGA	H1-1 (1,002 bp)
H1-1_R	ATCGAAAATCAATAATCTGGATGATGGACCCATAGCACC	
H1-2_F	TCCAGATTATTGATTTTCGATGCTG	H1-2 (243 bp)
H1-2_R	GGTGATGTCCGTTTAACTTAACCTC	
H2-1_F	CGACAAGCTTCATATGAGATCCTACTCA	H2-1 (1,006 bp)
H2-1_R	TTCGACAATCAACAACCTAGACTTTGG	
H2-2_F	TCTAGGTTGTTGATTGTCTGAAGCTG	H2-2 (243 bp)
H2-2_R	GGTGATGTCCGTTTAACTTAAGCTC	
H3-1_F	CGACAAGCTTCATATGAGATCCTACTC	H3-1 (1,108 bp)
H3-1_R	TTCTTTTTCAGTTCTTTCTTTACCACC	
H3-2_F	AAGAAAGAACTGAAAAAGAATTTGCAACTTTATTAGGTACAG	H3-1 (140 bp)
H3-2_R	GGTGATGTCCGTTTAACTTAAGCTC	
HM1-1_F	CGACAAGCTTCATATGAGATCCTACTC	HM1-1 (1,108 bp)
HM1-1_R	TTCTTTTCTGTCTTTCTTTACCACC	
HM1-2_F	AAGAAAGAACAGAAAAAGAAACCGCTGCTTTGTTGGATGCTG	HM1-1 (140 bp)
HM1-2_R	GGTGATGTCCGTTTAACTTAACCTC	
M2-1_F	CGACAAGCTTCATATGAGATCCTACTC	M2-1 (1,180 bp)
M2-1_R	ACCATGATGACCTGCCTTACCATG	
M2-2_F	GGTAAGGCAGGTCATCATGGTGTT	M2-2 (696 bp)
M2-2_R	AAACCGTCTATCAGGGCGATG	
M3-1_F	CGACAAGCTTCATATGAGATCCTACTC	M3-1 (1,186 bp)
M3-1_R	AATAACACCATGATGACCTGCTTGACCATGCCAACTCTAAC	
M3-2_F	AGAGTTTGCCATGGTCAAGCAGGTCATCATGGTGTTATTGAAGC	M3-2 (708 bp)
M3-2_R	AAACCGTCTATCAGGGCGATG	
M4-1_F	CGACAAGCTTCATATGAGATCCTACTC	M4-1 (1,183 bp)
M4-1_R	TTCAATAACACCTTGATGACCAGCTTGACCATGCCAAA	
M4-2_F	CATGGTCAAGCTGGTCATCAAGGTGTTATTGAAGCAAG	M4-2

M4-2_R	AAACCGTCTATCAGGGCGATG	(699 bp)
M5-1_F	CGACAAGCTTCATATGAGATCCTACTC	M5-1
M5-1_R	GAATAACAGCATCGACAATCAATA	(993 bp)
M5-2_F	TTATTGATTGTCGATGCTGTTATTC	M5-2
M5-2_R	GGTGATGTCCGTTTAACTTAACCTC	(237 bp)
M6-1_F	CGACAAGCTTCATATGAGATCCTACTC	M6-1
M6-1_R	TCTTTCTTTACCACCCATAGCCAAACCAACGATATCGAT	(1,096 bp)
M6-2_F	ATCGTTGGTTTGGCTATGGGTGGTAAAGAAAGAACTGAA	M6-2
M6-2_R	GGTGATGTCCGTTTAACTTAACCTC	(165 bp)
M7-1_F	CGACAAGCTTCATATGAGATCCTACTC	M6-1
M7-1_R	TCTTTCTTTACCACCCATAGCCAAACCAACGATATCGAT	(1,096 bp)
M7-2_F	ATCGTTGGTTTGGCTATGGGTGGTAAAGAAAGAACTGAA	M6-2
M7-2_R	GGTGATGTCCGTTTAACTTAACCTC	(165 bp)
M8-1_F	CGACAAGCTTCATATGAGATCCTACTC	M6-1
M8-1_R	TCTTTCTTTACCACCCATAGCCAAACCAACGATATCGAT	(1,096 bp)
M8-2_F	ATCGTTGGTTTGGCTATGGGTGGTAAAGAAAGAACTGAA	M6-2
M8-2_R	GGTGATGTCCGTTTAACTTAACCTC	(165 bp)
M9-1_F	CGACAAGCTTCATATGAGATCCTACTC	M4-1
M9-1_R	TTCAATAACACCTTGATGACCAGCTTGACCATGCCAAA	(1,183 bp)
M9-2_F	CATGGTCAAGCTGGTCATCAAGGTGTTATTGAAGCAAG	M4-2
M9-2_R	AAACCGTCTATCAGGGCGATG	(699 bp)
M10-1_F	CGACAAGCTTCATATGAGATCCTACTC	M10-1
M10-1_R	ACCATGATGTCTTGCTTGACCATG	(1,180 bp)
M10-2_F	GGTCAAGCAAGACATCATGGTGTT	M10-2
M10-2_R	AAACCGTCTATCAGGGCGATG	(696 bp)
M11-1_F	CGACAAGCTTCATATGAGATCCTACTC	M11-1
M11-1_R	ACCATGCCATCTTGCCTTACCATG	(1,180 bp)
M11-2_F	GGTAAGGCAAGATGGCATGGTGTT	M11-2
M11-2_R	AAACCGTCTATCAGGGCGATG	(696 bp)
M12-1_F	CGACAAGCTTCATATGAGATCCTACTC	M12-1
M12-1_R	ACCTTGATGTCTTGCCTTACCATG	(1,180 bp)
M12-2_F	GGTAAGGCAAGACATCAAGGTGTT	M12-2
M12-2_R	AAACCGTCTATCAGGGCGATG	(696 bp)
M13-1_F	CGACAAGCTTCATATGAGATCCTACTC	M13-1
M13-1_R	TGCTTCAATAACACCTTGCCATCTTGCCTTACCATGCCA	(1,192 bp)
M13-2_F	CATGGTAAGGCAAGATGGCAAGGTGTTATTGAAGCAAGA	M13-2
M13-2_R	AAACCGTCTATCAGGGCGATG	(699 bp)
M14-1_F	CGACAAGCTTCATATGAGATCCTACTC	M14-1
M14-1_R	TGCTTCAATAACACCTTGATGACCTGCCTTACCATGCCAAAC	(1,192 bp)

M14-2_F	TGGCATGGTAAGGCAGGTCATCAAGGTGTTATTGAAGCAAGA	M14-2
M14-2_R	AAACCGTCTATCAGGGCGATG	(702 bp)
M15-1_F	CGACAAGCTTCATATGAGATCCTACTC	M15-1
M15-1_R	TTCAATAACACCATGCCAACCTGCCTTACCATGCCAAAC	(1,189 bp)
M15-2_F	TGGCATGGTAAGGCAGGTTGGCATGGTGTATTGAAGCA	M15-2
M15-2_R	AAACCGTCTATCAGGGCGATG	(702 bp)
M16-1_F	CGACAAGCTTCATATGAGATCCTACTC	M16-1
M16-1_R	TGCTTCAATAACACCTTGATGTCTTGCTTGACCATGCCAAACTCTA AC	(1,192 bp)
M16-2_F	AGAGTTTGGCATGGTCAAGCAAGACATCAAGGTGTTATTGAAGCA AGATTG	M16-2
M16-2_R	AAACCGTCTATCAGGGCGATG	(708 bp)
M17-1_F	CGACAAGCTTCATATGAGATCCTACTC	M17-1
M17-1_R	TTCAATAACACCATGCCATCTTGCTTGACCATGCCAAACTCTAAC	(1,192 bp)
M17-2_F	AGAGTTTGGCATGGTCAAGCAAGATGGCATGGTGTATTGAAGCA AG	M17-2
M17-2_R	AAACCGTCTATCAGGGCGATG	(708 bp)
M18-1_F	CGACAAGCTTCATATGAGATCCTACTC	M18-1
M18-1_R	ACCTTGCCAACCAGCCTTACCATGCCAAACTCTAACAA	(1,180 bp)
M18-2_F	AGAGTTTGGCATGGTAAGGCTGGTTGGCAAGGTGTTAT	M18-2
M18-2_R	AAACCGTCTATCAGGGCGATG	(708 bp)
M19-1_F	CGACAAGCTTCATATGAGATCCTACTC	M19-1
M19-1_R	AATAACACCTTGCCATCTAGCTTGACCATGCCAAACTC	(1,186 bp)
M19-2_F	TGGCATGGTCAAGCTAGATGGCAAGGTGTTATTGAAGC	M19-2
M19-2_R	AAACCGTCTATCAGGGCGATG	(702 bp)
M20-1_F	CGACAAGCTTCATATGAGATCCTACTC	M20-1
M20-1_R	TGCTTCAATAACACCATGCCAACCAGCTTGACCATGCC	(1,192 bp)
M20-2_F	GGTCAAGCTGGTTGGCATGGTGTATTGAAGCAAGATT	M20-2
M20-2_R	AAACCGTCTATCAGGGCGATG	(696 bp)

3 SI Figures.

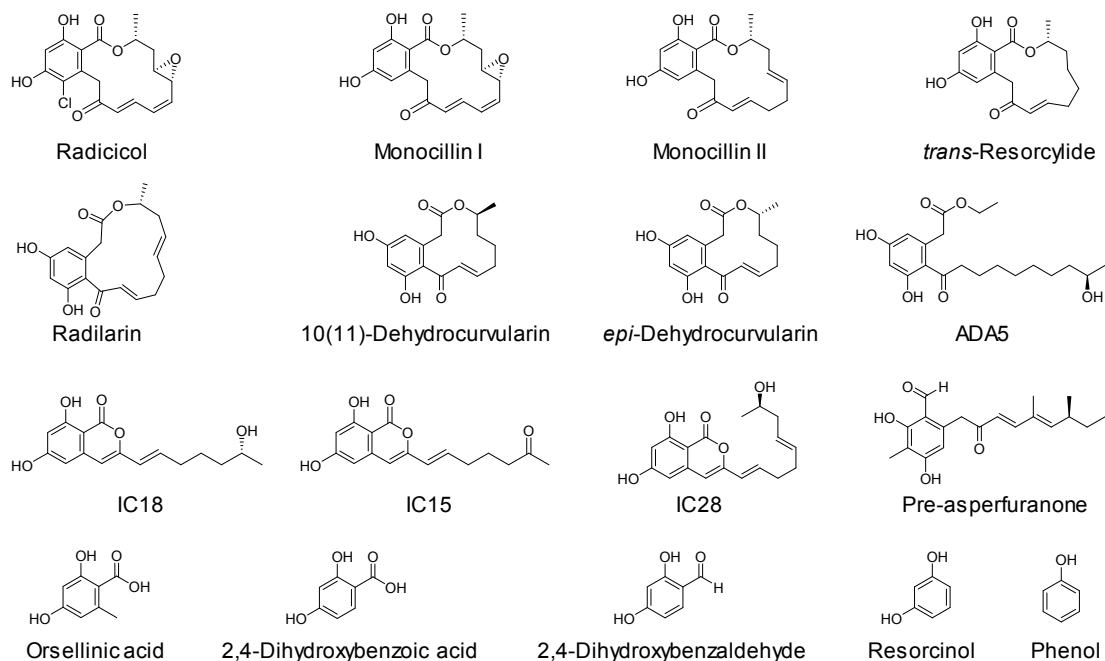
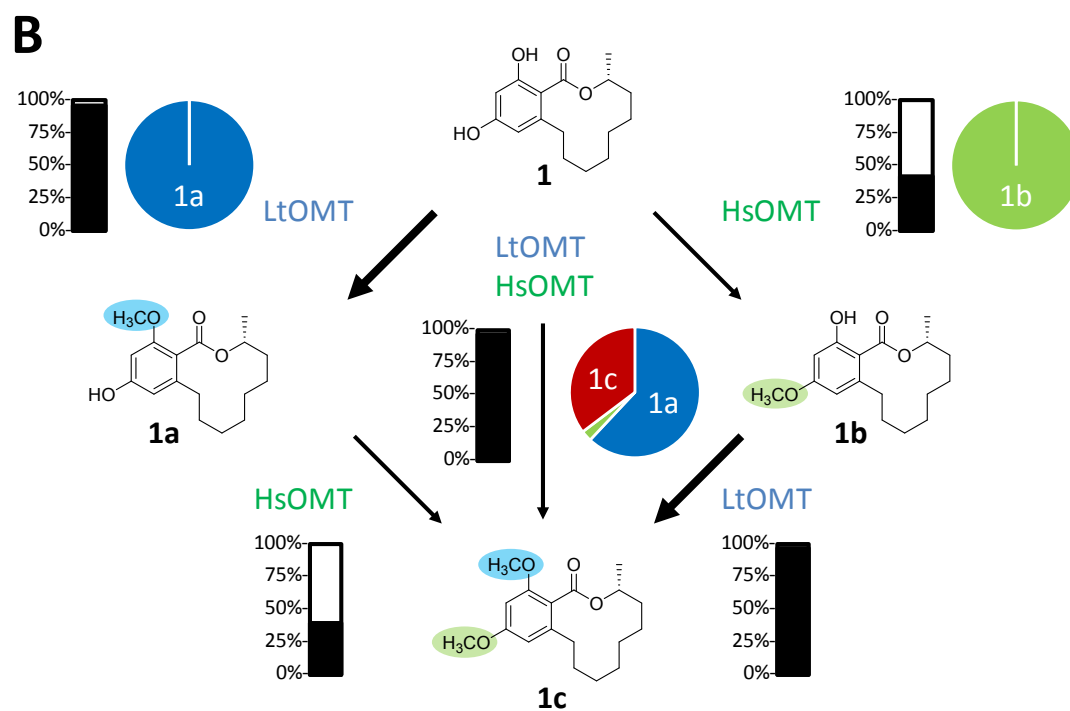
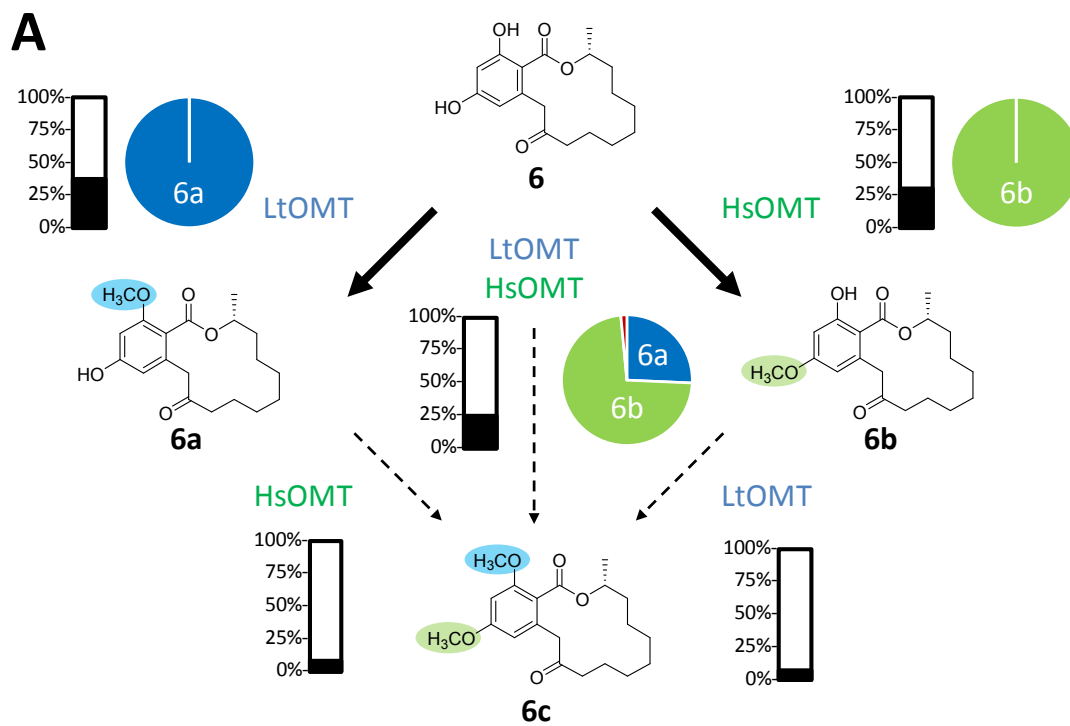
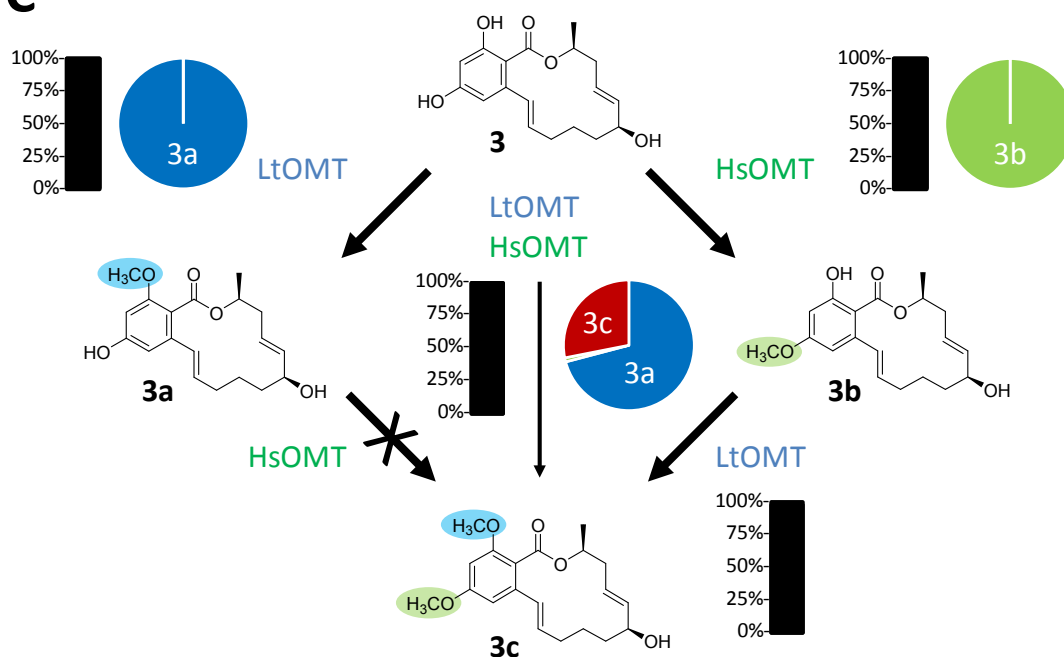


Figure S1. Compounds not accepted as substrates by LtOMT and HsOMT.



C



D

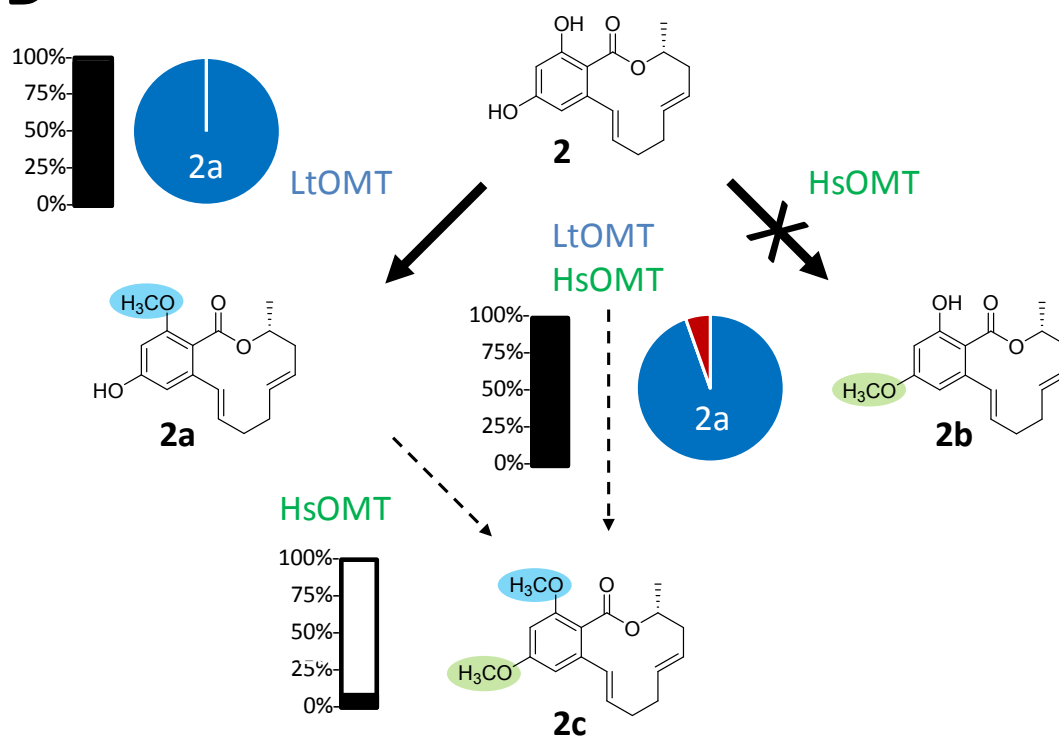


Figure S2. Influence of preexisting methylation on the activities of LtOMT and HsOMT.

Unmethylated compounds were fed to cultures of *Saccharomyces cerevisiae* BJ5464-NpgA co-expressing LtOMT and HsOMT, or LtOMT and HsOMT separately. *o*-Methoxy or *p*-methoxy compounds were fed to cultures of *Saccharomyces cerevisiae* BJ5464-NpgA expressing HsOMT or LtOMT separately. *Bars* show the overall conversion percentage of the indicated substrate into all corresponding methylated products. *Pie charts* show the distribution of *O*-methylated product congeners (Yields of the individual products divided by the total yield of all products, multiplied by 100). See Table S3 for tabulated percent conversion values as the mean \pm SD from three independent experiments of three replicates each (n=9). **A.** LCL (**6**) is converted at moderate efficiency to **6a** by LtOMT and to **6b** by HsOMT, with small additional amounts of the *o,p*-dimethoxy product **6c** also forming when both LtOMT and HsOMT are present. *O*-methylated congeners **6a** or **6b** can be converted at low efficiency to **6c** by HsOMT or LtOMT, respectively. **B.** LtOMT converts DLD (**1**) to the *O*-methylated product **1a** efficiently. Conversion of DLD (**1**) by HsOMT to **1b** occurs at moderate levels. In the presence of both LtOMT and HsOMT, **1a** and **1c** are the main products. The *o,p*-dimethoxy congener **1c** can also be produced by HsOMT from **1a** at moderate efficiency, and from **1b** by LtOMT at high efficiency. **C.** DHZ (**3**) is efficiently converted to **3a** or **3b** by LtOMT or HsOMT, respectively. In the presence of both enzymes, **3a** and **3c** are the main products. The *o*-methoxy congener **3a** is not a substrate for HsOMT, while **3b** is efficiently converted to **3c** by LtOMT. **D.** RDN (**2**) is efficiently converted to **2a** by LtOMT. However, RDN (**2**) is not a substrate for HsOMT, thus the *p*-methoxy congener **2b** is not produced. In the presence of both enzymes, **2a** forms efficiently.

A small amount of the *o,p*-dimethoxy product **2c** is also produced, since the *o*-methoxy congener **2a** is a marginal substrate for HsOMT.”

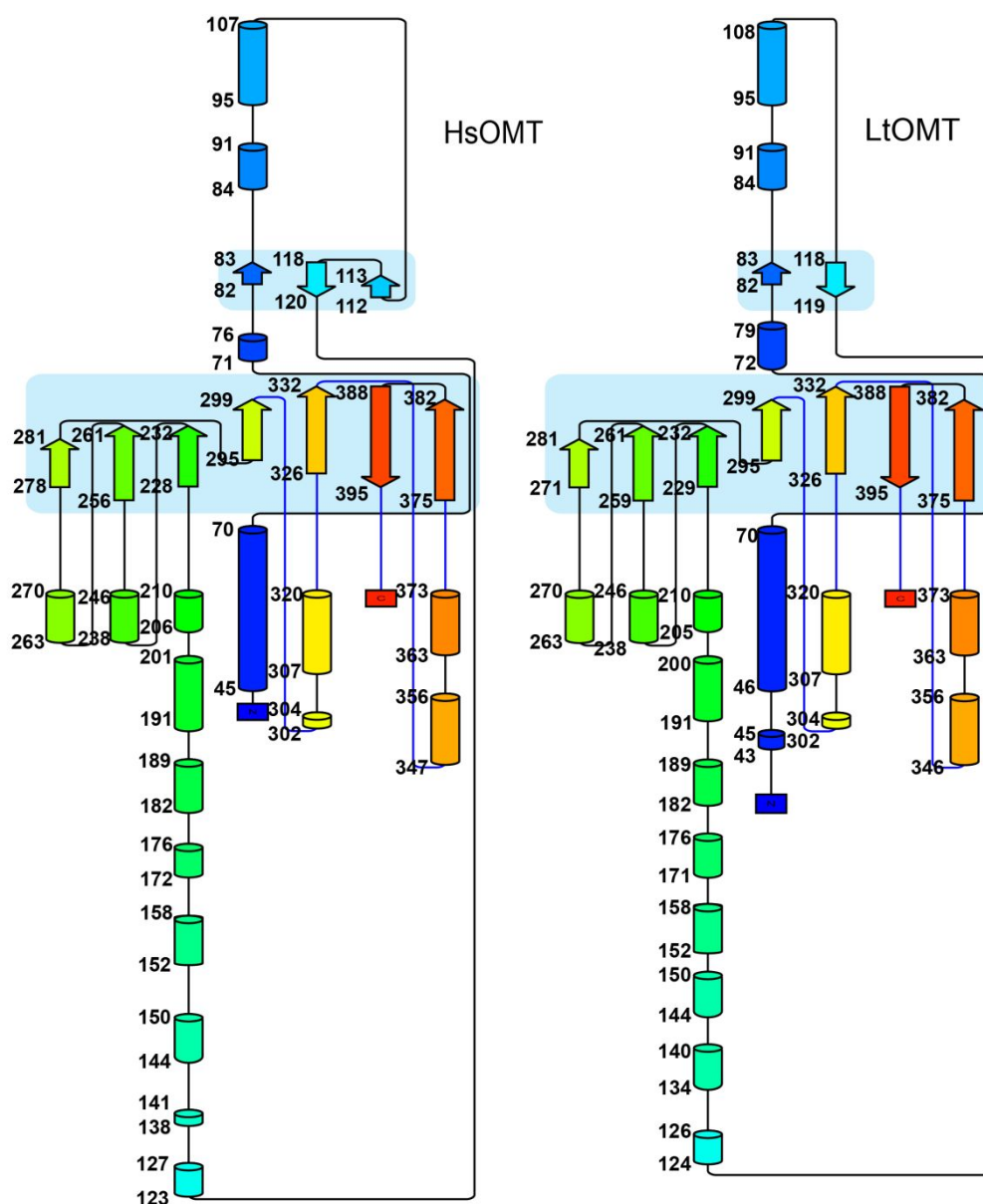


Figure S3. Topology of LtOMT and HsOMT.

β -strands are shown as *arrows*, α -helices indicated as *cylinders*, β -sheets are highlighted by *blue boxes*. Structural elements are colored as a gradient starting at the *N*-terminus (*dark blue*) and ending at the *C*-terminus (*red*). Amino acid residues at the start and at the end of each structural element are labeled by their residue number. The figure was generated using the Pro-Origami server (<http://munk.csse.unimelb.edu.au/pro-origami/>).

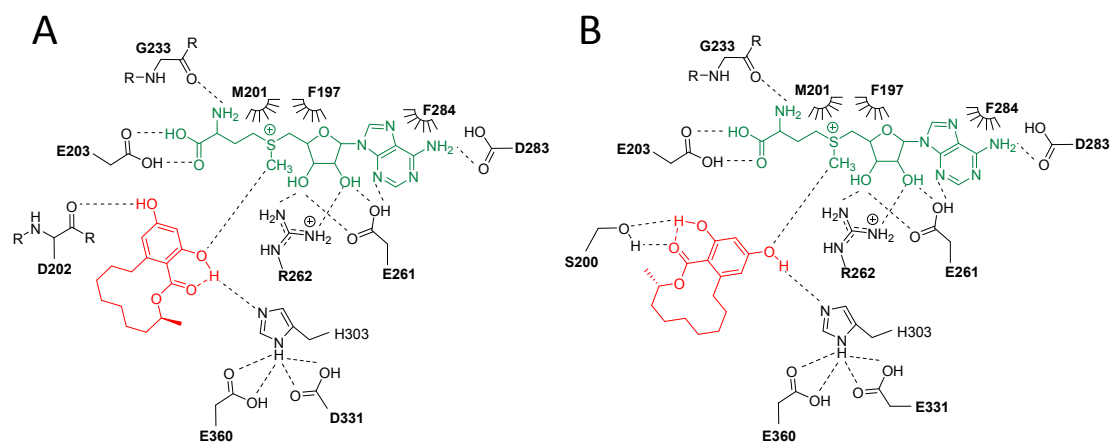


Figure S4. Docking models of DLD and SAM for LtOMT and HsOMT.

Predicted polar and hydrophobic interactions for *S*-adenosyl-methionine (SAM, in *green*), and polar interactions for DLD 1 (in *red*), with **A.** LtOMT, and **B.** HsOMT.

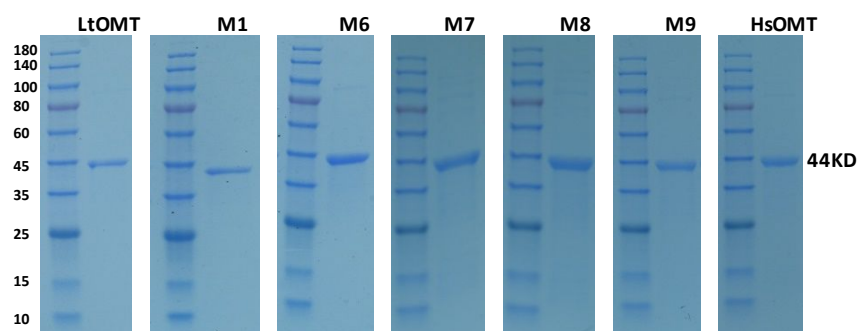


Figure S5. SDS-PAGE analysis of purified methyltransferases.

Recombinant methyltransferase enzymes were expressed as soluble ~44 kDa His-tagged proteins in *E. coli* Arctic Express (DE3) RIL cells and purified to substantial homogeneity as described in the SI Materials and Methods.

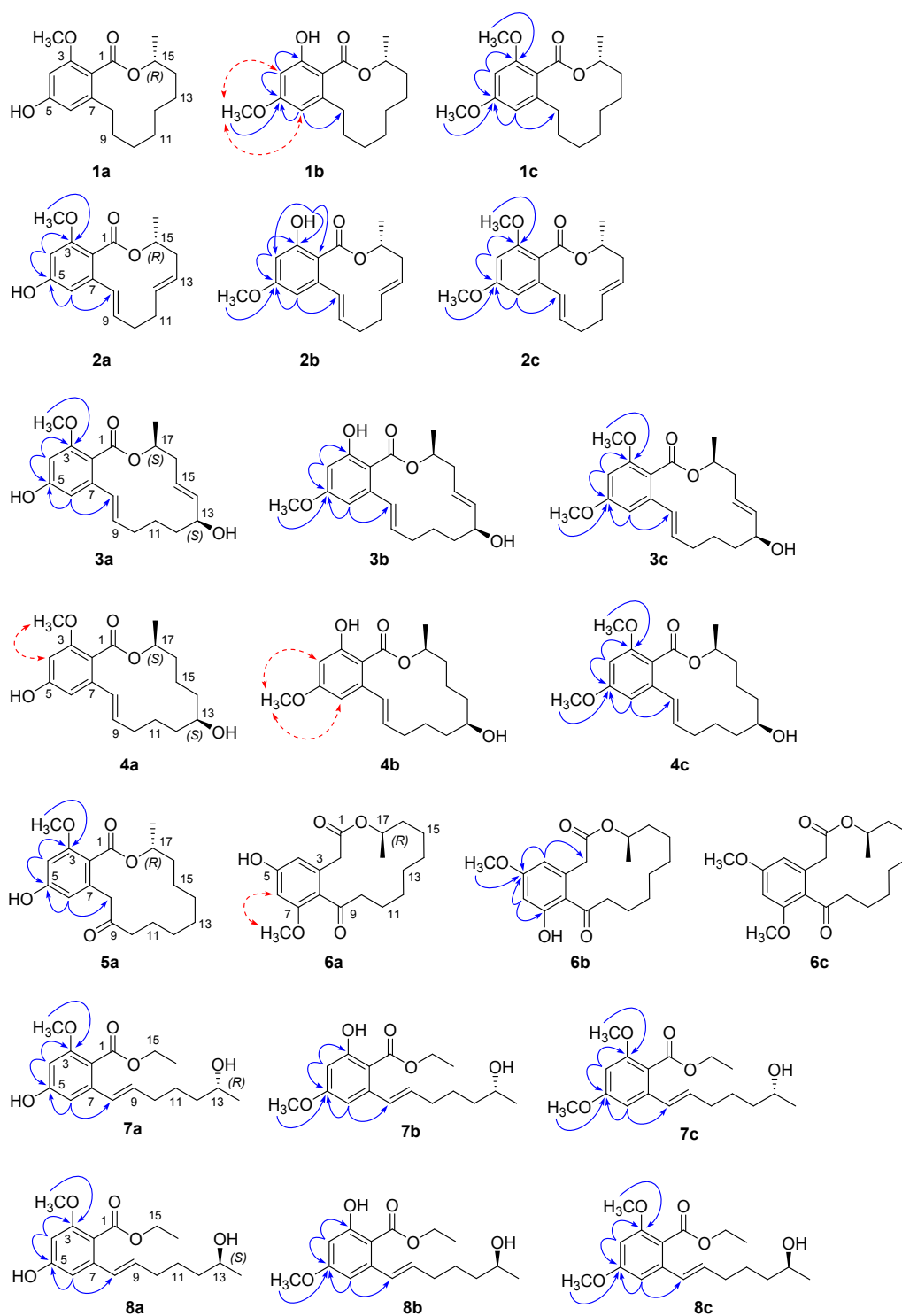


Figure S6. Chemical structures and key HMBC (\rightarrow) and NOE (\dashrightarrow) correlations of isolated compounds.

Figure S7. NMR spectra.

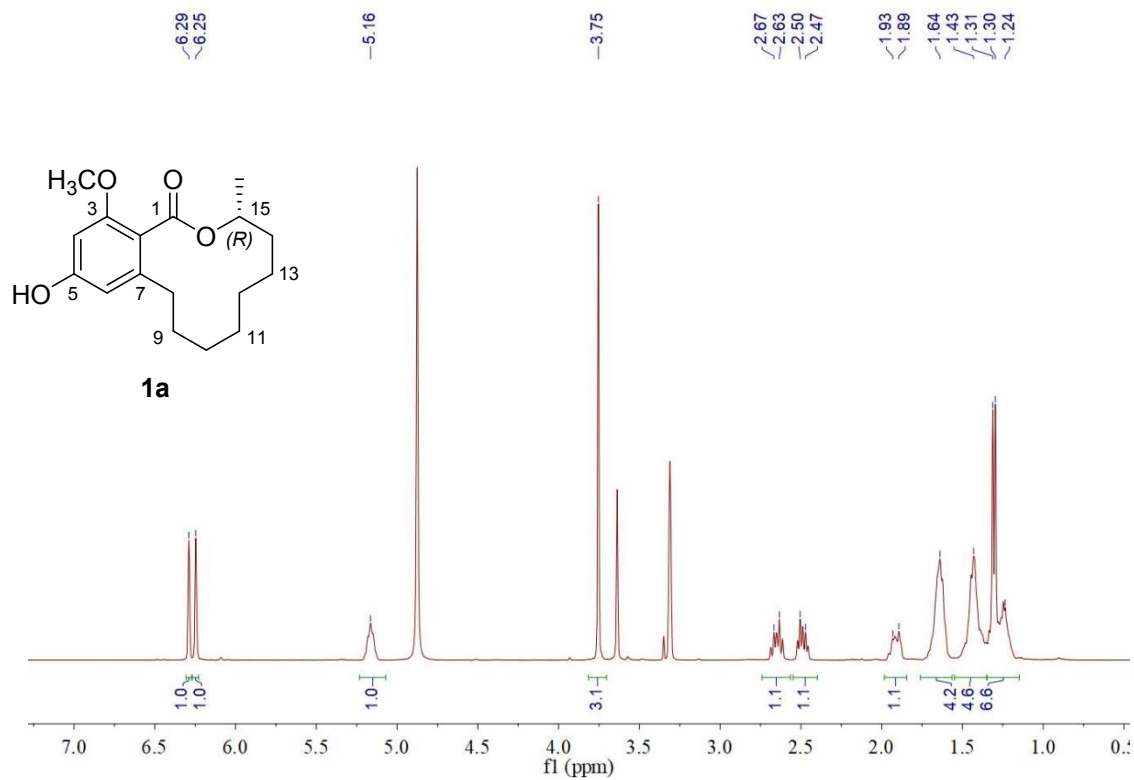


Figure S7.1. ¹H NMR spectrum of compound 1a in methanol-*d*₄

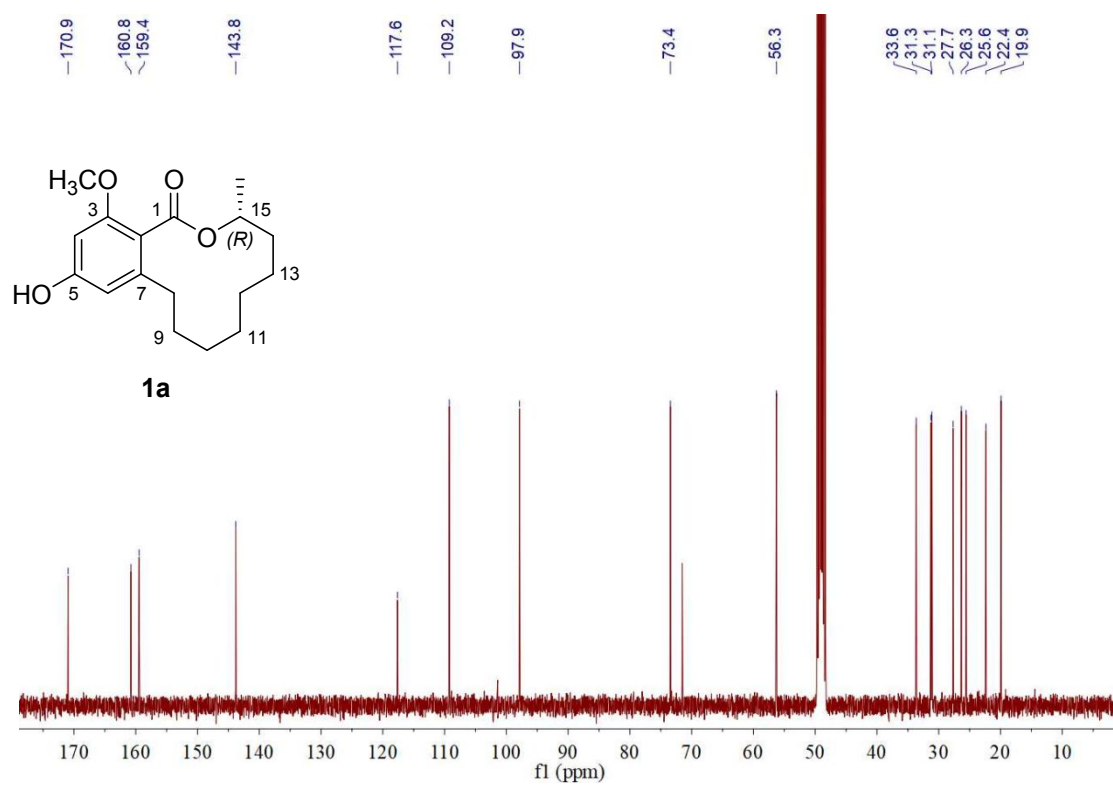


Figure S7.2. ¹³C NMR spectrum of compound **1a** in methanol-*d*₄

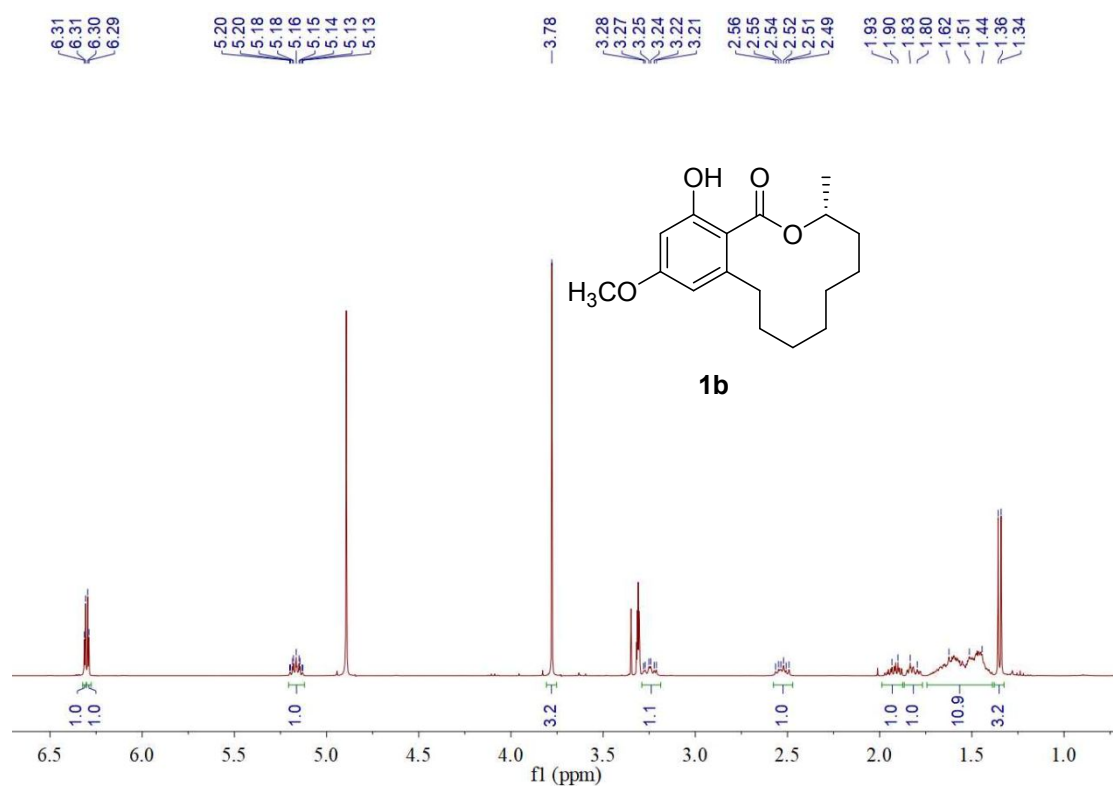


Figure S7.3. ¹H NMR spectrum of compound **1b** in methanol-*d*₄

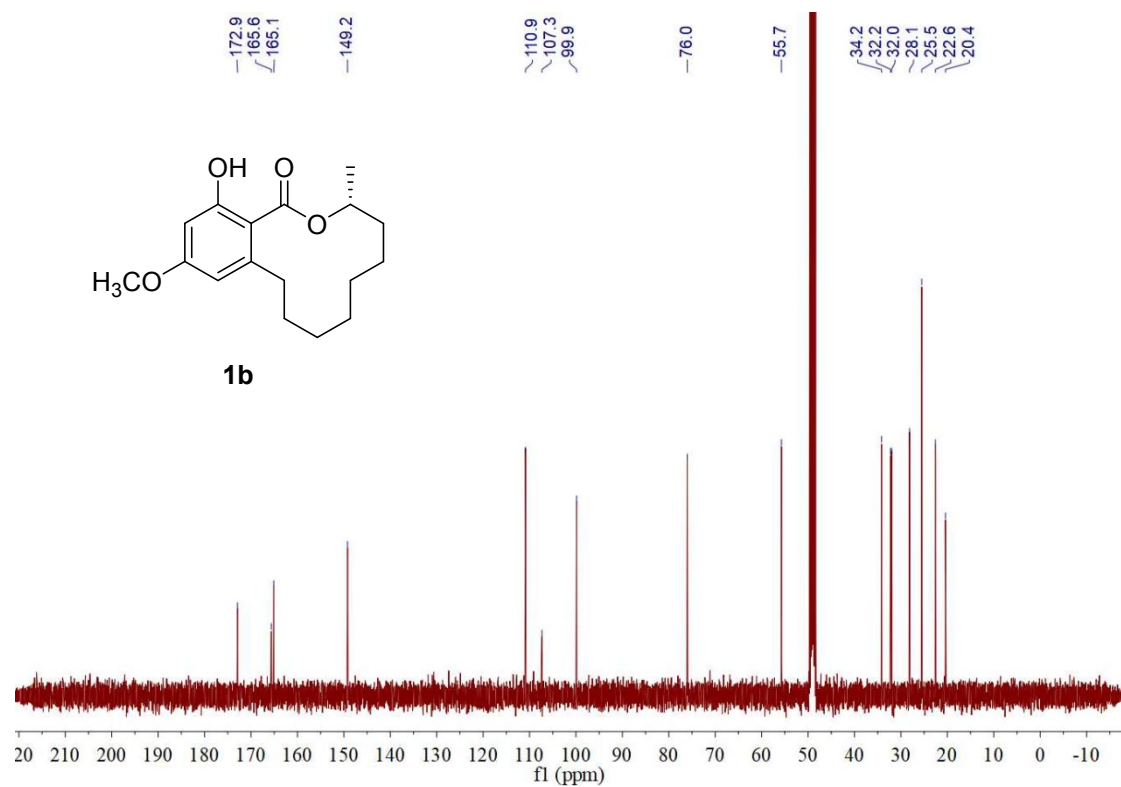


Figure S7.4. ^{13}C NMR spectrum of compound **1b** in methanol- d_4

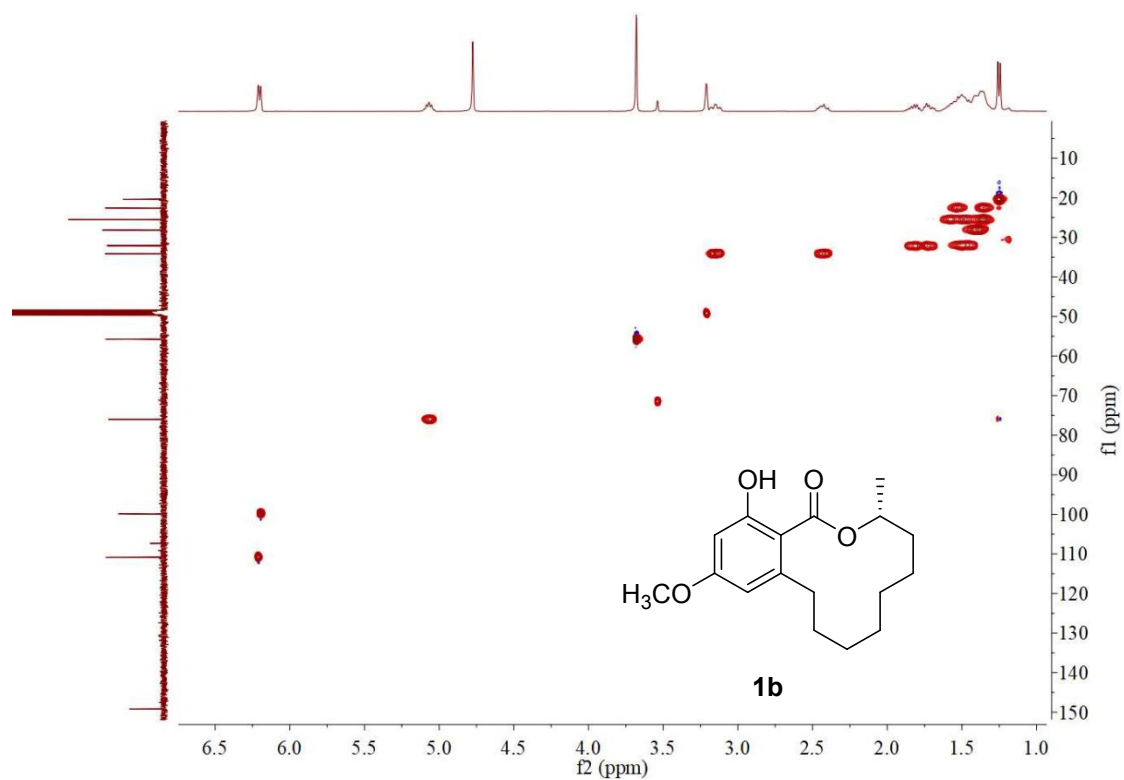


Figure S7.5. HSQC spectrum of compound **1b** in methanol- d_4

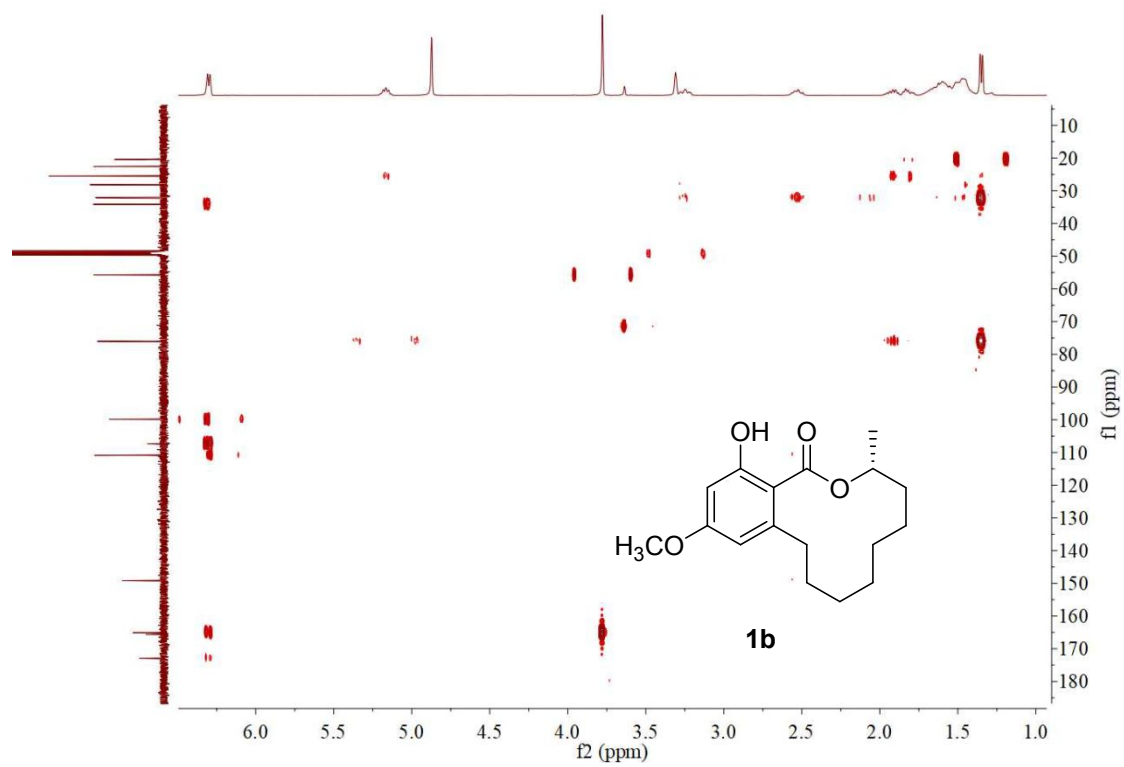


Figure S7.6. HMBC spectrum of compound **1b** in methanol- d_4

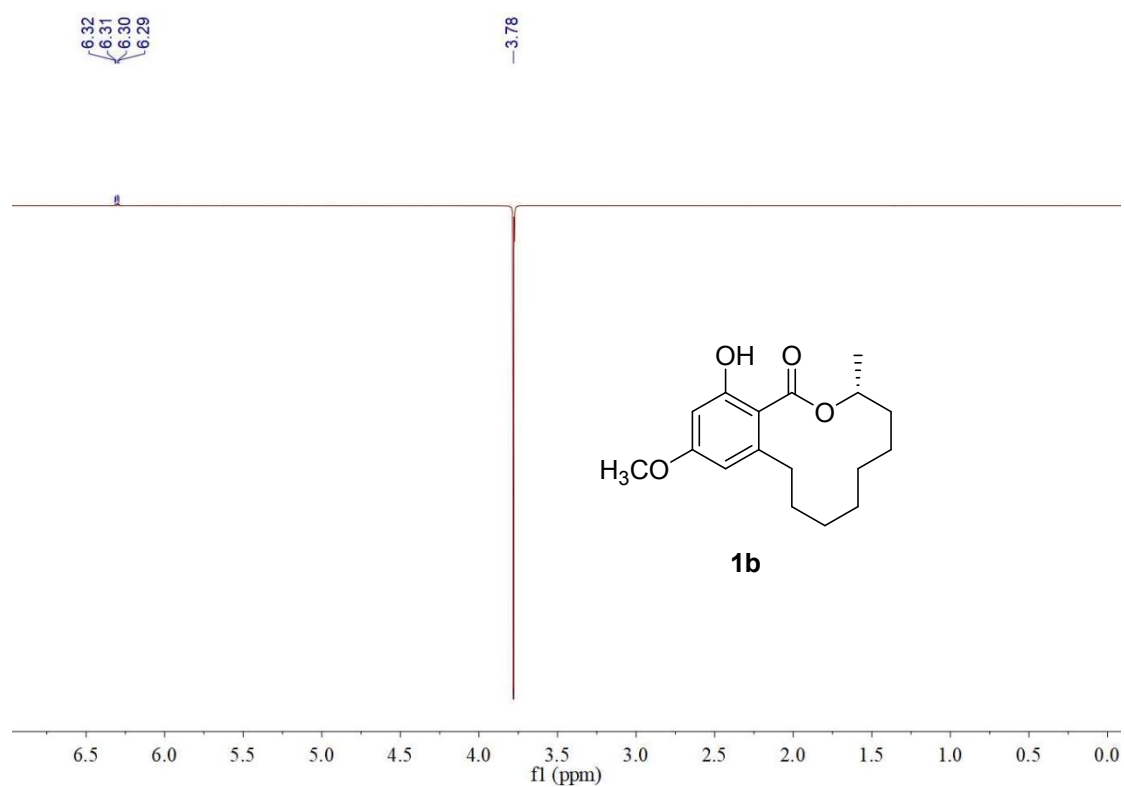


Figure S7.7. 1D NOESY spectrum of compound **1b** in methanol-*d*₄

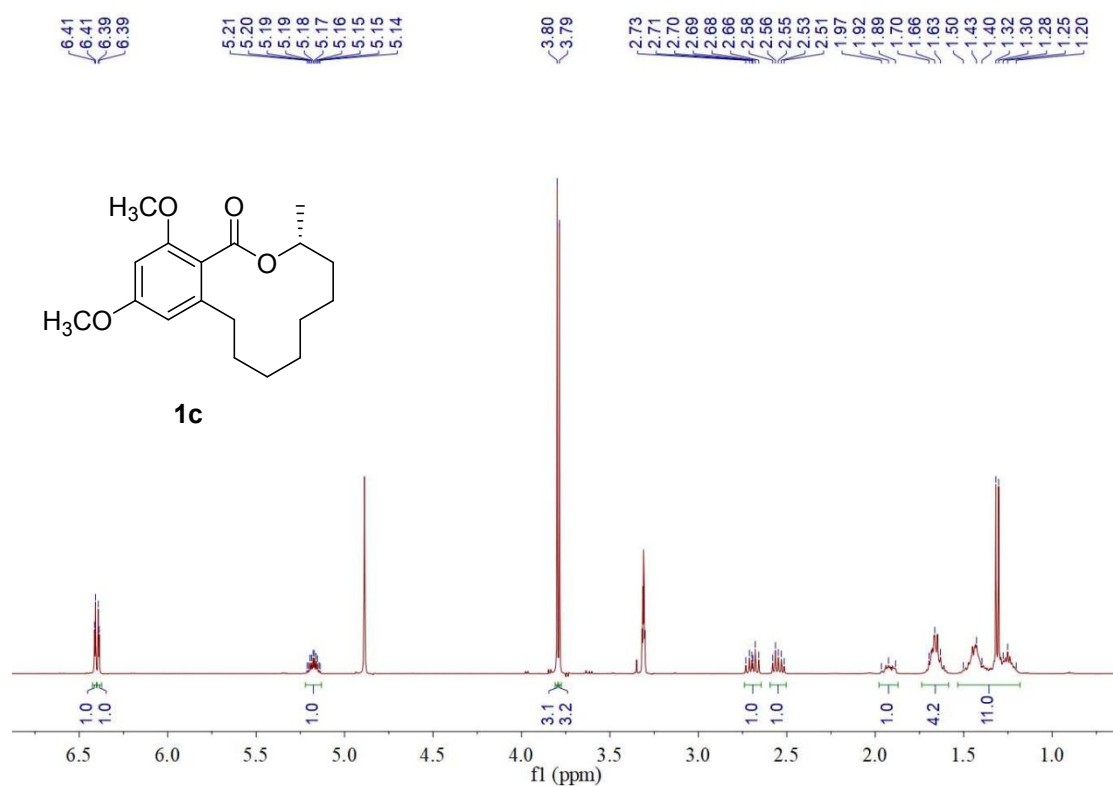


Figure S7.8. ¹H NMR spectrum of compound **1c** in methanol-*d*₄

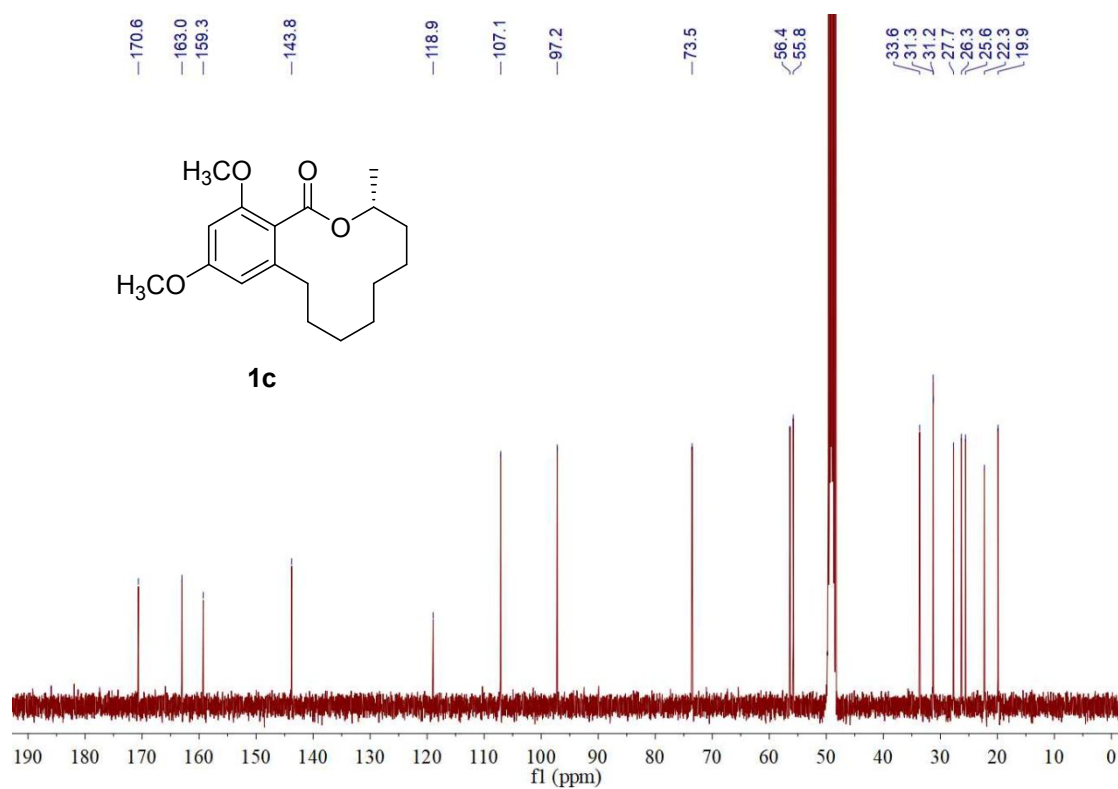


Figure S7.9. ¹³C NMR spectrum of compound **1c** in methanol-*d*₄

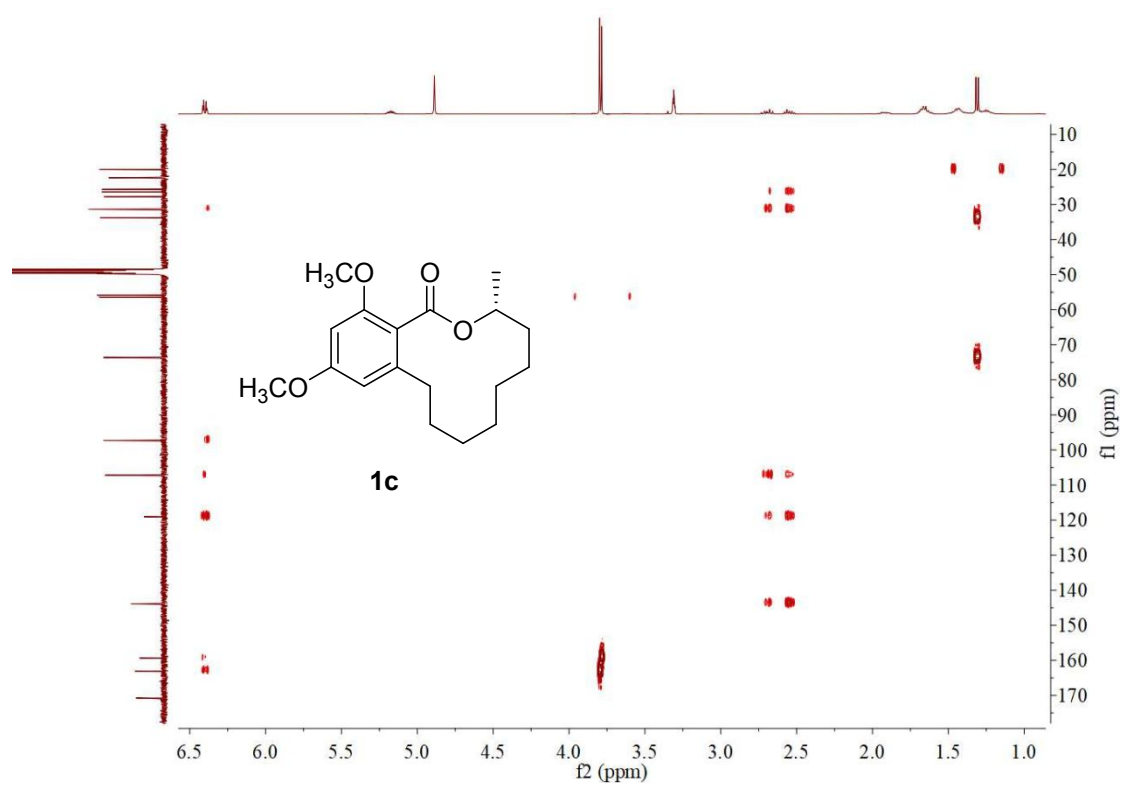


Figure S7.10. HMBC spectrum of compound **1c** in methanol- d_4

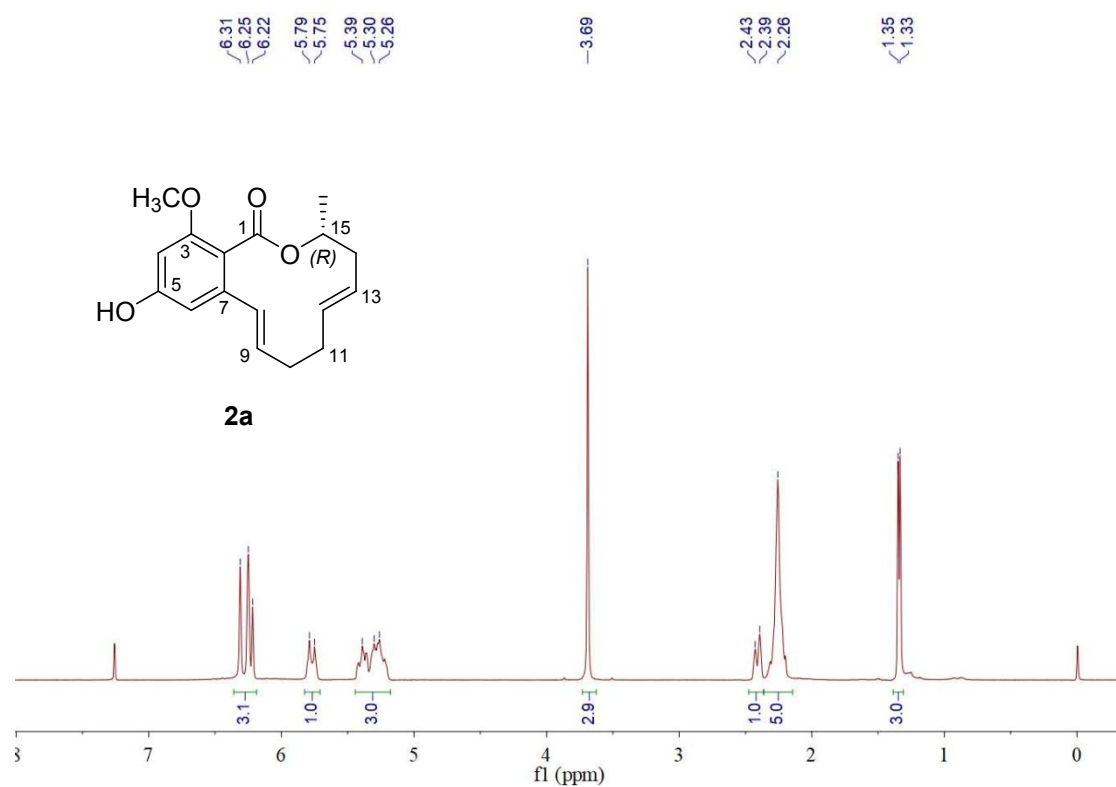


Figure S7.11. ¹H NMR spectrum of compound **2a** in CDCl₃

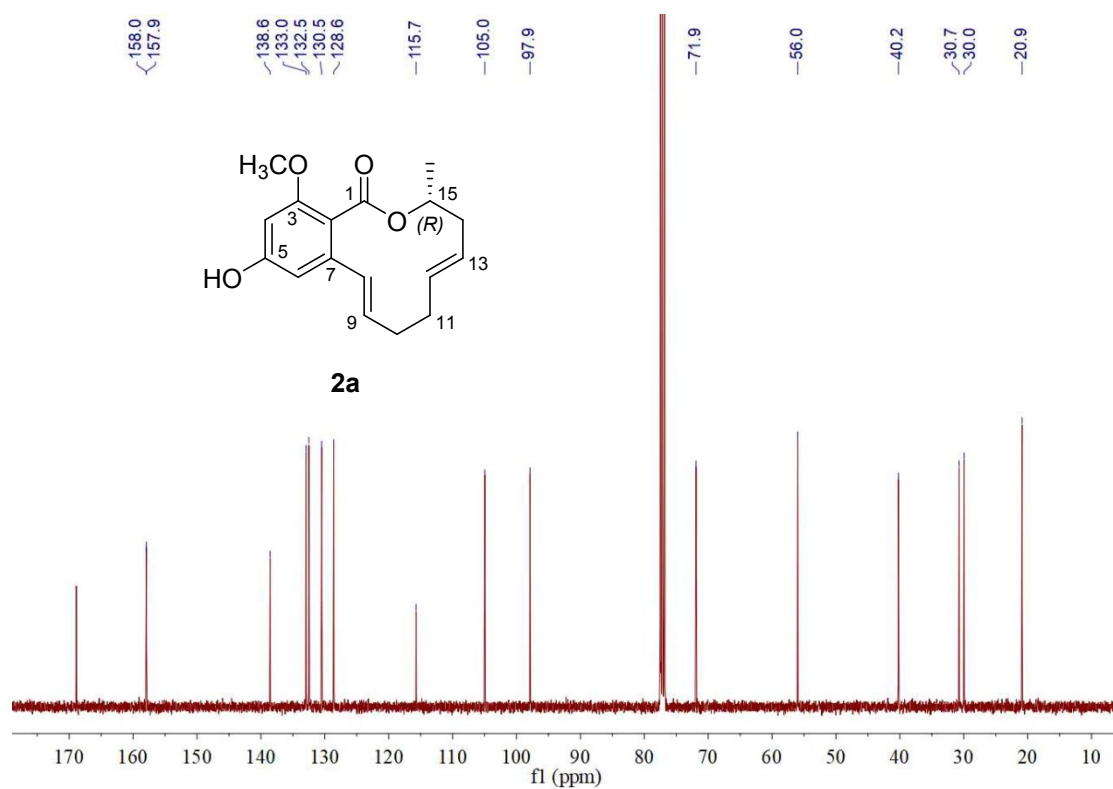


Figure S7.12. ¹³C NMR spectrum of compound **2a** in CDCl₃

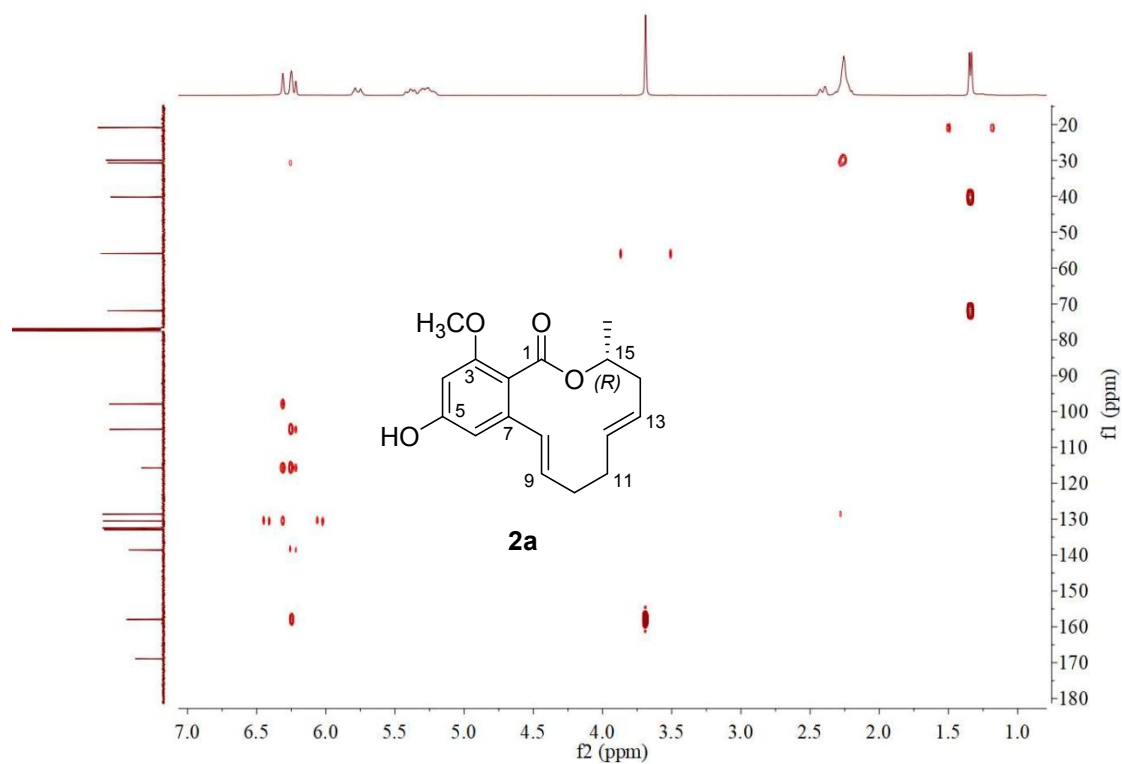


Figure S7.13. HMBC spectrum of compound **2a** in CDCl_3

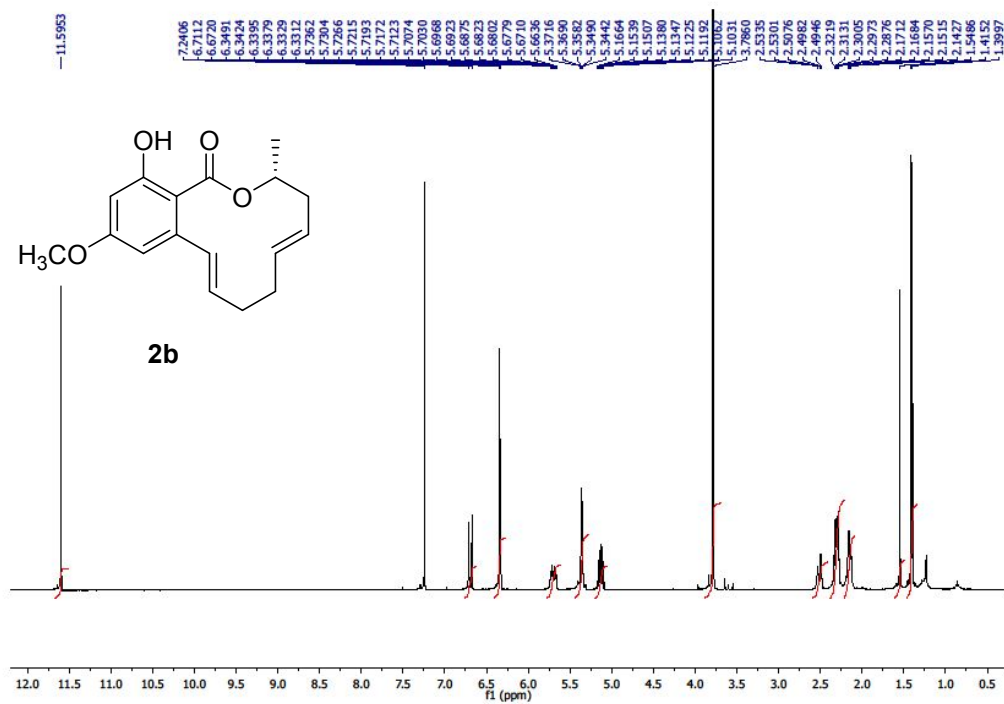


Figure S7.14. ^1H NMR spectrum of compound **2b** in CDCl_3

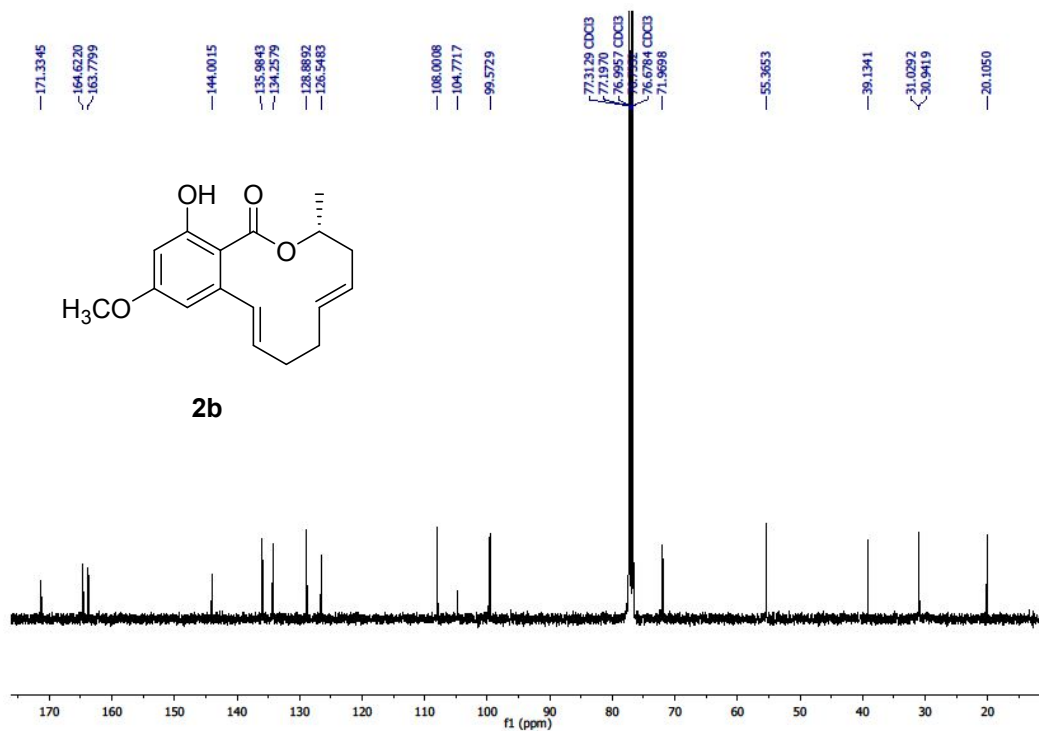


Figure S7.15. ^{13}C NMR spectrum of compound **2b** in CDCl₃

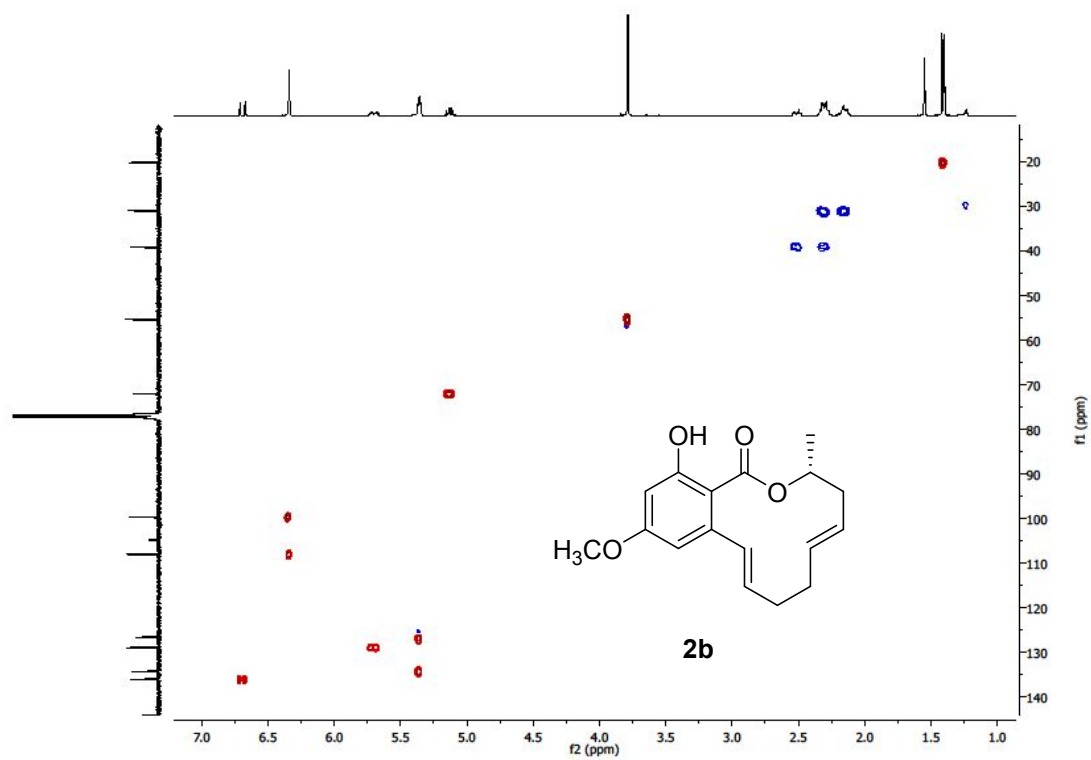


Figure S7.16. HSQC spectrum of compound **2b** in CDCl_3

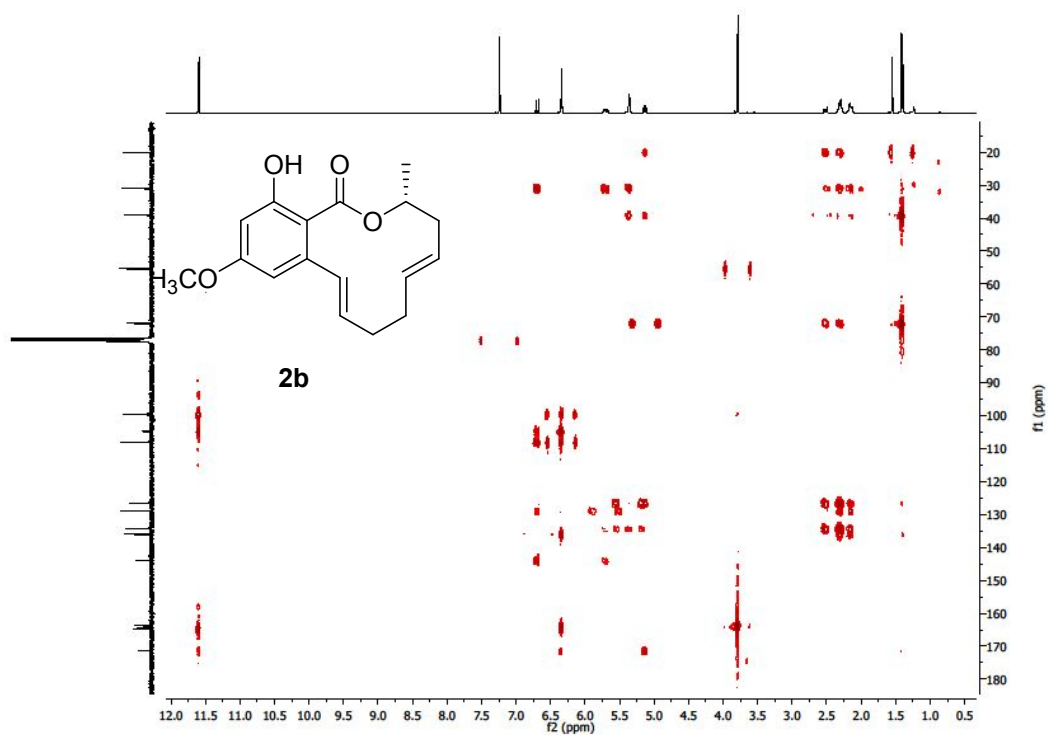


Figure S7.17. HMBC spectrum of compound **2b** in CDCl_3

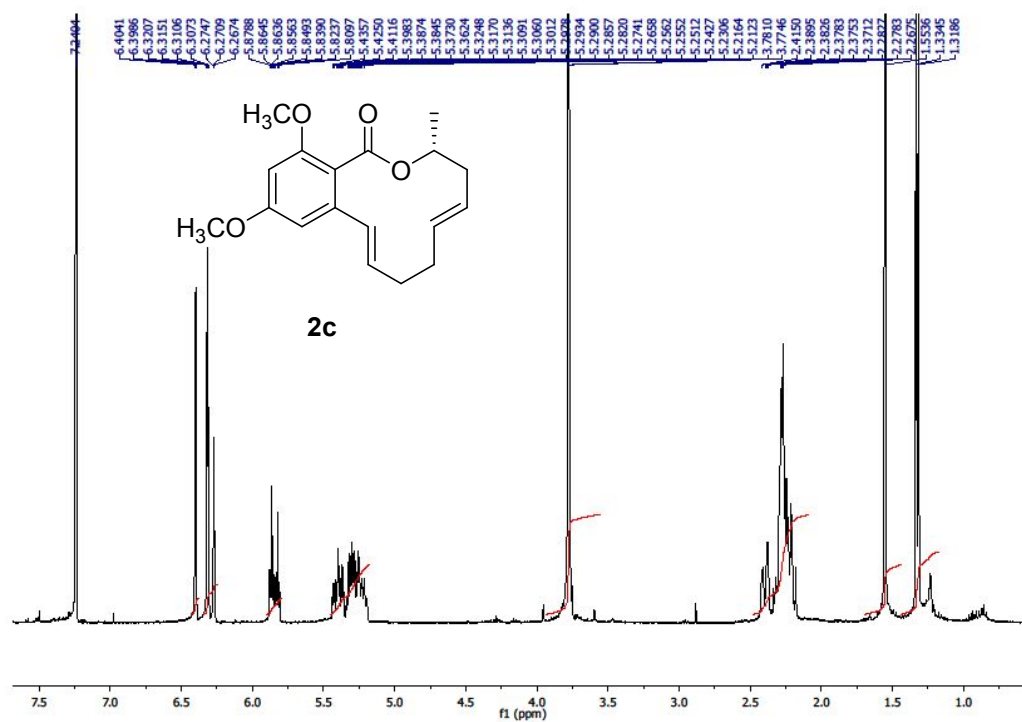


Figure S7.18. ^1H NMR spectrum of compound 2c in CDCl_3

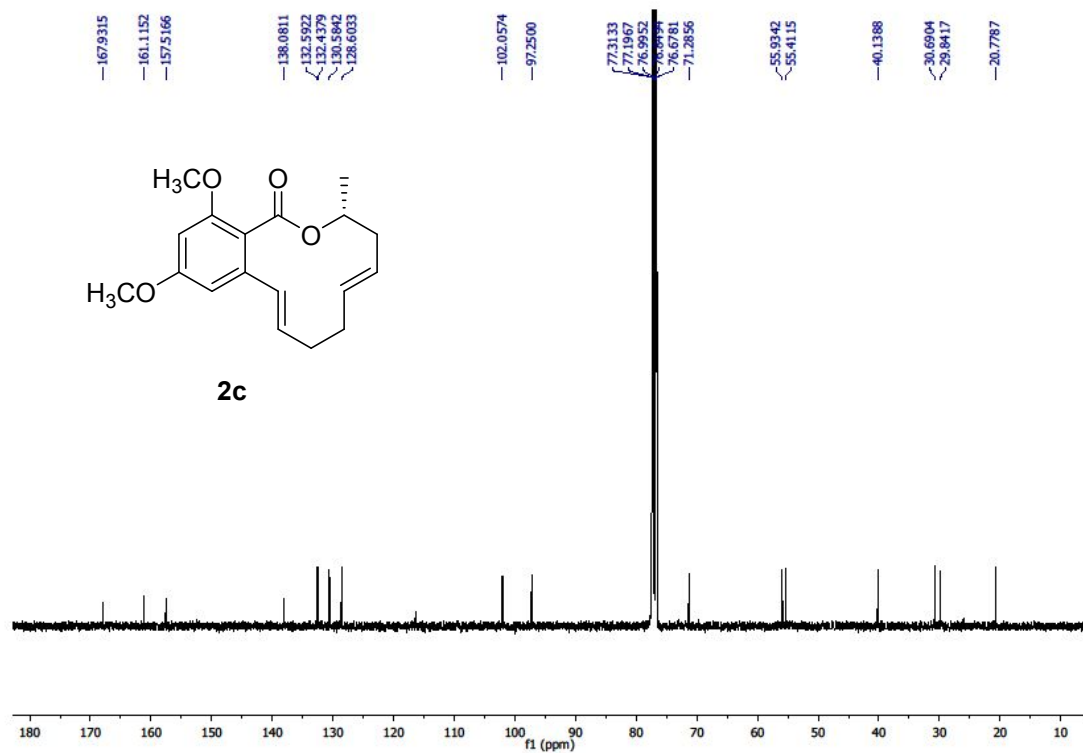


Figure S7.19. ¹³C NMR spectrum of compound **2c** in CDCl₃

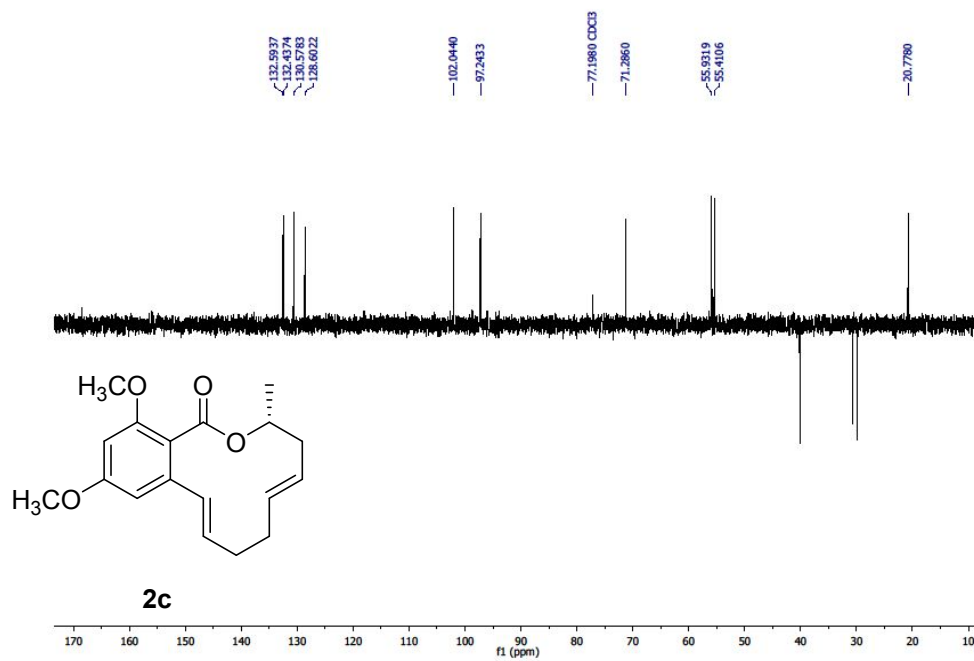


Figure S7.20. DEPT 135 spectrum of compound **2c** in CDCl_3

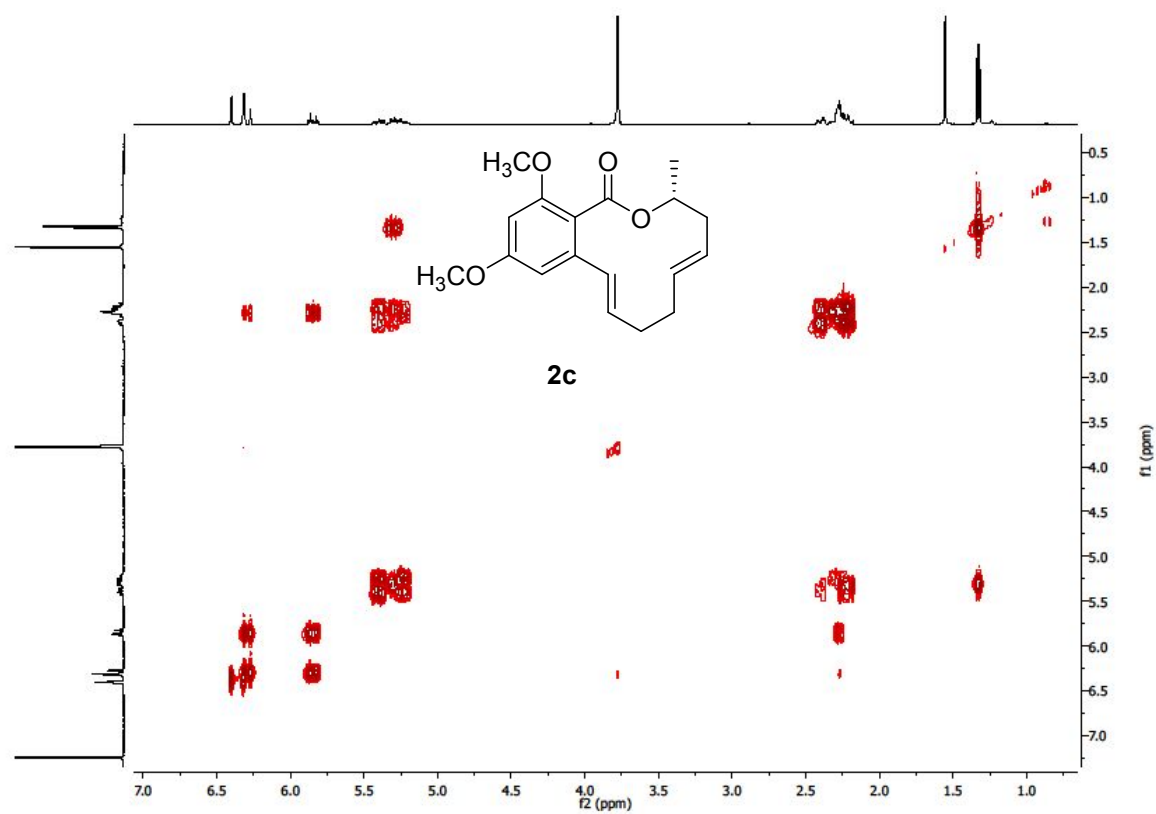


Figure S7.21. ^1H - ^1H COSY spectrum of compound **2c** in CDCl_3

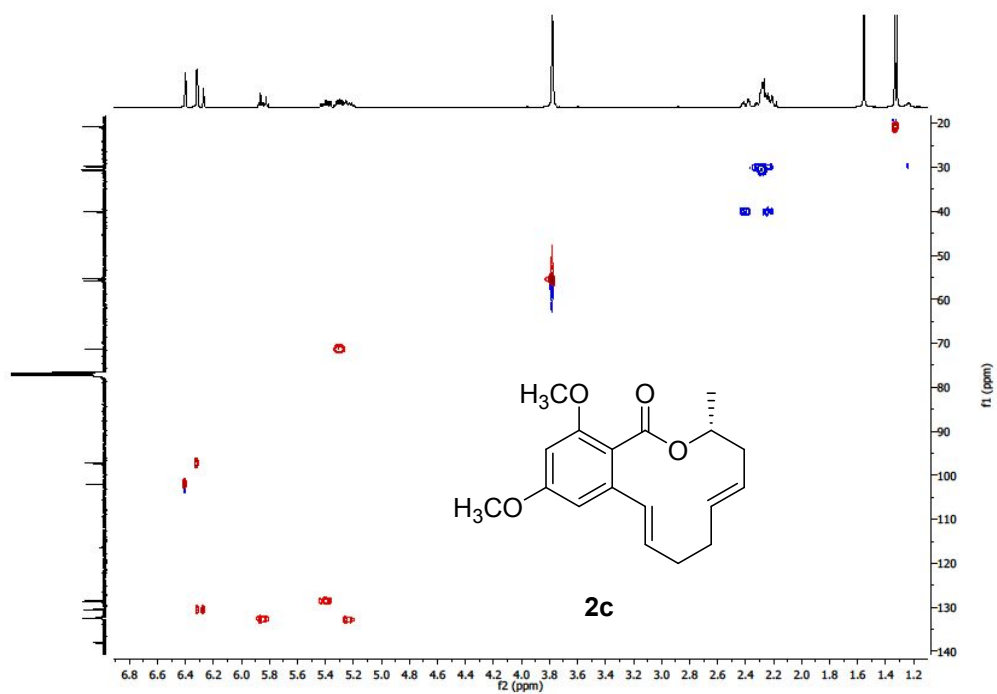


Figure S7.22. HSQC spectrum of compound **2c** in CDCl_3

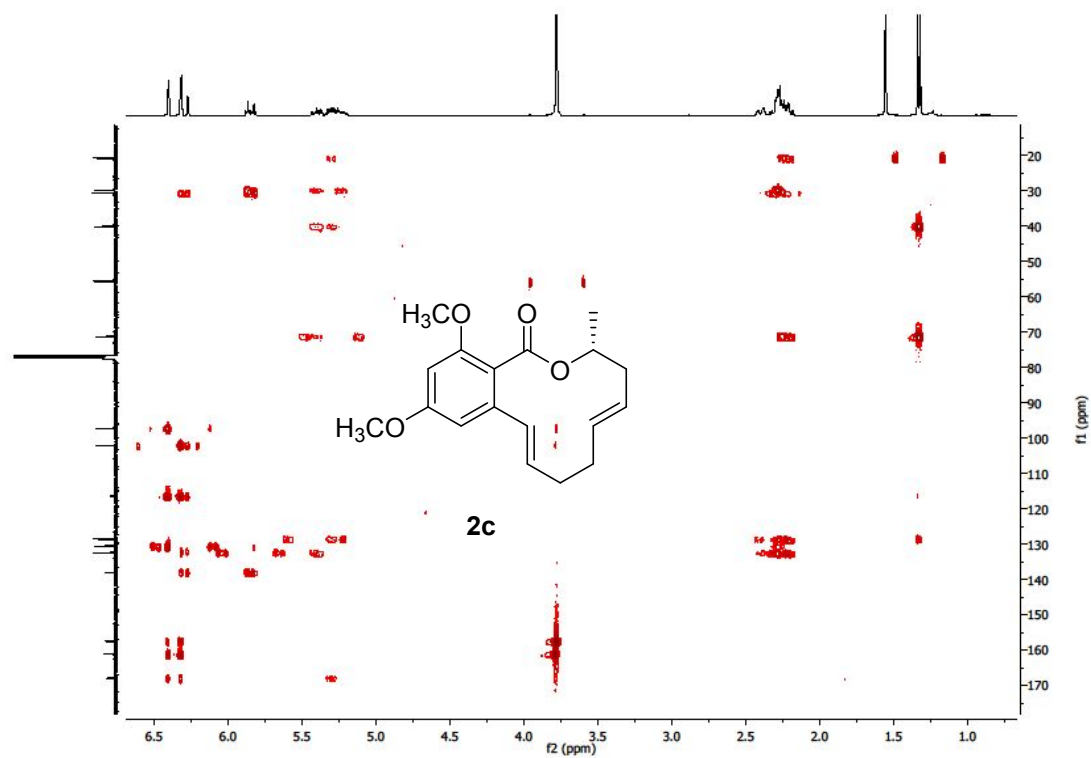


Figure S7.23. HMBC spectrum of compound **2c** in CDCl_3

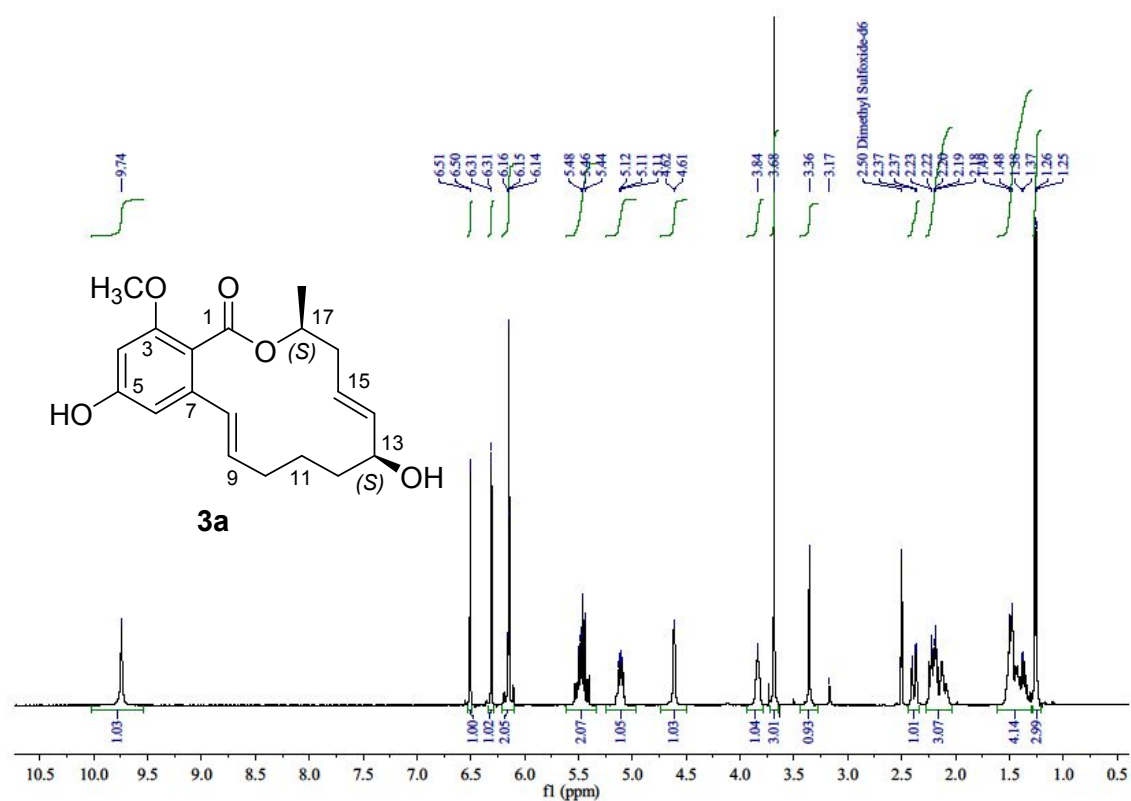


Figure S7.24. ^1H NMR spectrum of compound **3a** in $\text{DMSO}-d_6$

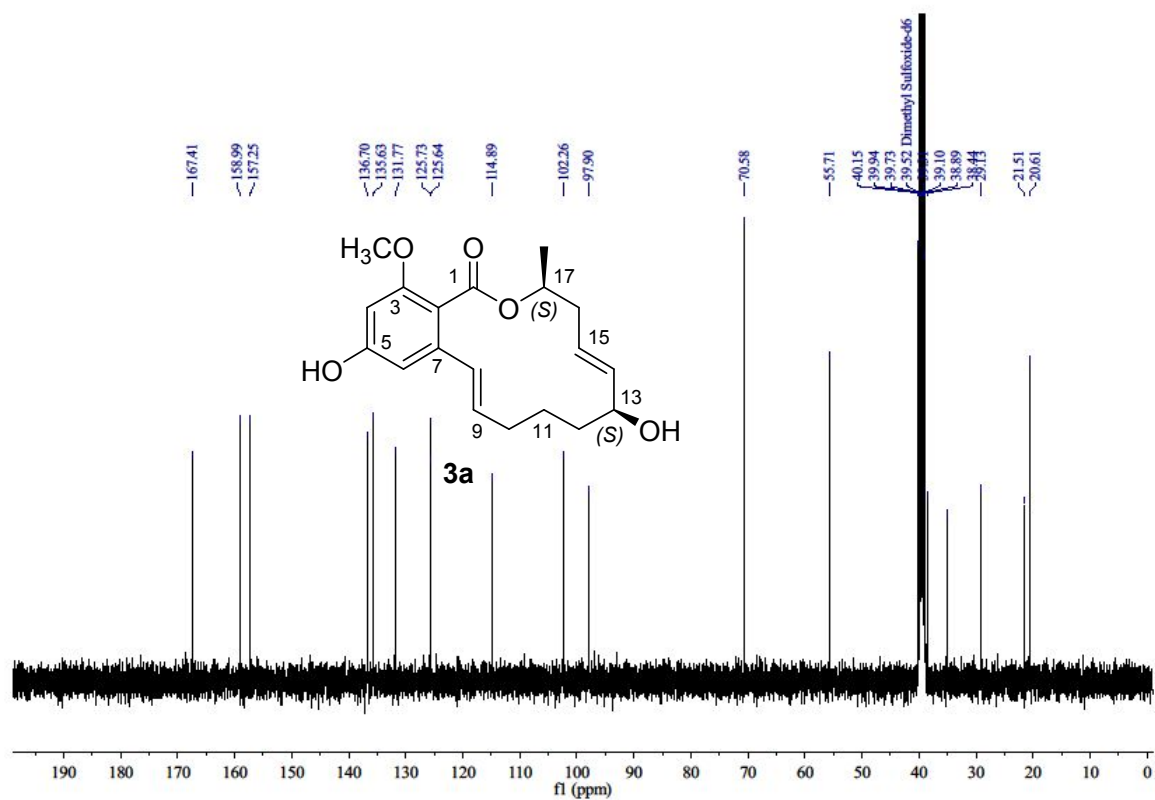


Figure S7.25. ¹³C NMR spectrum of compound **3a** in DMSO-*d*₆

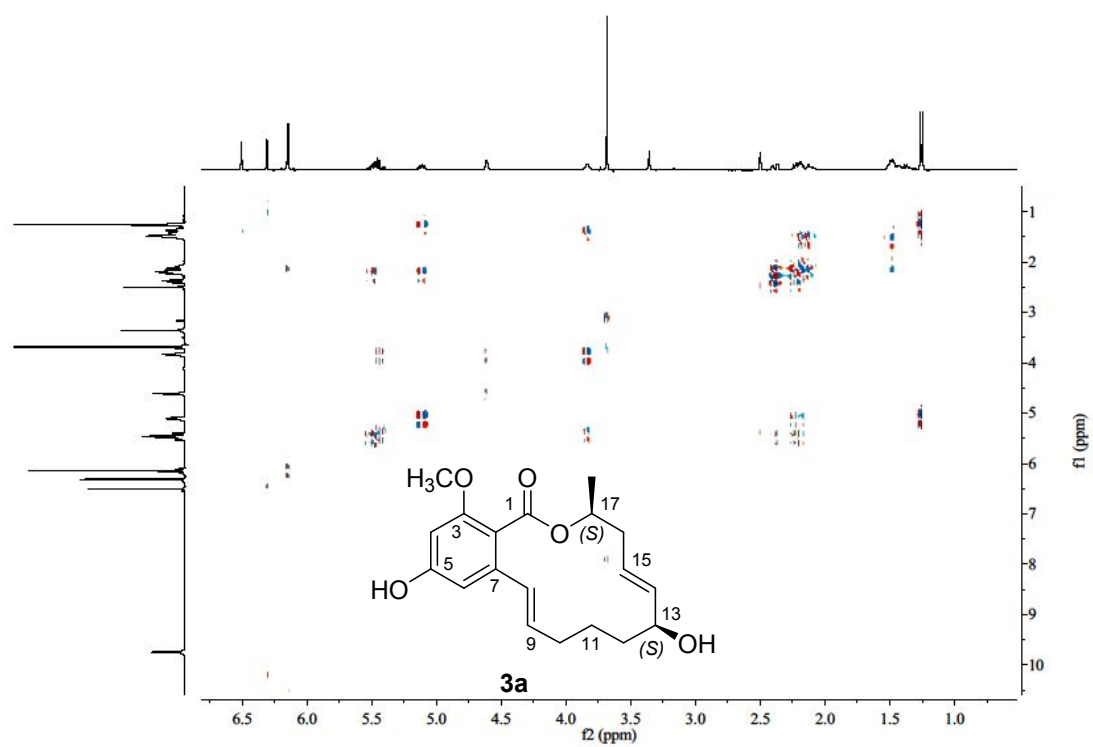


Figure S7.26. ^1H - ^1H COSY spectrum of compound **3a** in $\text{DMSO}-d_6$

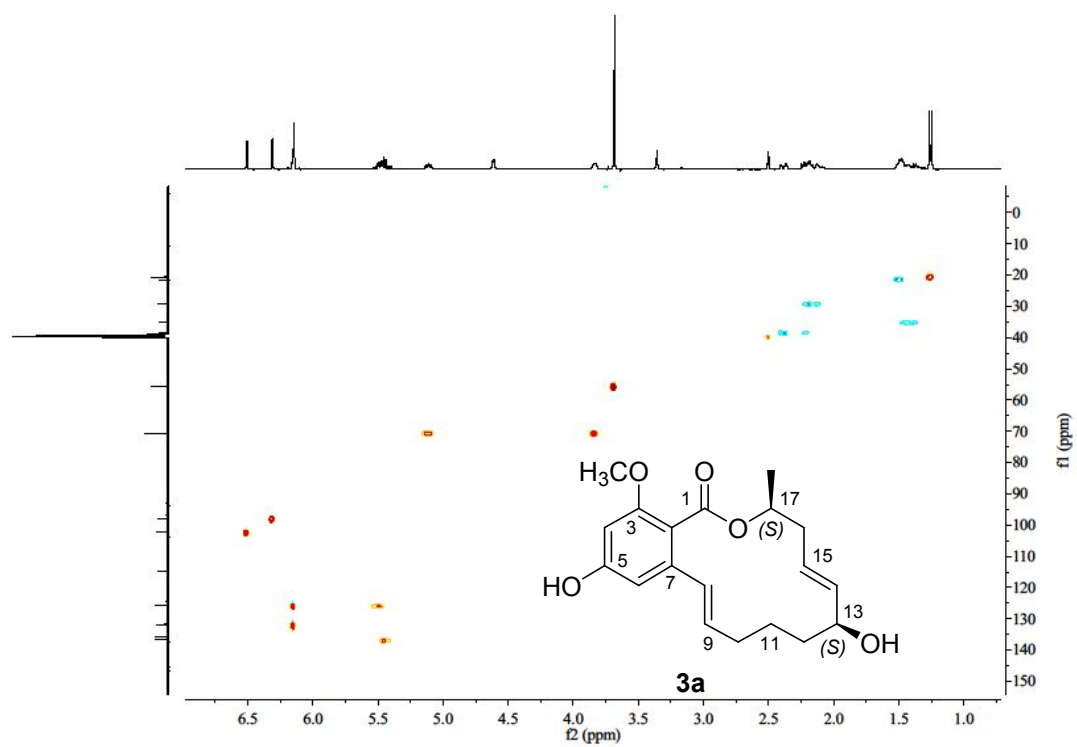


Figure S7.27. HSQC spectrum of compound **3a** in $\text{DMSO}-d_6$

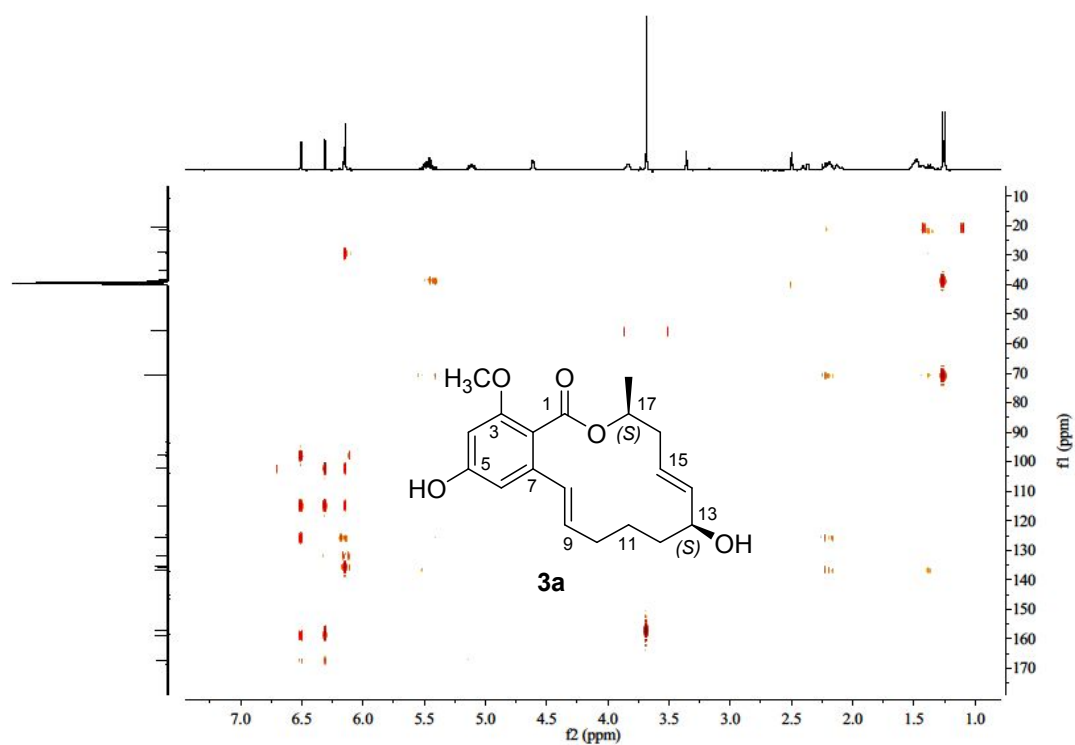


Figure S7.28. HMBC spectrum of compound **3a** in DMSO-*d*₆

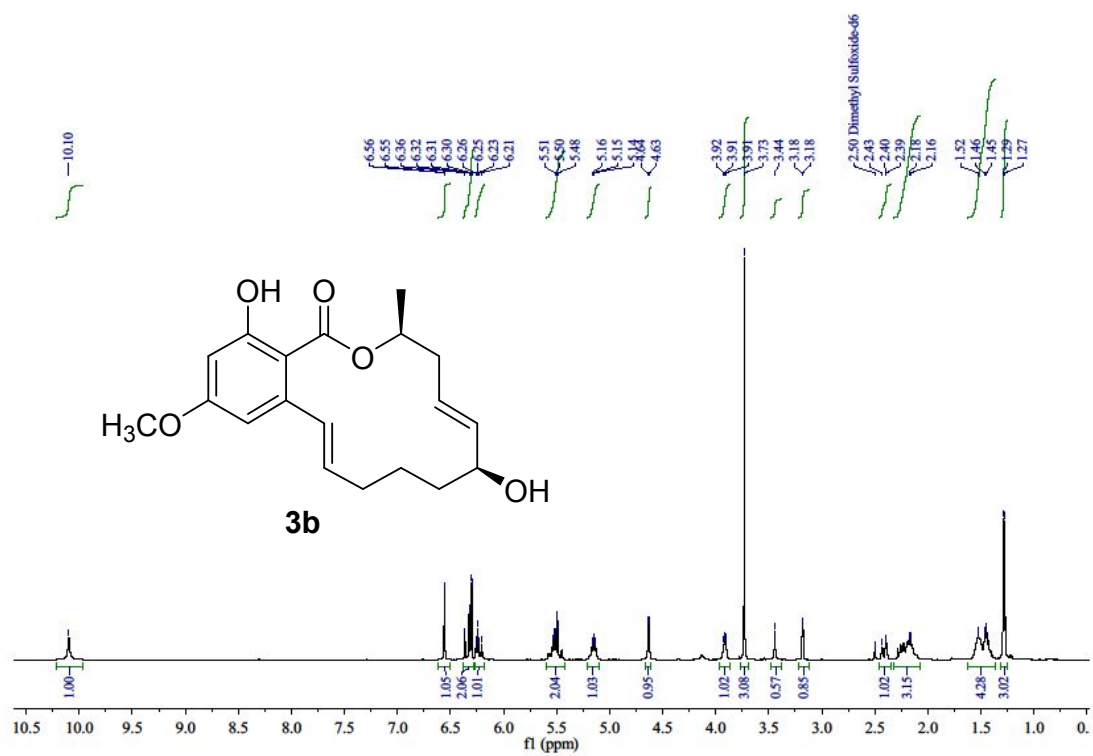


Figure S7.29. ^1H NMR spectrum of compound **3b** in $\text{DMSO}-d_6$

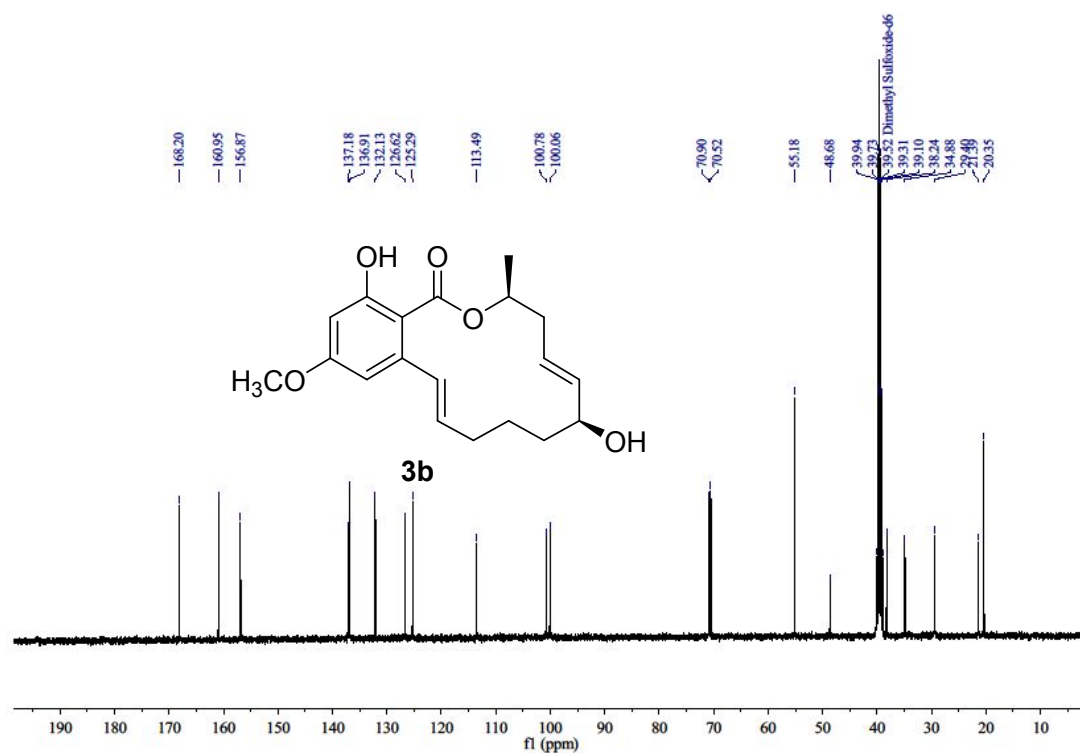


Figure S7.30. ¹³C NMR spectrum of compound 3b in DMSO-*d*₆

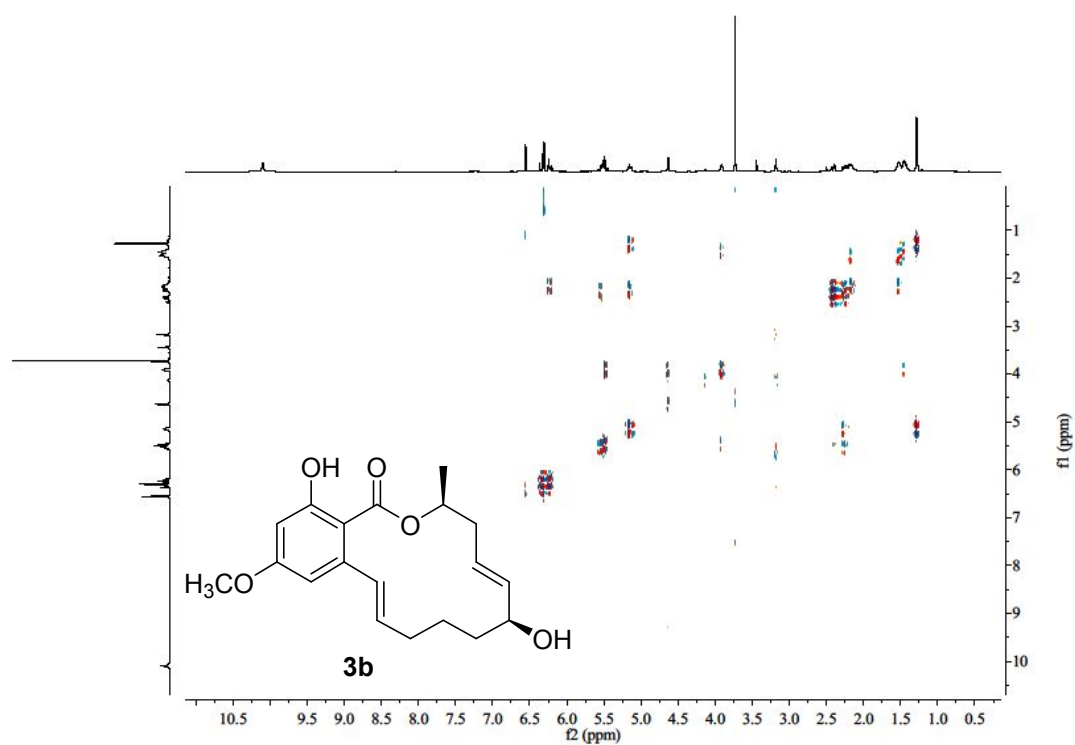


Figure S7.31. ^1H - ^1H COSY spectrum of compound **3b** in $\text{DMSO}-d_6$

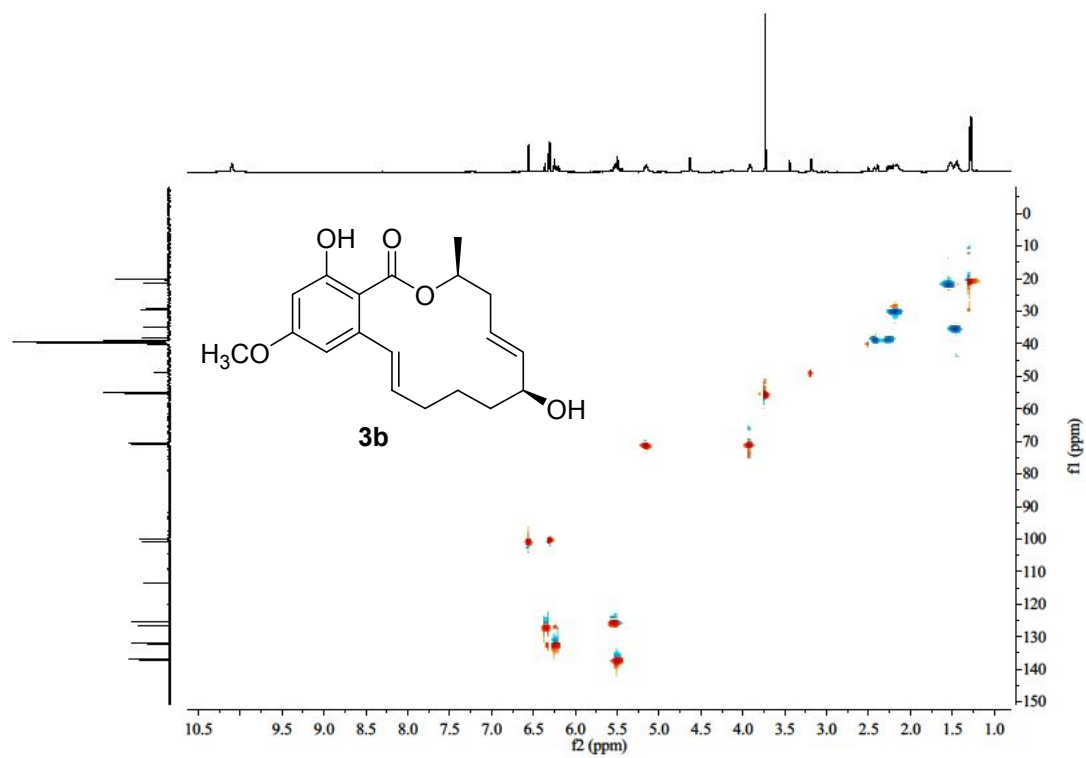


Figure S7.32. HSQC spectrum of compound **3b** in $\text{DMSO-}d_6$

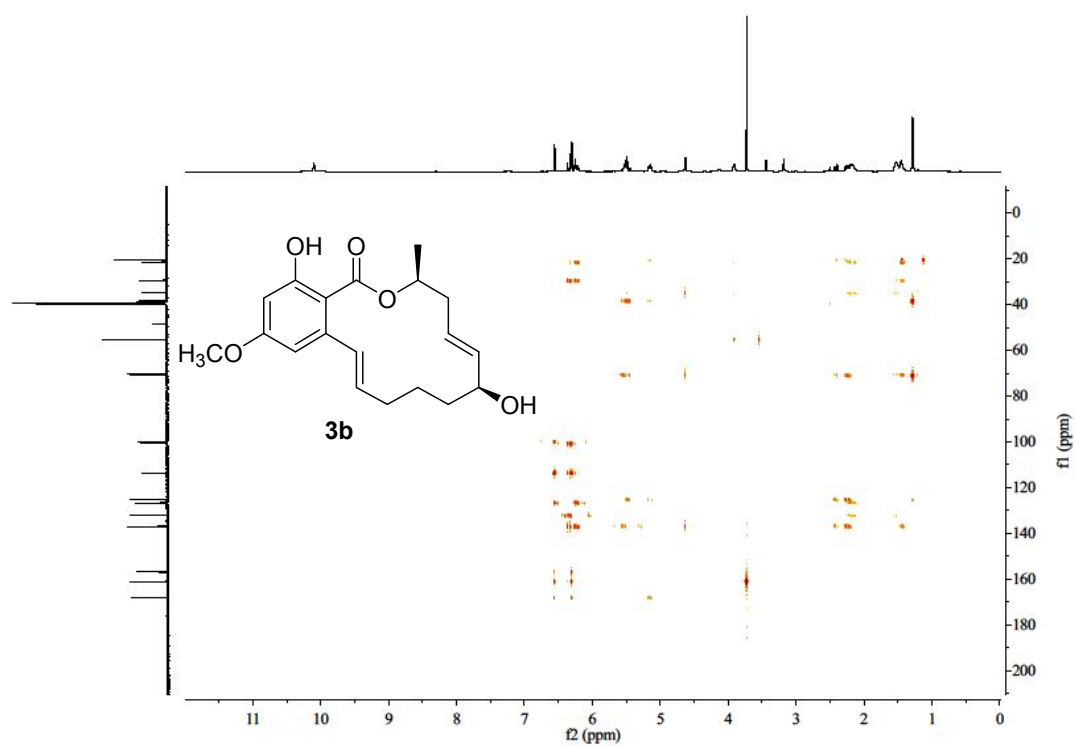


Figure S7.33. HMBC spectrum of compound **3b** in $\text{DMSO}-d_6$

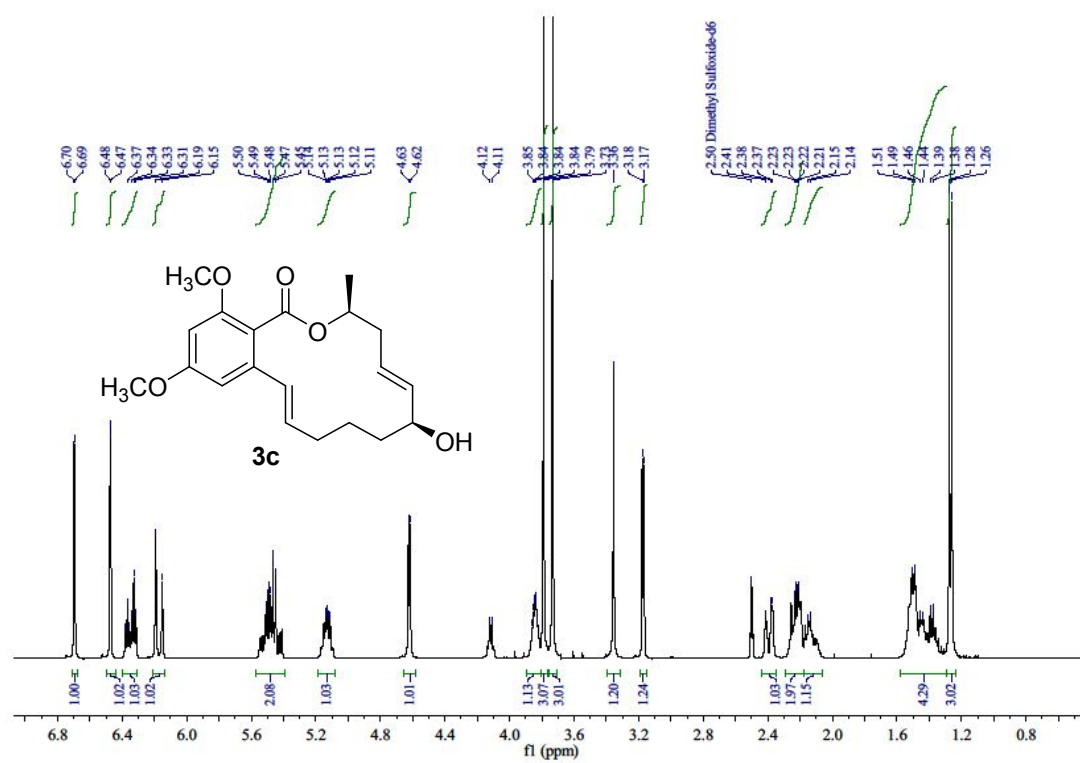


Figure S7.34. ^1H NMR spectrum of compound 3c in $\text{DMSO}-d_6$

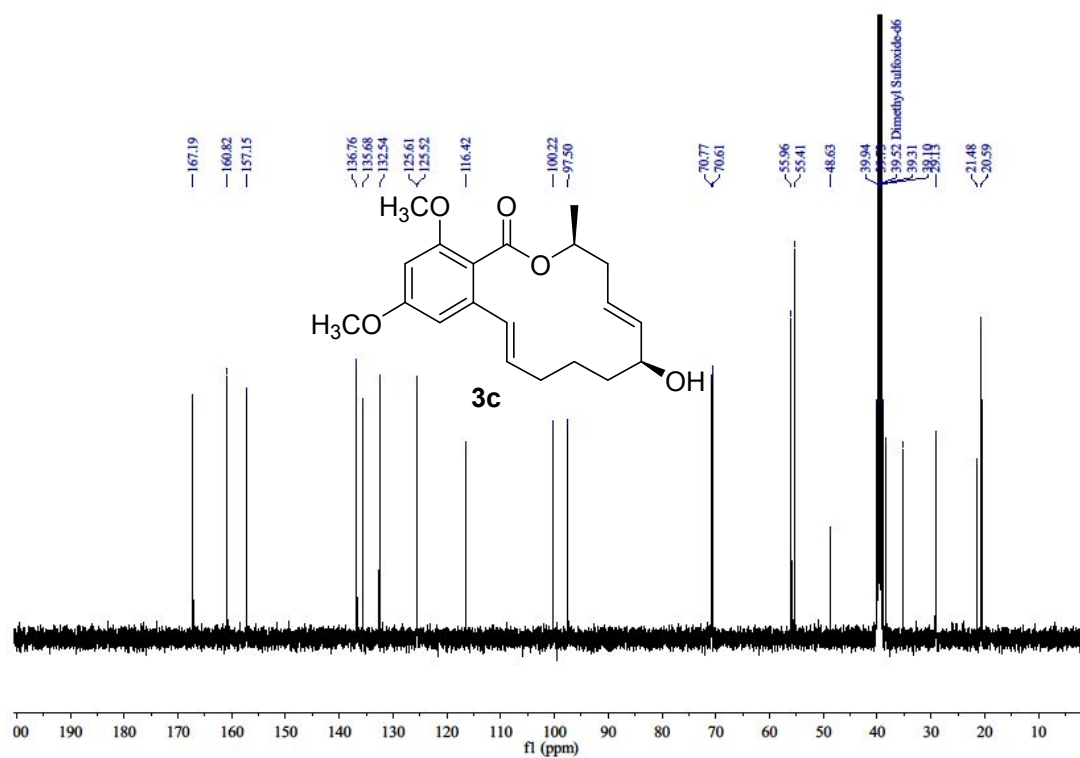


Figure S7.35. ^{13}C NMR spectrum of compound **3c** in $\text{DMSO}-d_6$

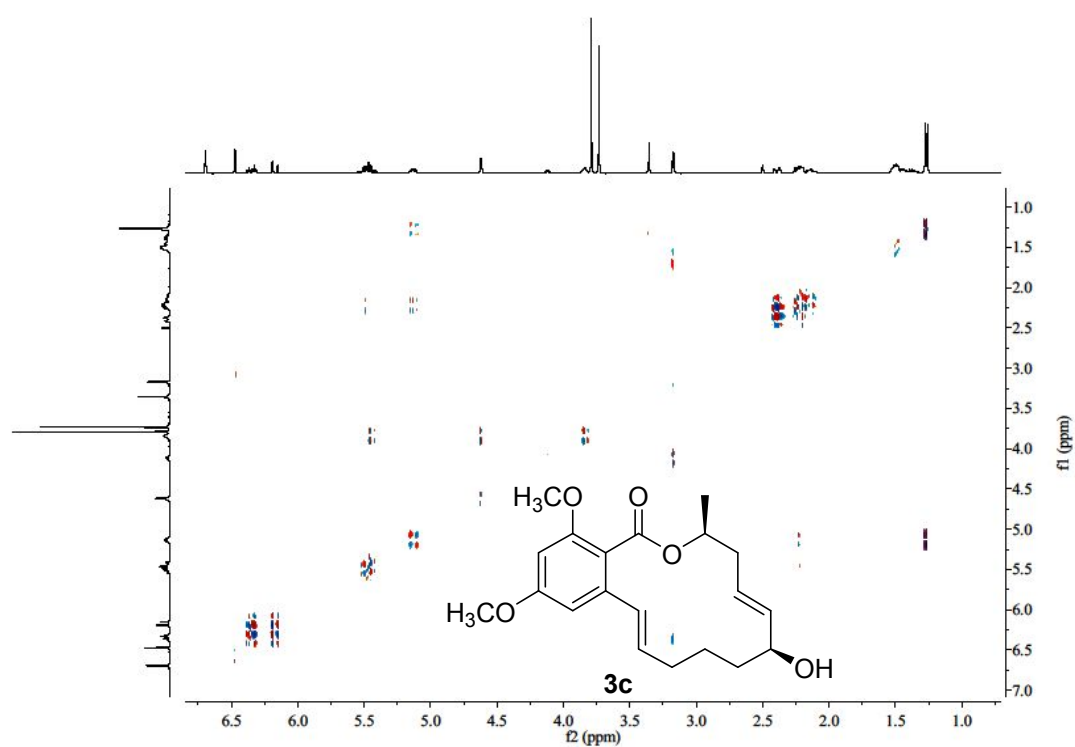


Figure S7.36. ^1H - ^1H COSY spectrum of compound **3c** in $\text{DMSO}-d_6$

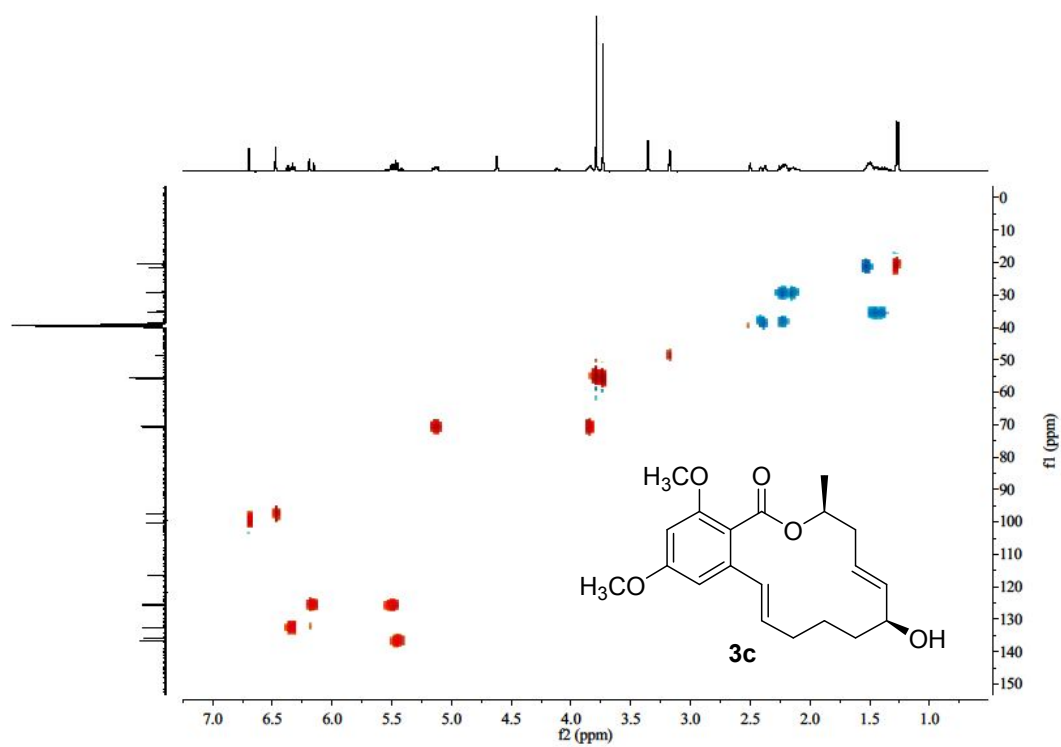


Figure S7.37. HSQC spectrum of compound **3c** in $\text{DMSO-}d_6$

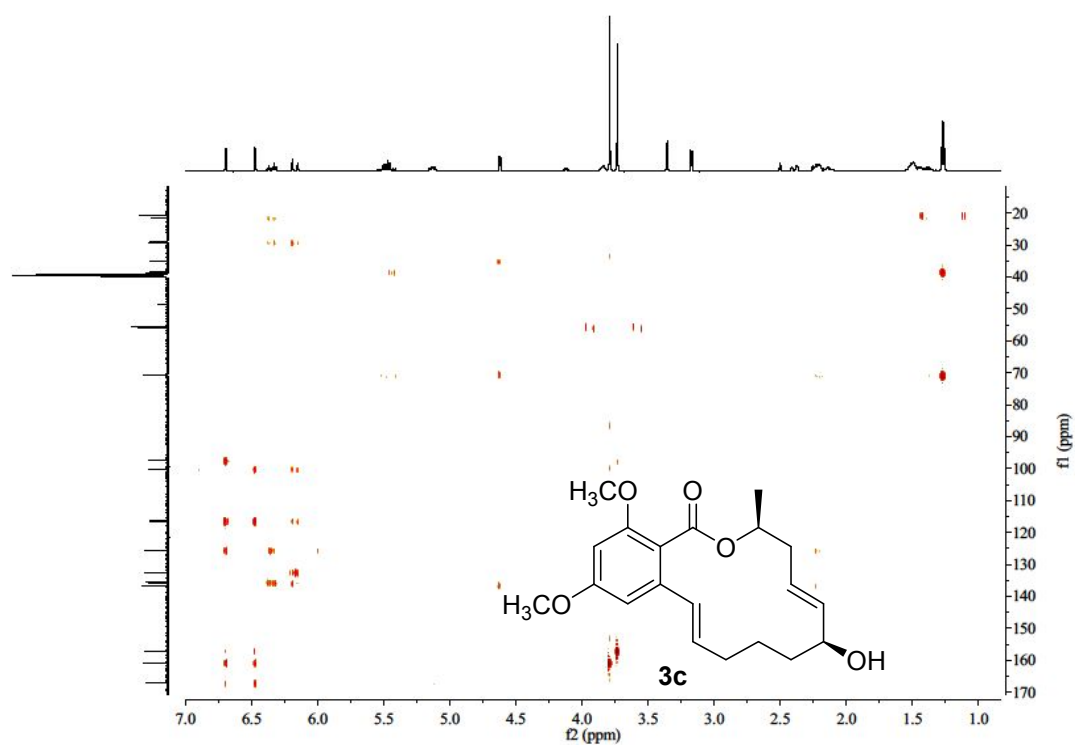


Figure S7.38. HMBC spectrum of compound **3c** in DMSO-*d*₆

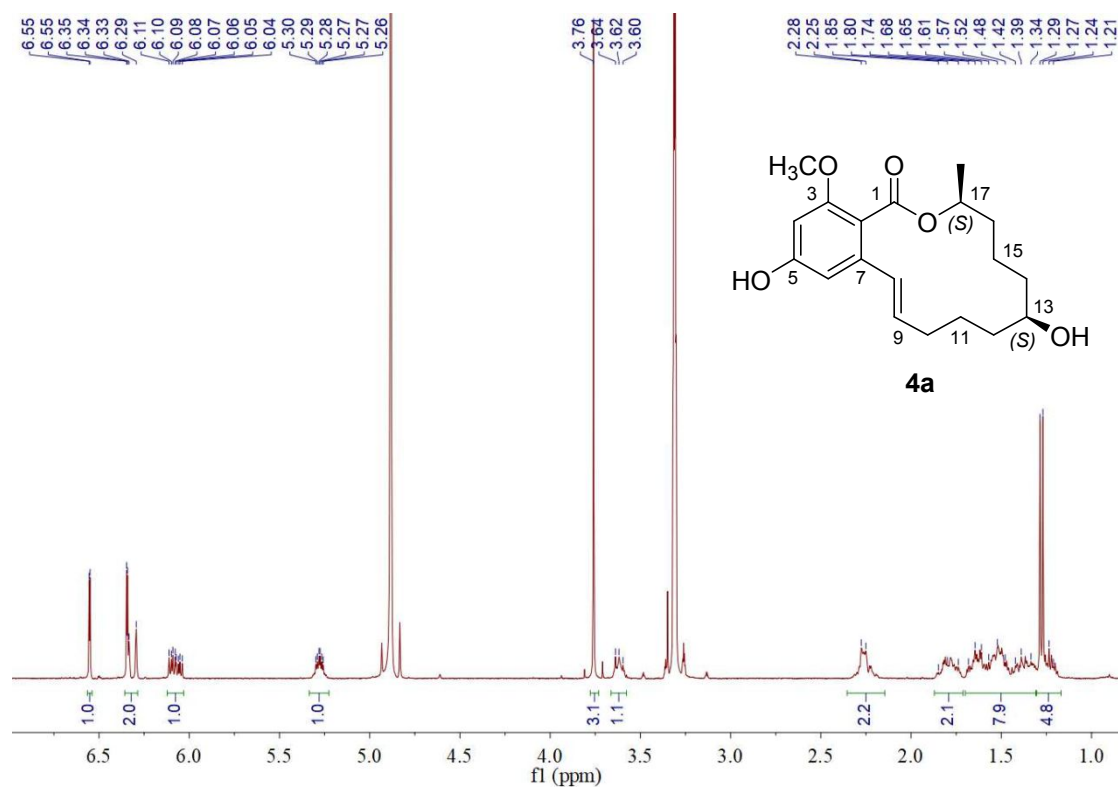


Figure S7.39. ^1H NMR spectrum of compound 4a in methanol- d_4

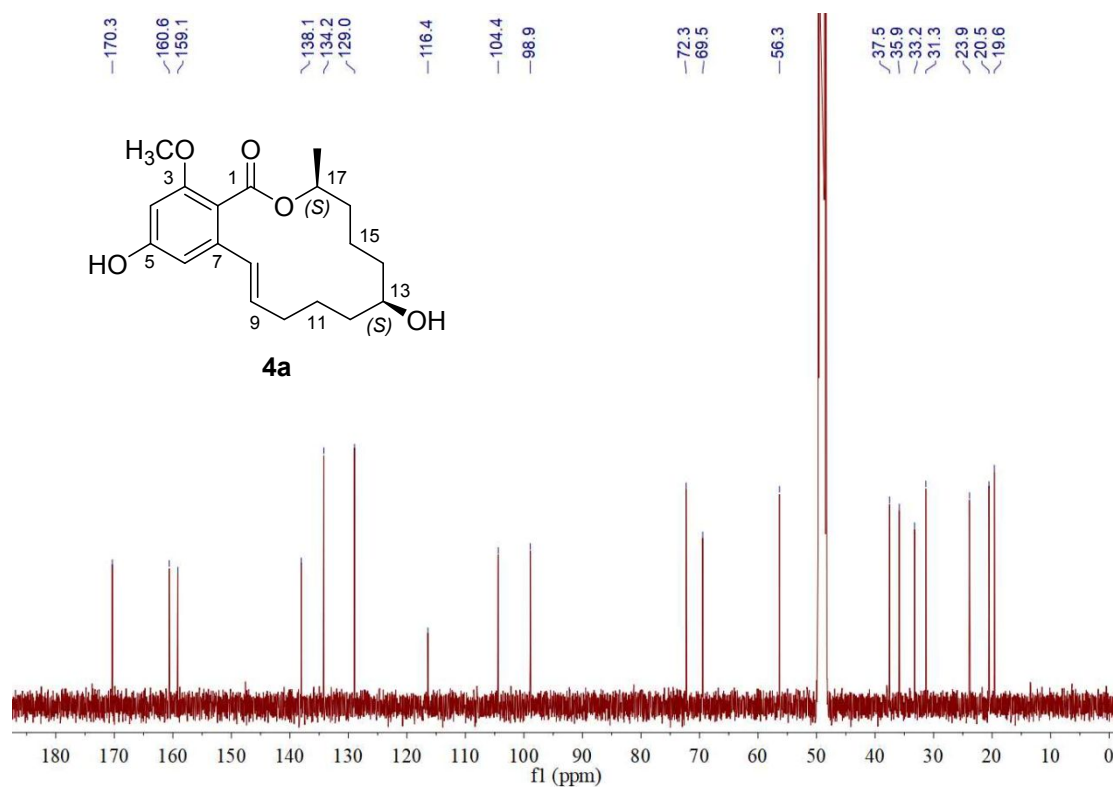


Figure S7.40. ^{13}C NMR spectrum of compound **4a** in methanol- d_4

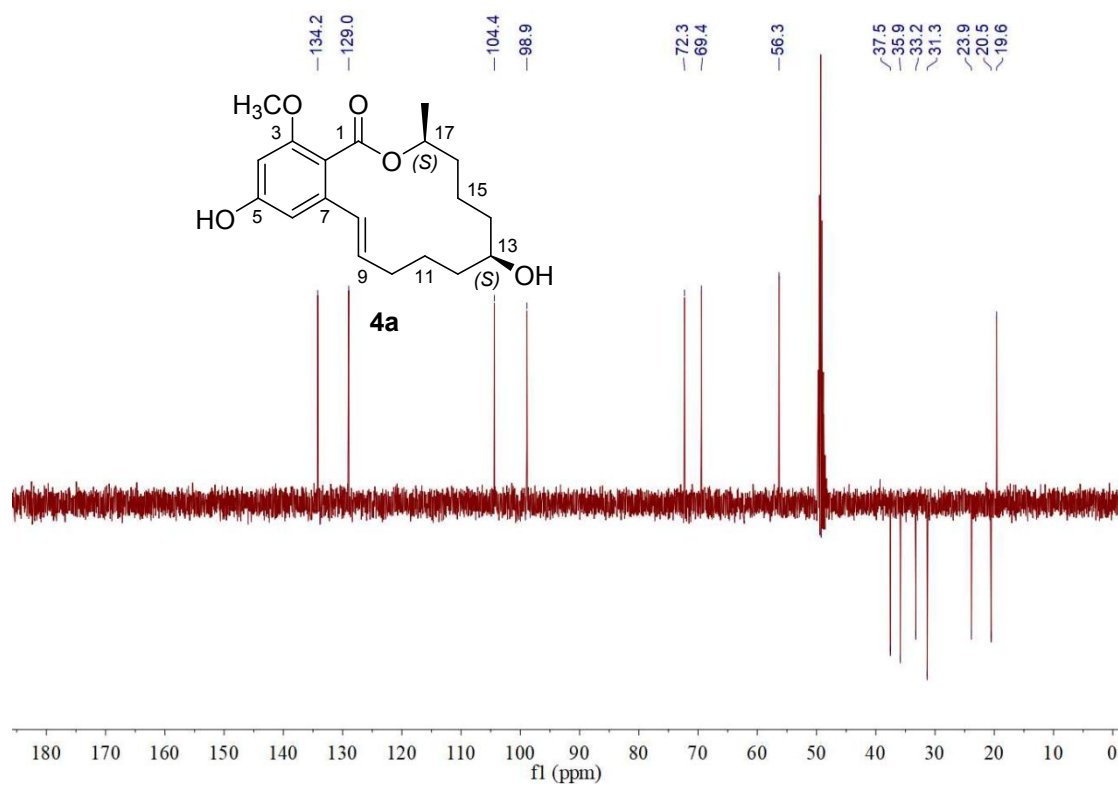


Figure S7.41. DEPT 135 spectrum of compound 4a in methanol-*d*₄

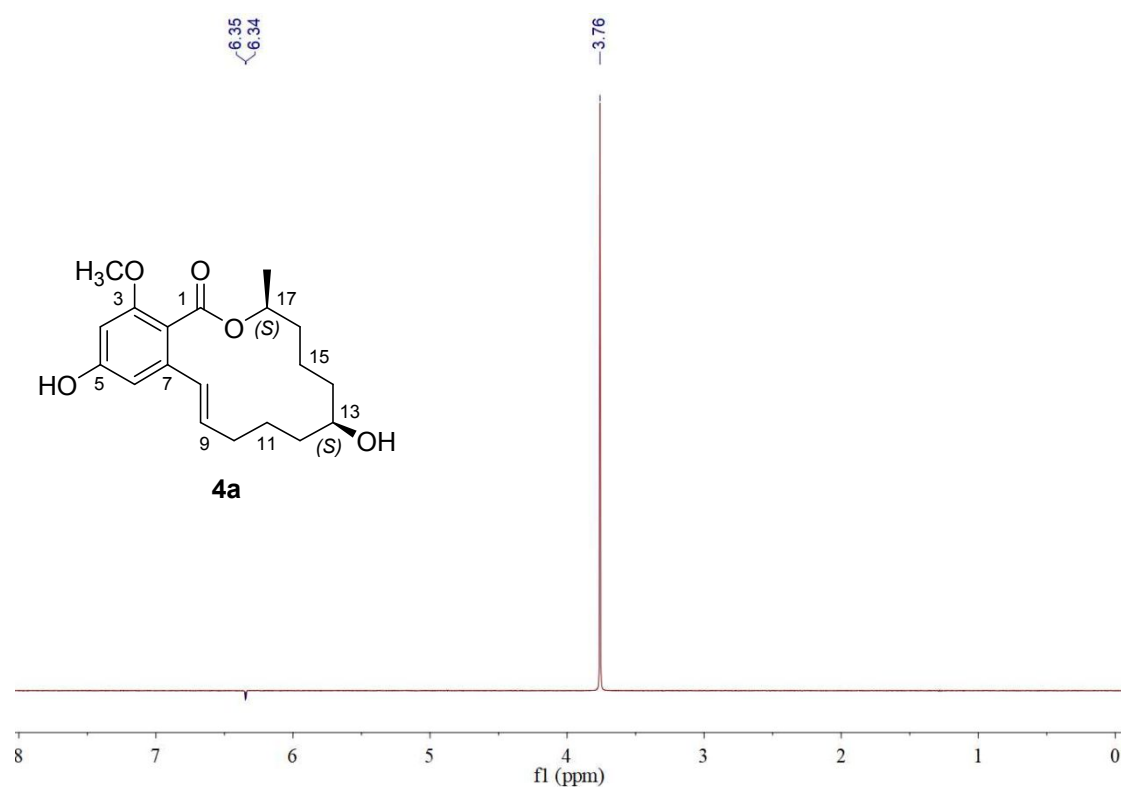


Figure S7.42. 1D NOESY spectrum of compound **4a** in methanol-*d*₄

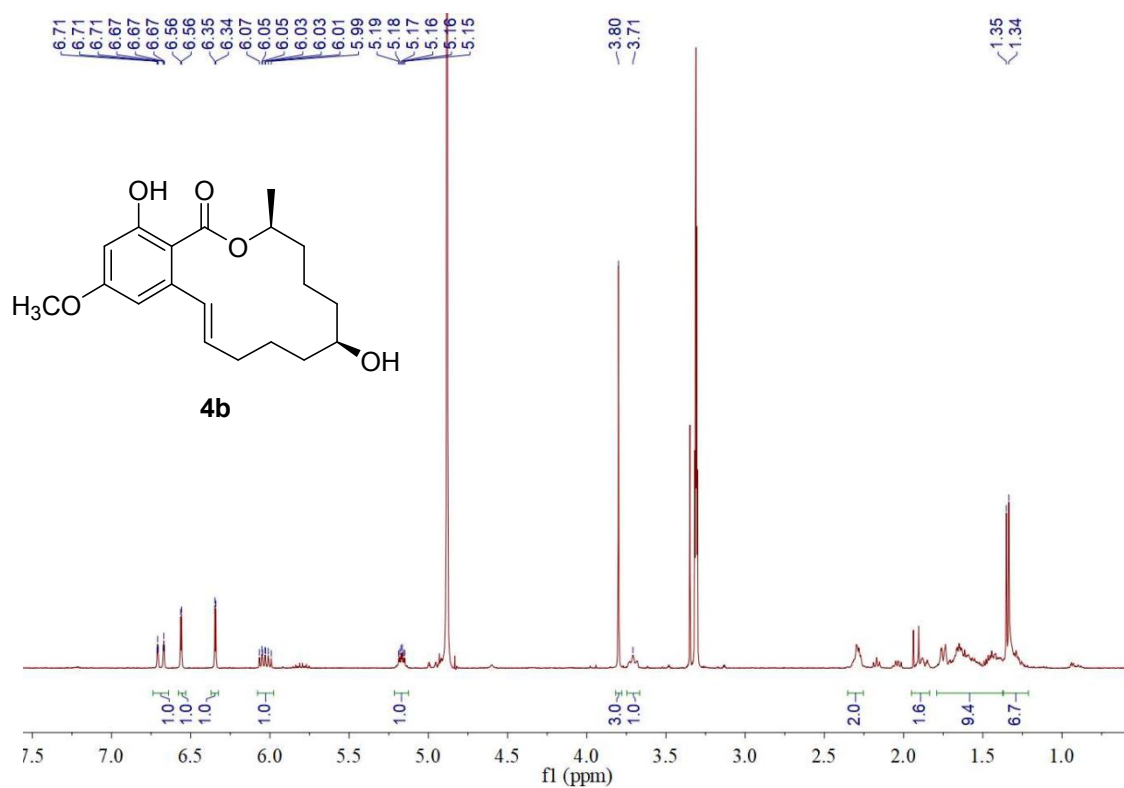


Figure S7.43. ^1H NMR spectrum of compound **4b** in methanol- d_4

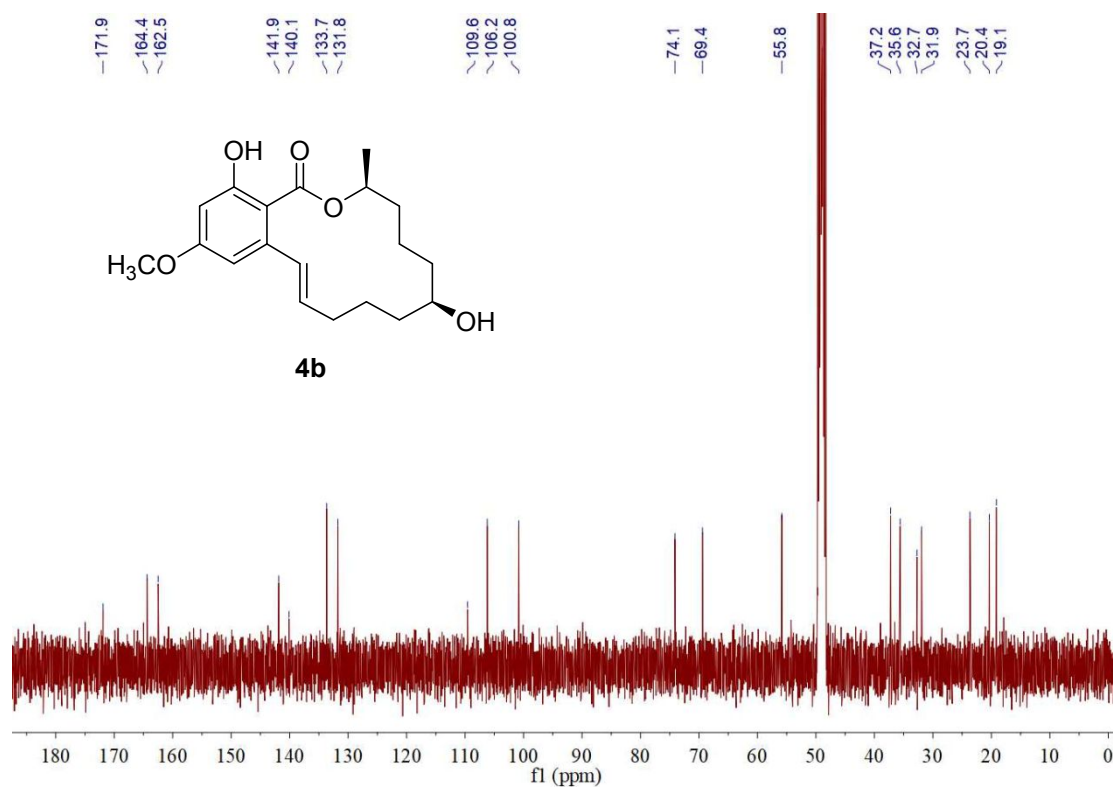


Figure S7.44. ^{13}C NMR spectrum of compound **4b** in methanol- d_4

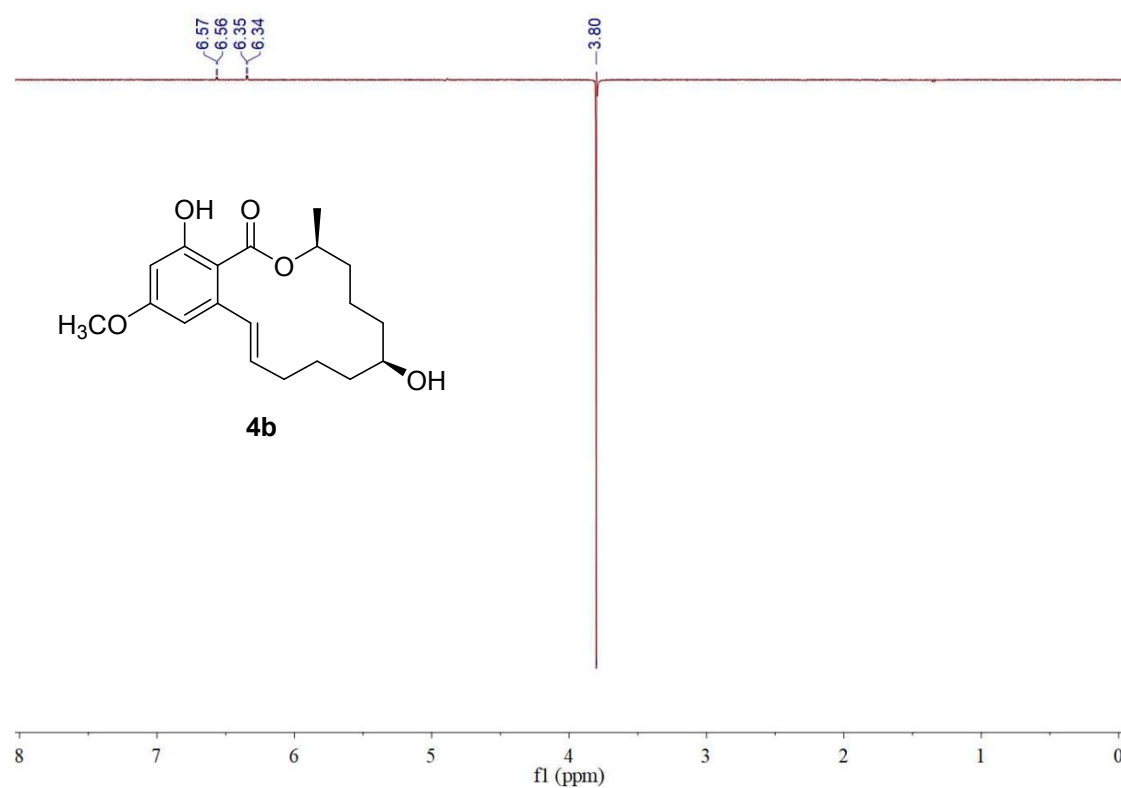


Figure S7.45. 1D NOESY NMR spectrum of compound **4b** in methanol- d_4

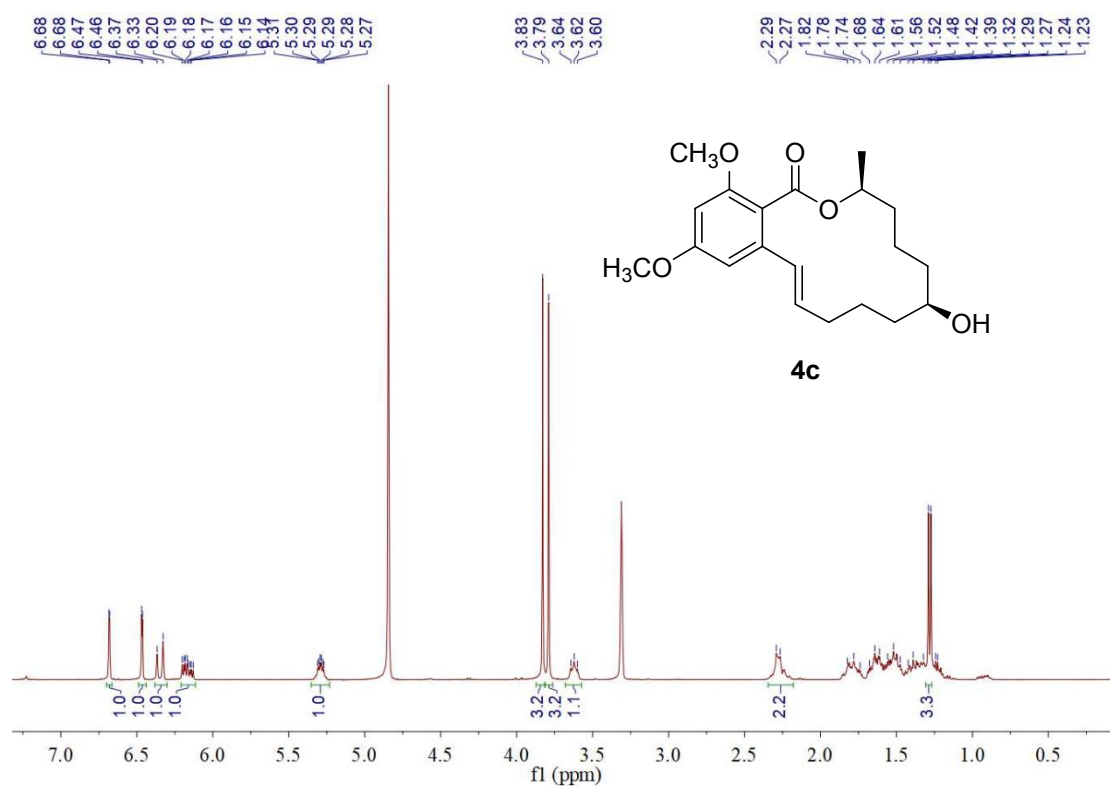


Figure S7.46. ¹H NMR spectrum of compound **4c** in methanol-*d*₄

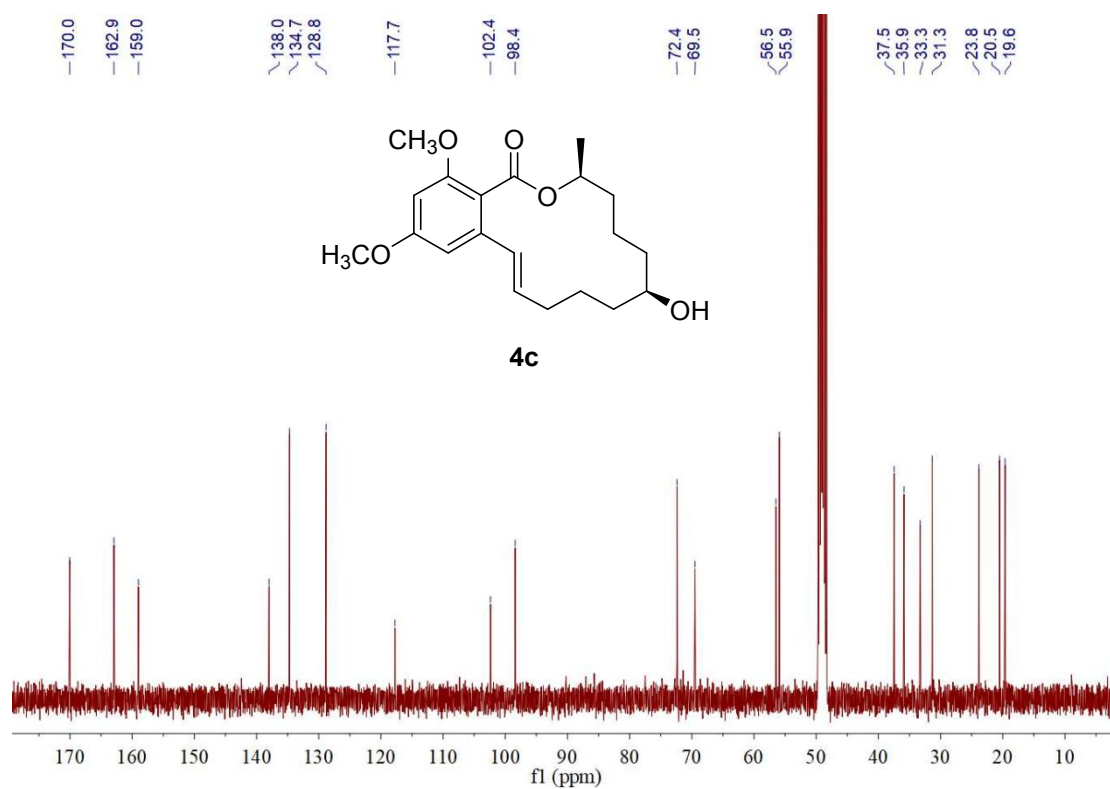


Figure S7.47. ¹³C NMR spectrum of compound 4c in methanol-*d*₄

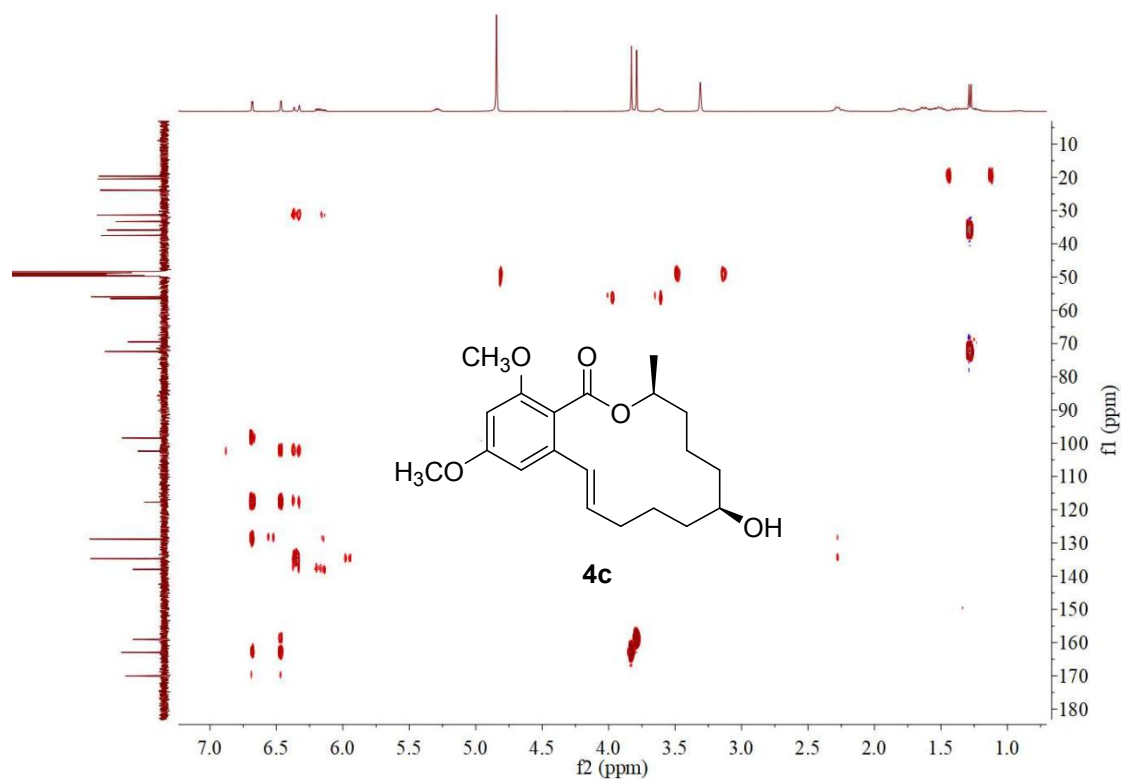


Figure S7.48. HMBC spectrum of compound 4c in methanol- d_4

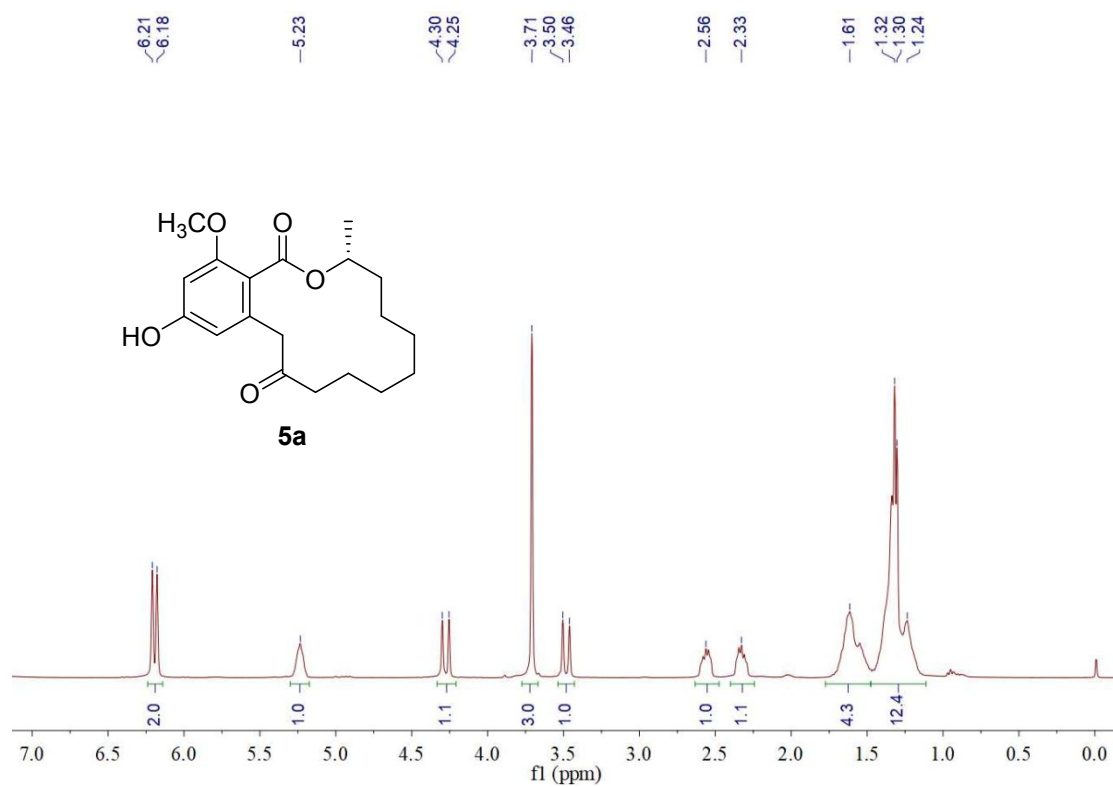


Figure S7.49. ¹H NMR spectrum of compound **5a** in CDCl₃

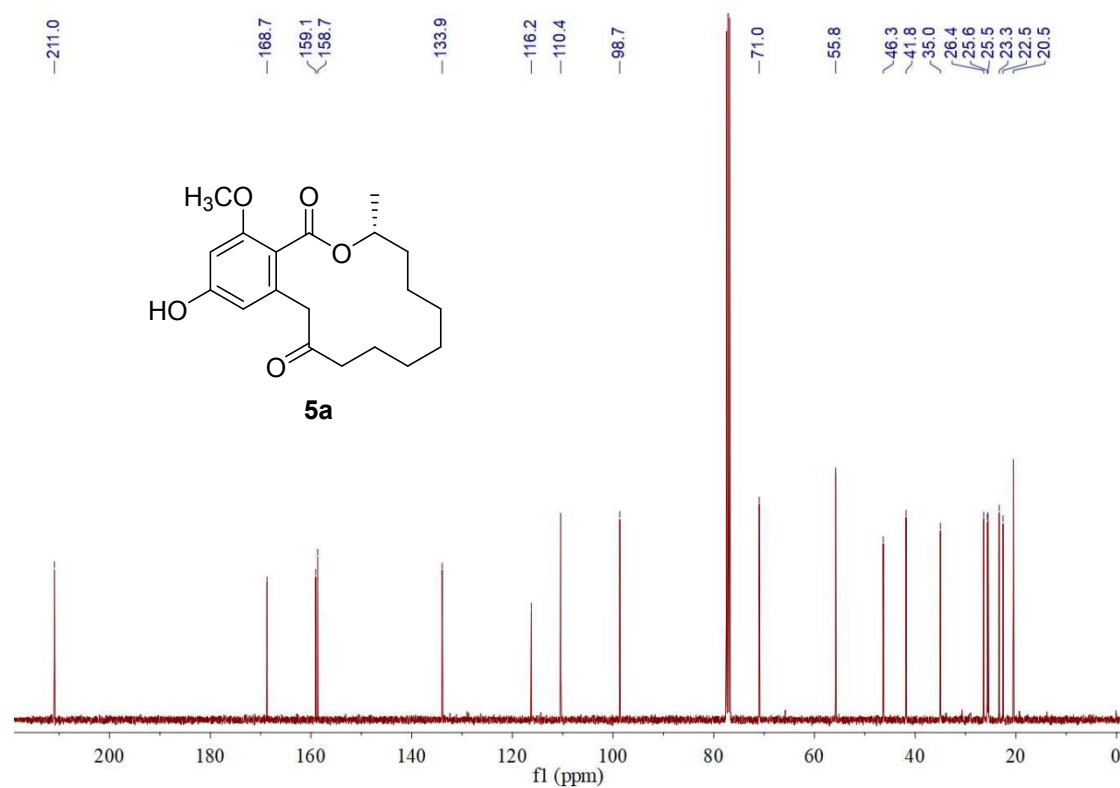


Figure S7.50. ¹³C NMR spectrum of compound **5a** in CDCl₃

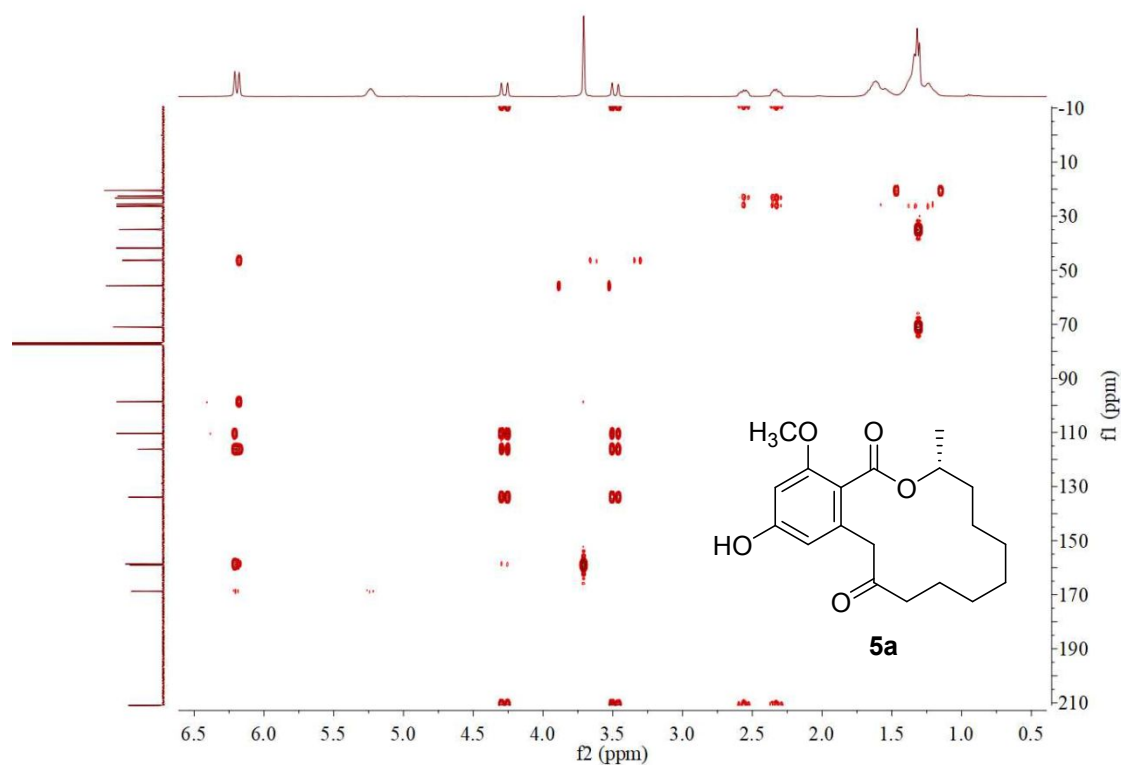


Figure S7.51. HMBC spectrum of compound **5a** in CDCl_3

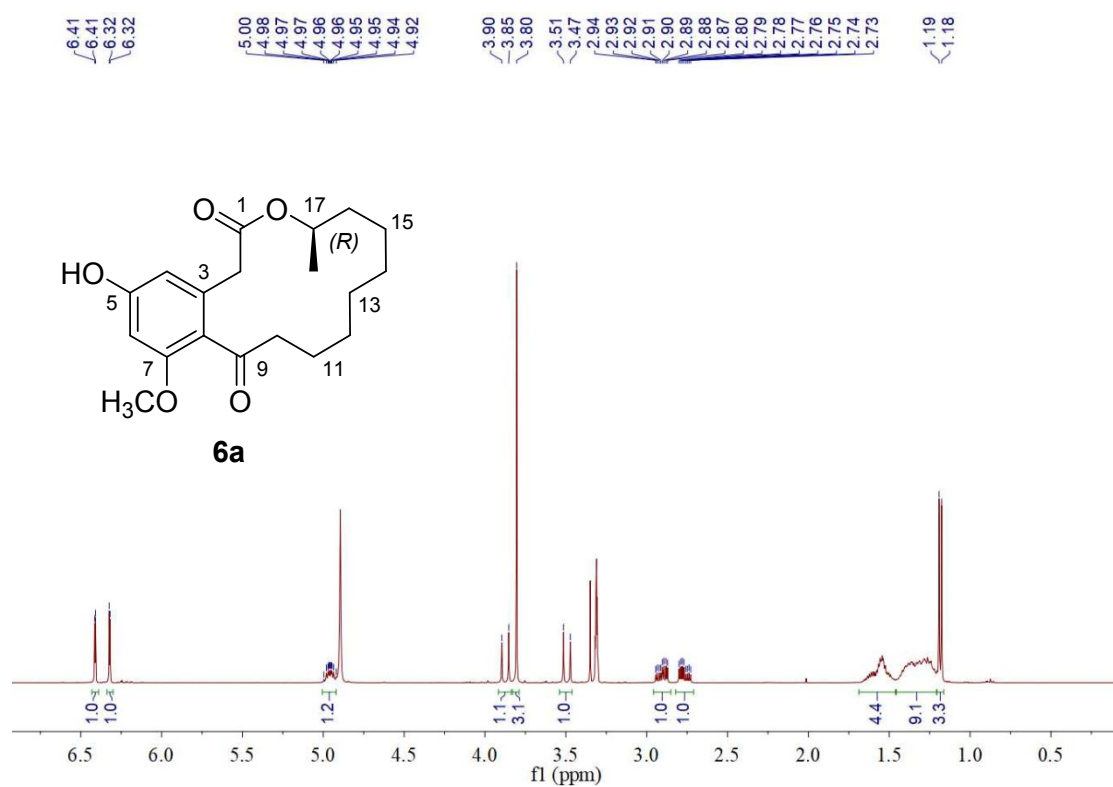


Figure S7.52. ^1H NMR spectrum of compound **6a** in methanol- d_4

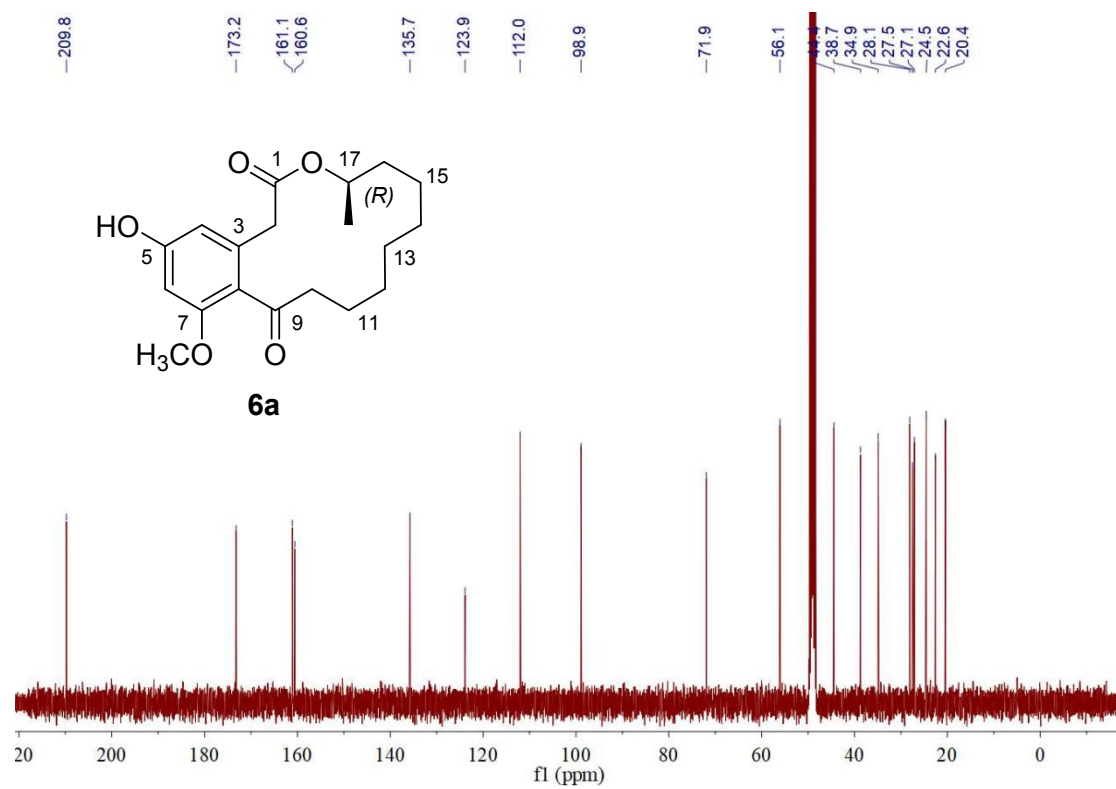


Figure S7.53. ^{13}C NMR spectrum of compound **6a** in methanol- d_4

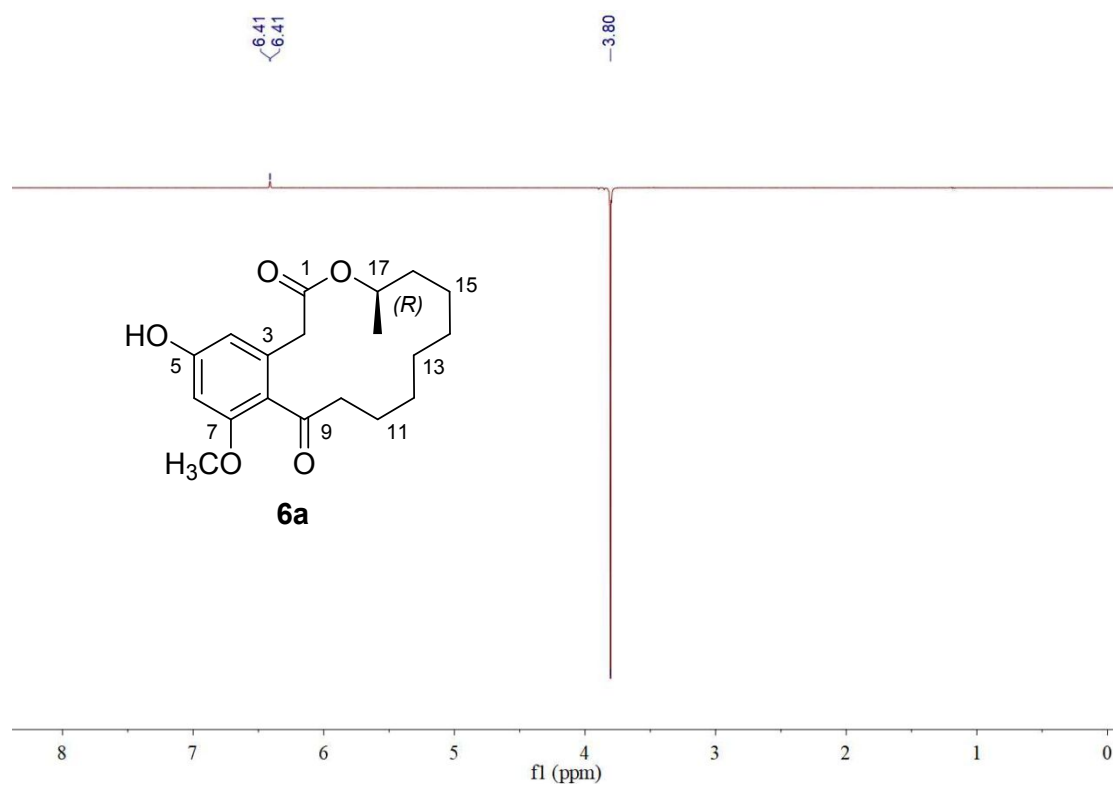


Figure S7.54. 1D NOESY spectrum of compound **6a** in methanol-*d*₄

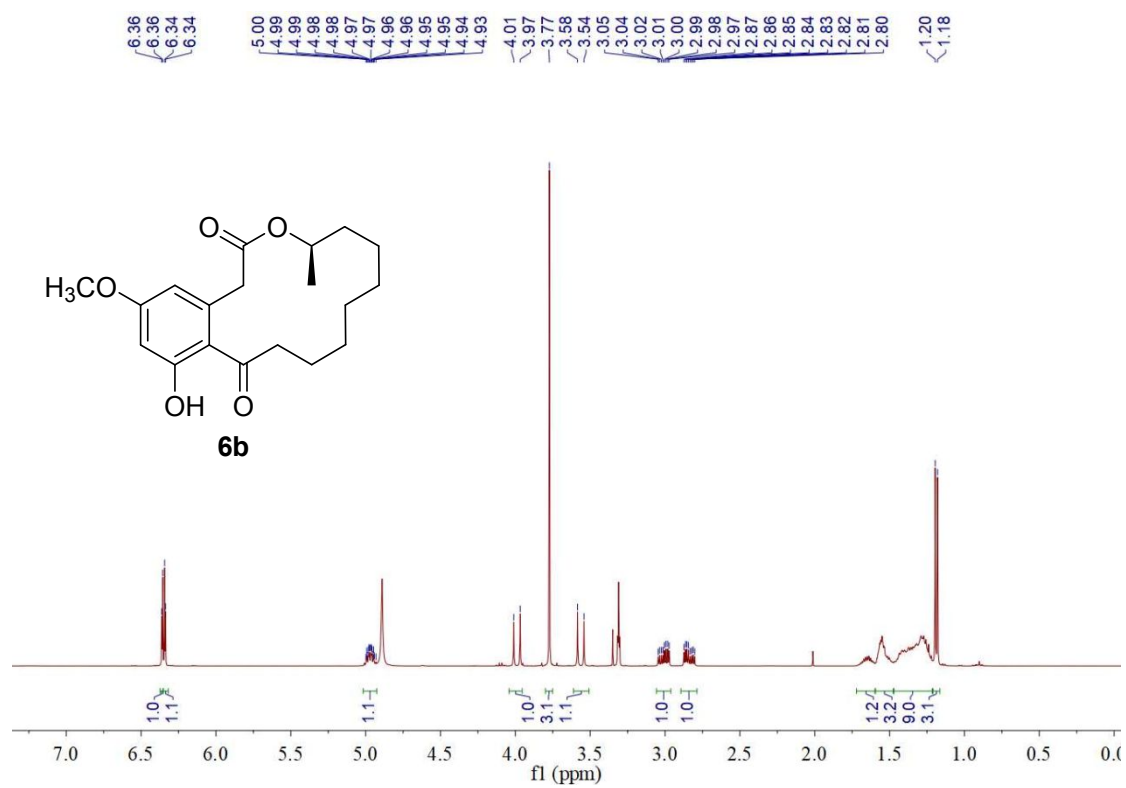


Figure S7.55. ¹H NMR spectrum of compound **6b** in methanol-*d*₄

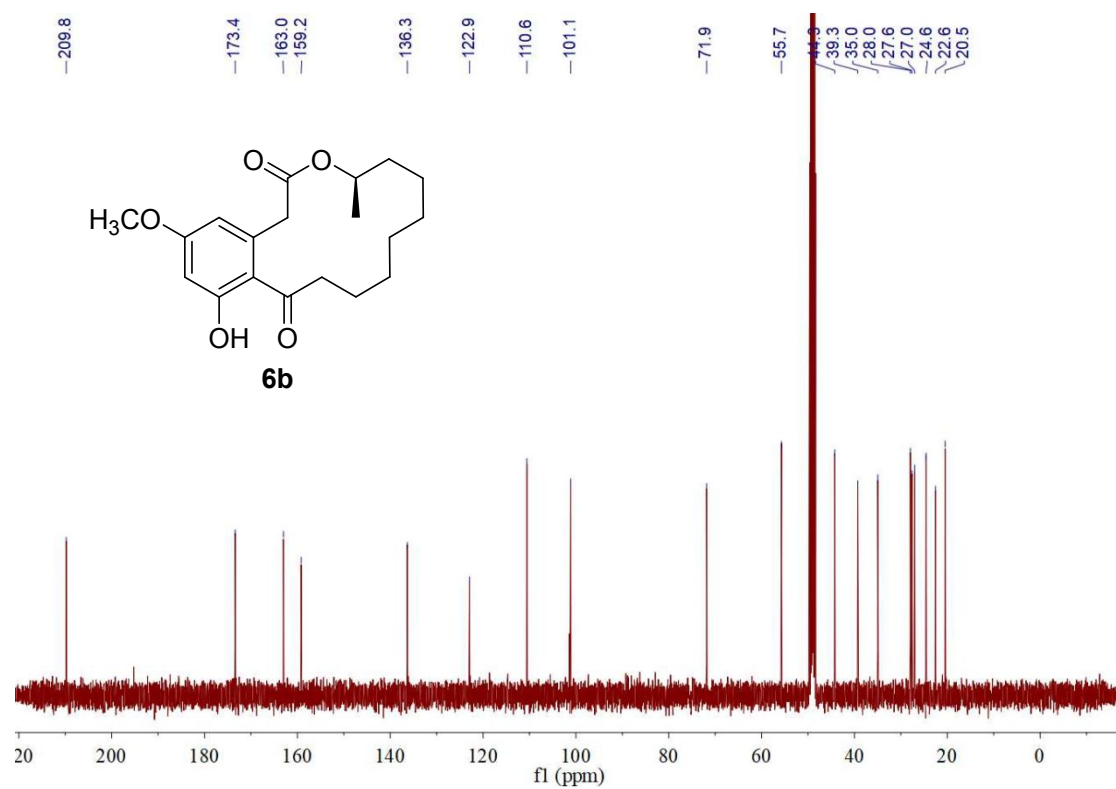


Figure S7.56. ¹³C NMR spectrum of compound **6b** in methanol-*d*₄

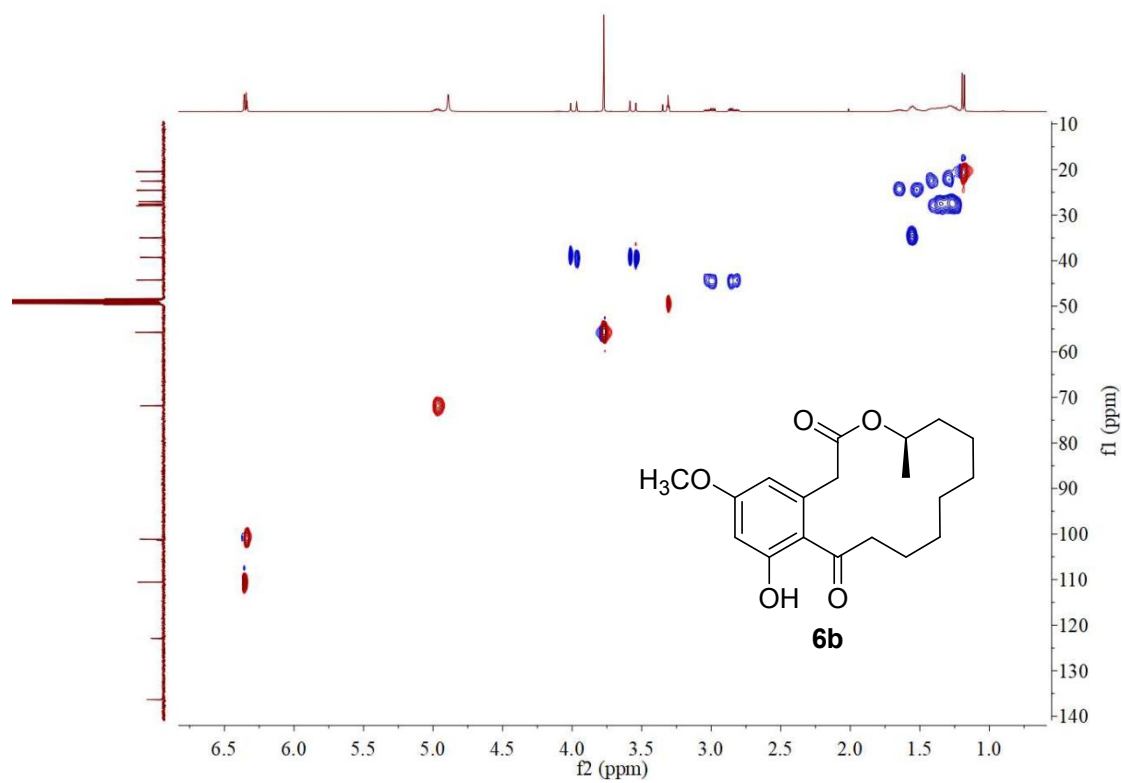


Figure S7.57. HSQC spectrum of compound 6b in methanol- d_4

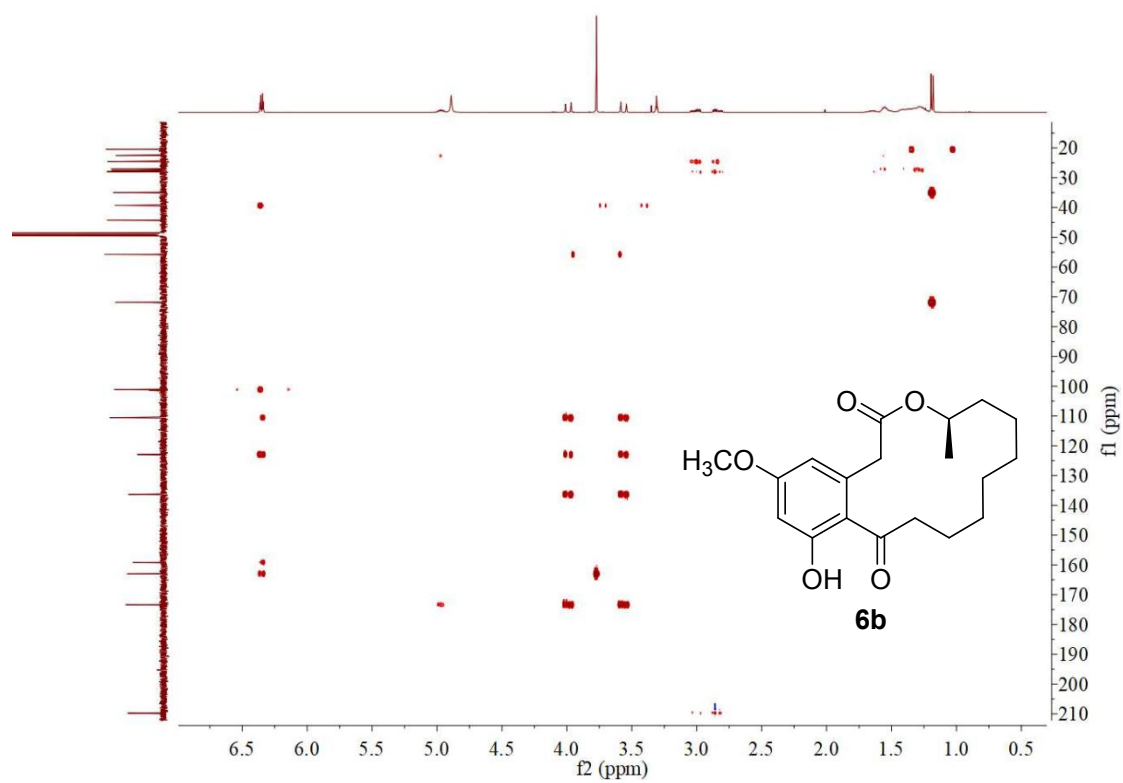


Figure S7.58. HMBC spectrum of compound **6b** in methanol- d_4

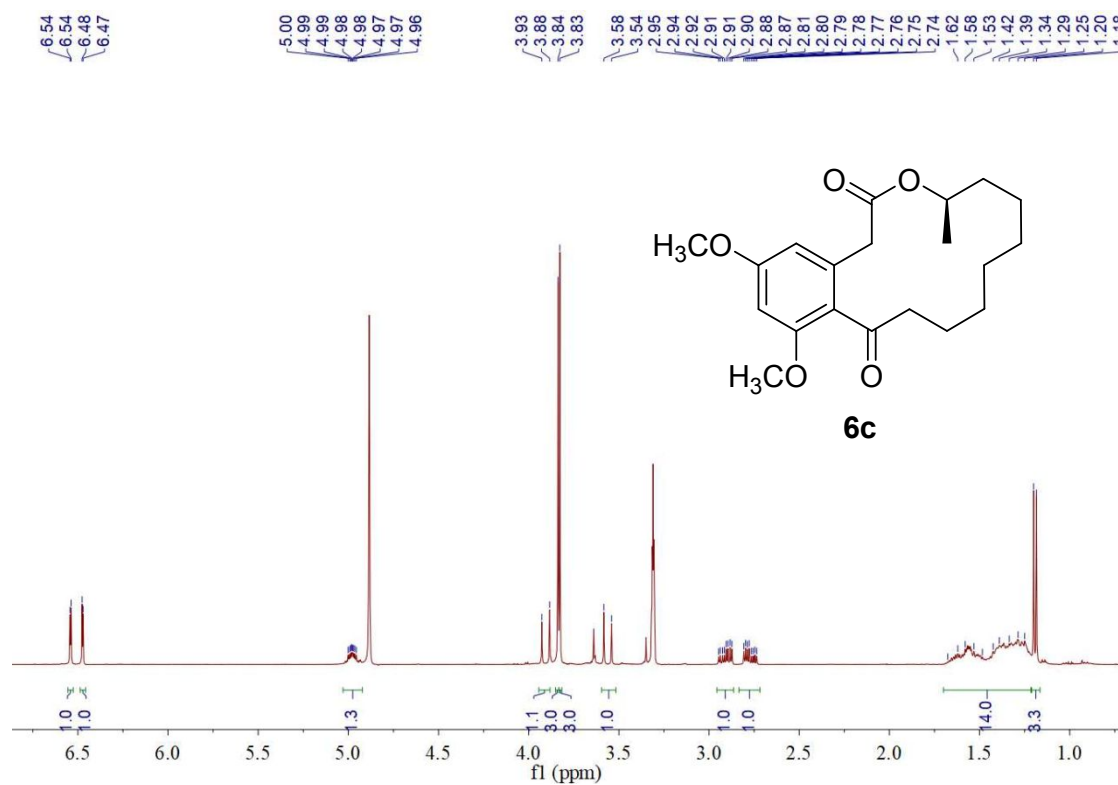


Figure S7.59. ^1H NMR spectrum of compound **6c** in methanol- d_4

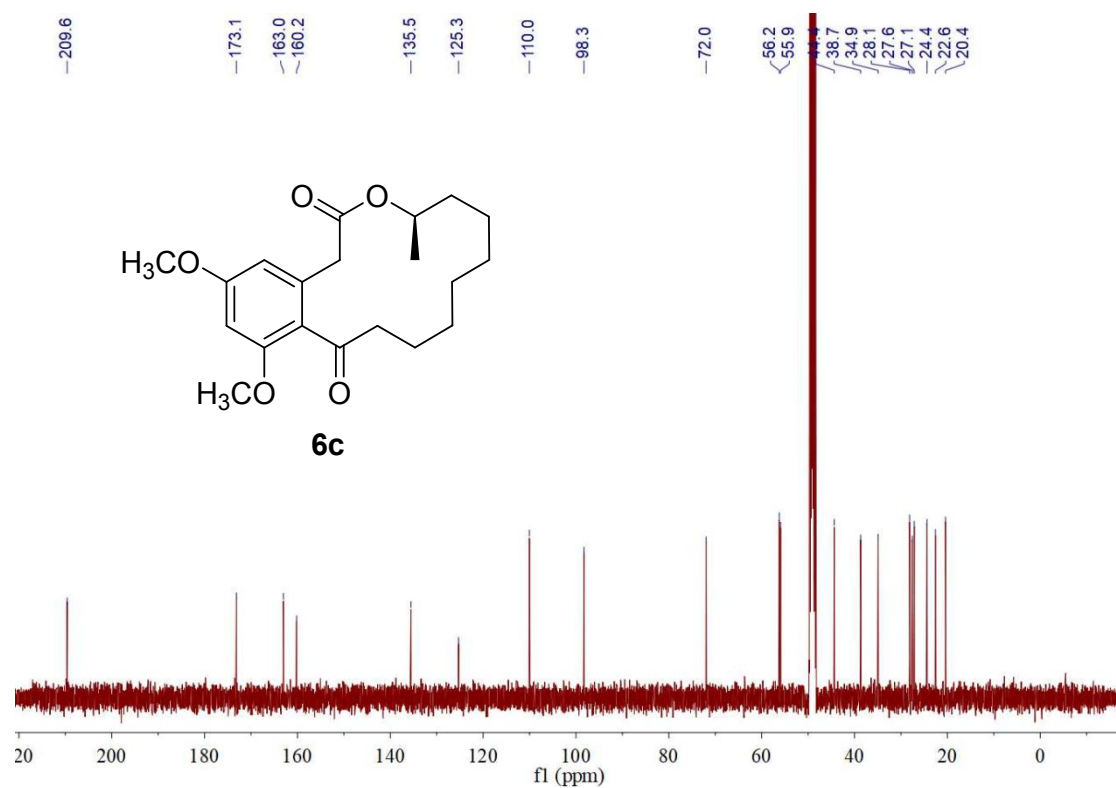


Figure S7.60. ^{13}C NMR spectrum of compound **6c** in methanol- d_4

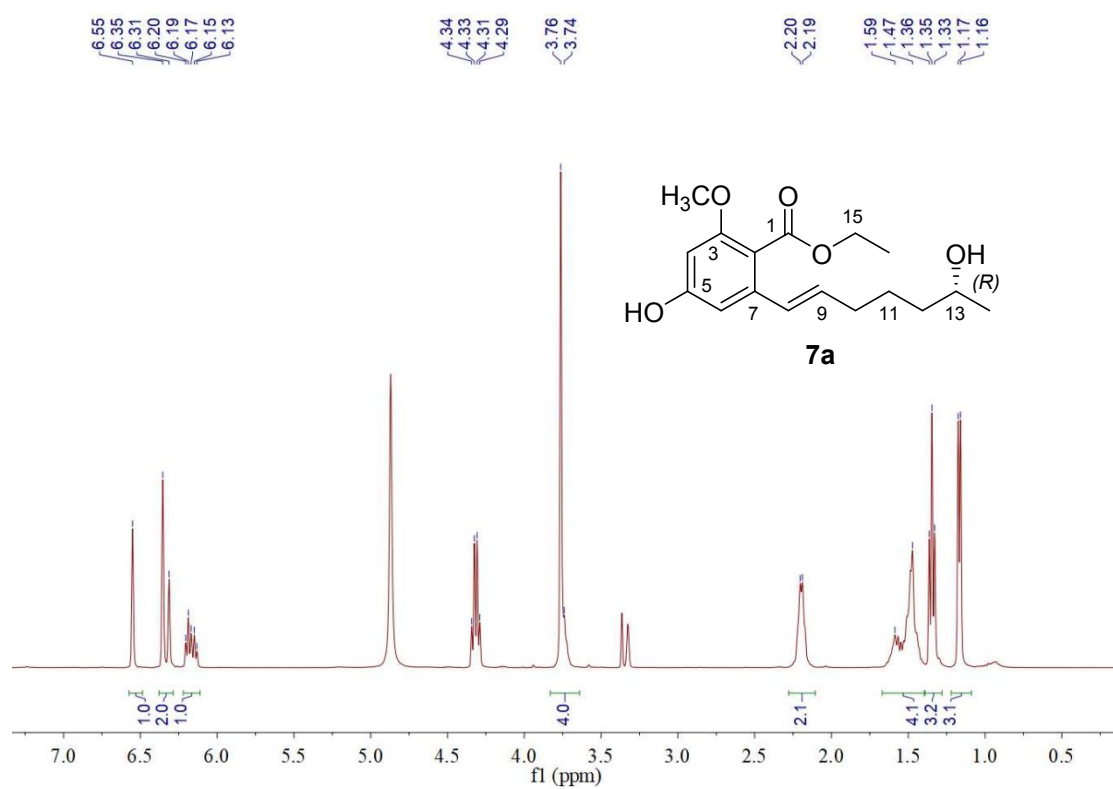


Figure S7.61. ¹H NMR spectrum of compound **7a** in methanol-*d*₄

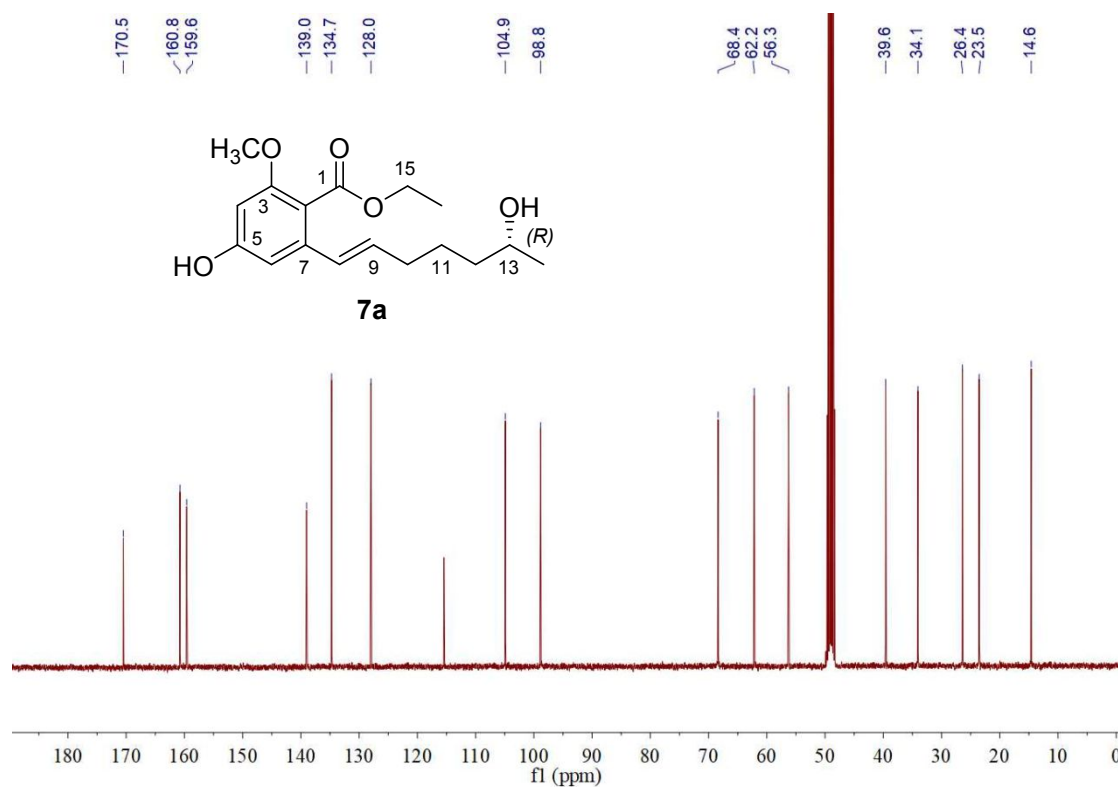


Figure S7.62. ¹³C NMR spectrum of compound **7a** in methanol-*d*₄

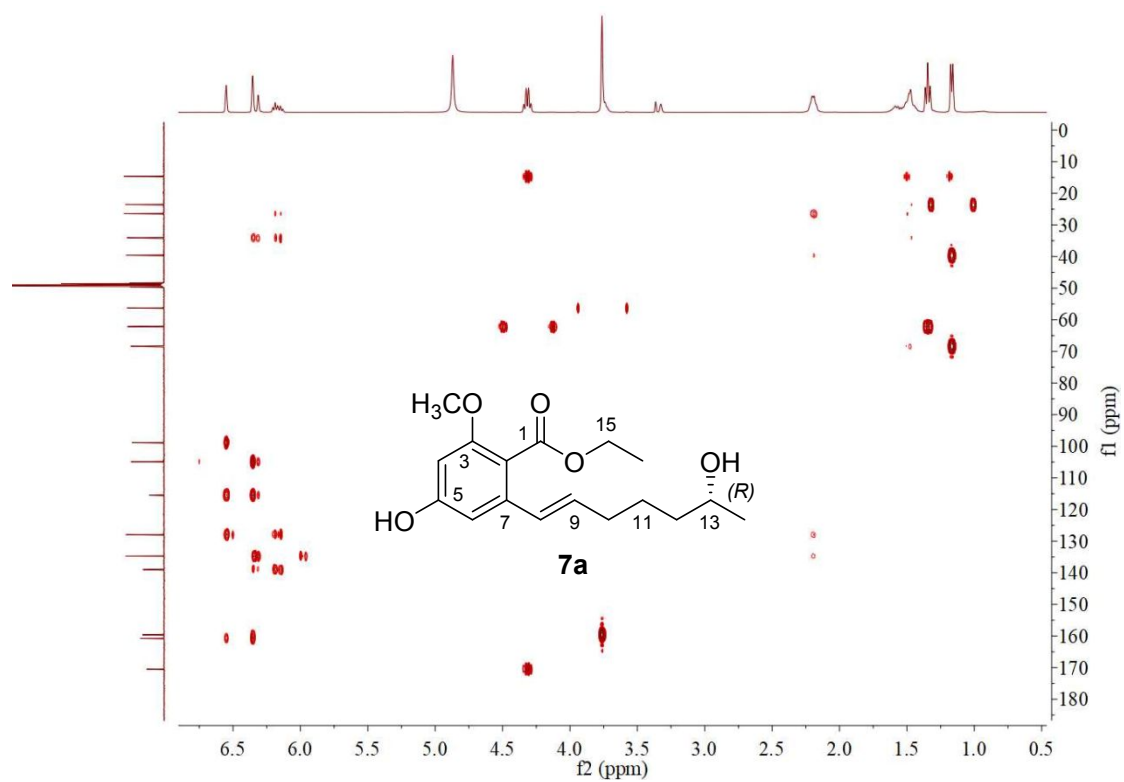


Figure S7.63. HMBC spectrum of compound **7a** in methanol-*d*₄

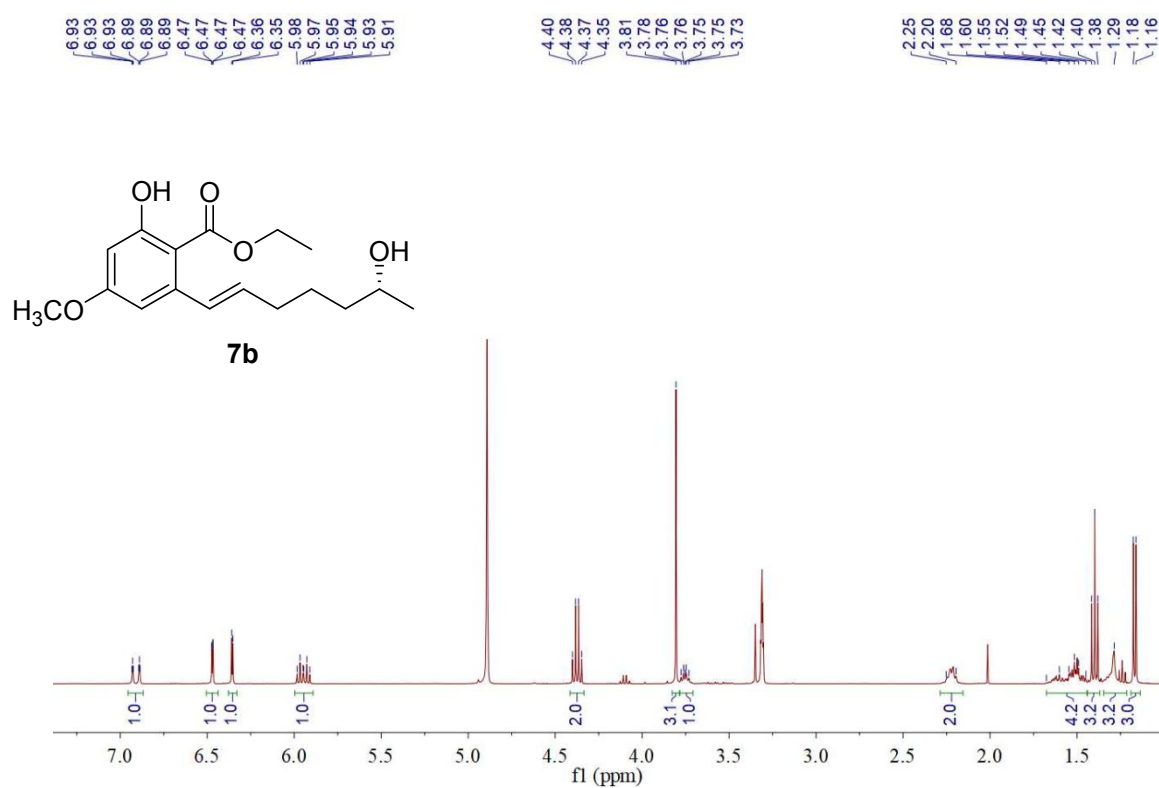


Figure S7.64. ^1H NMR spectrum of compound **7b** in methanol- d_4

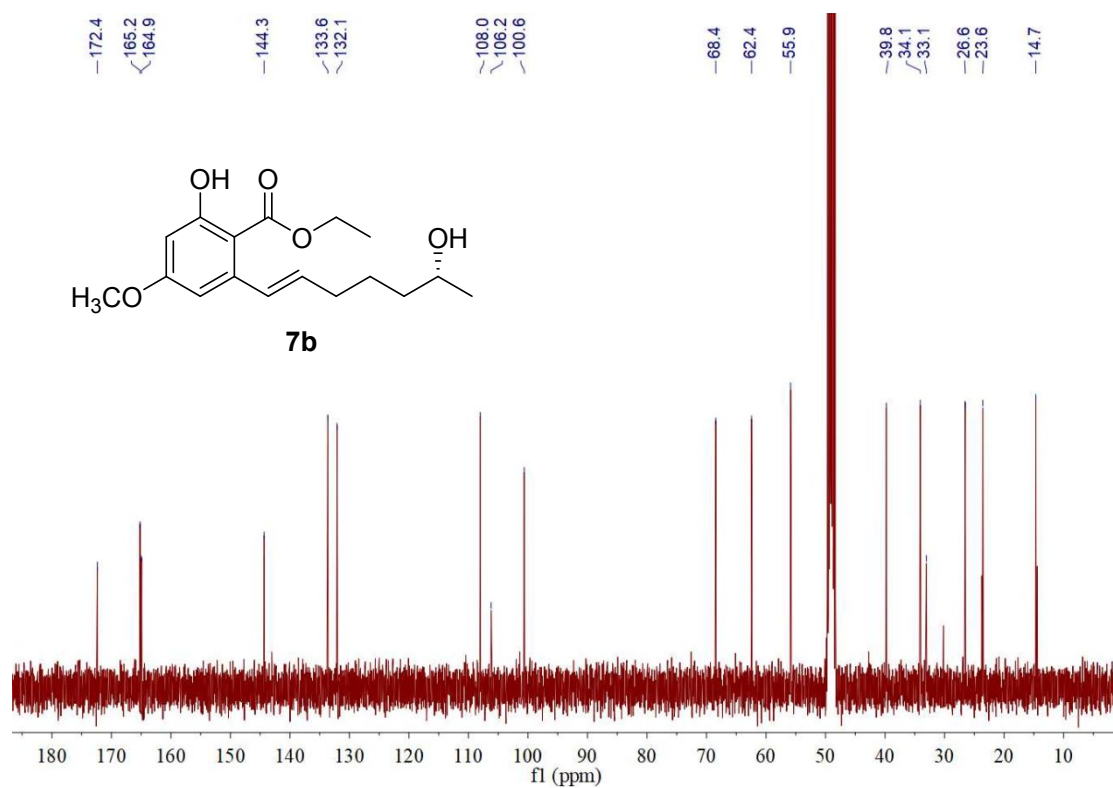


Figure S7.65. ¹³C NMR spectrum of compound **7b** in methanol-*d*₄

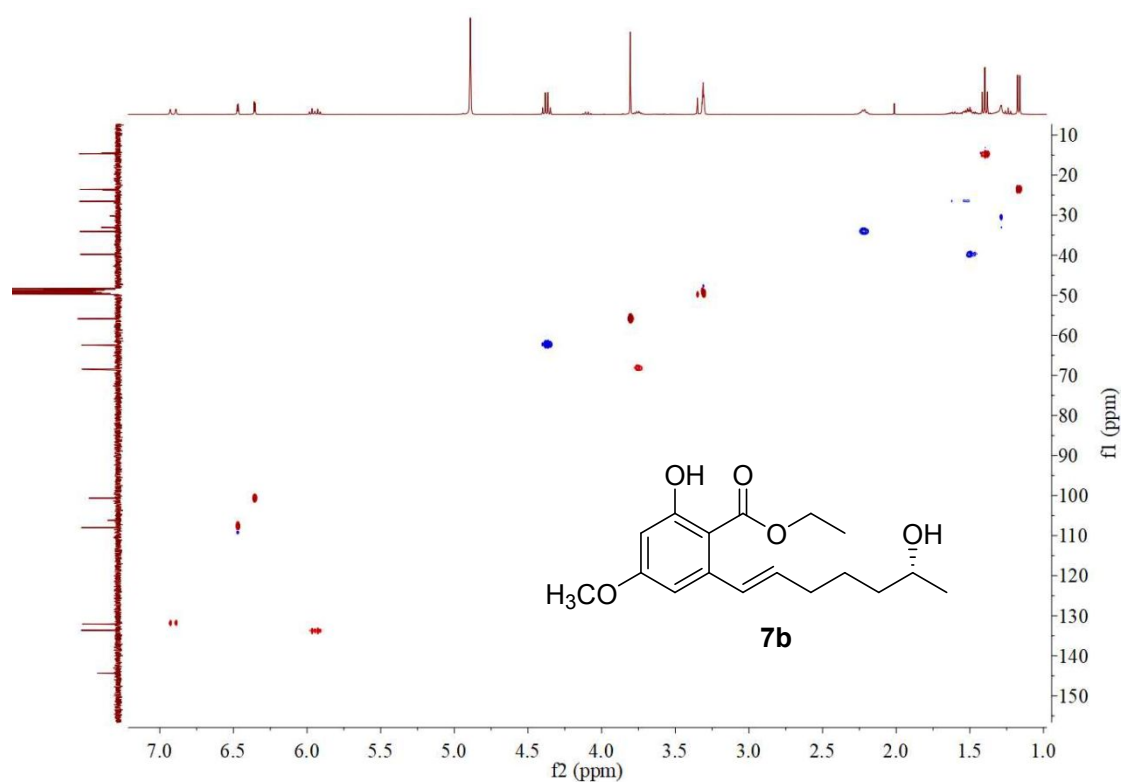


Figure S7.66. HSQC spectrum of compound **7b** in methanol-*d*₄

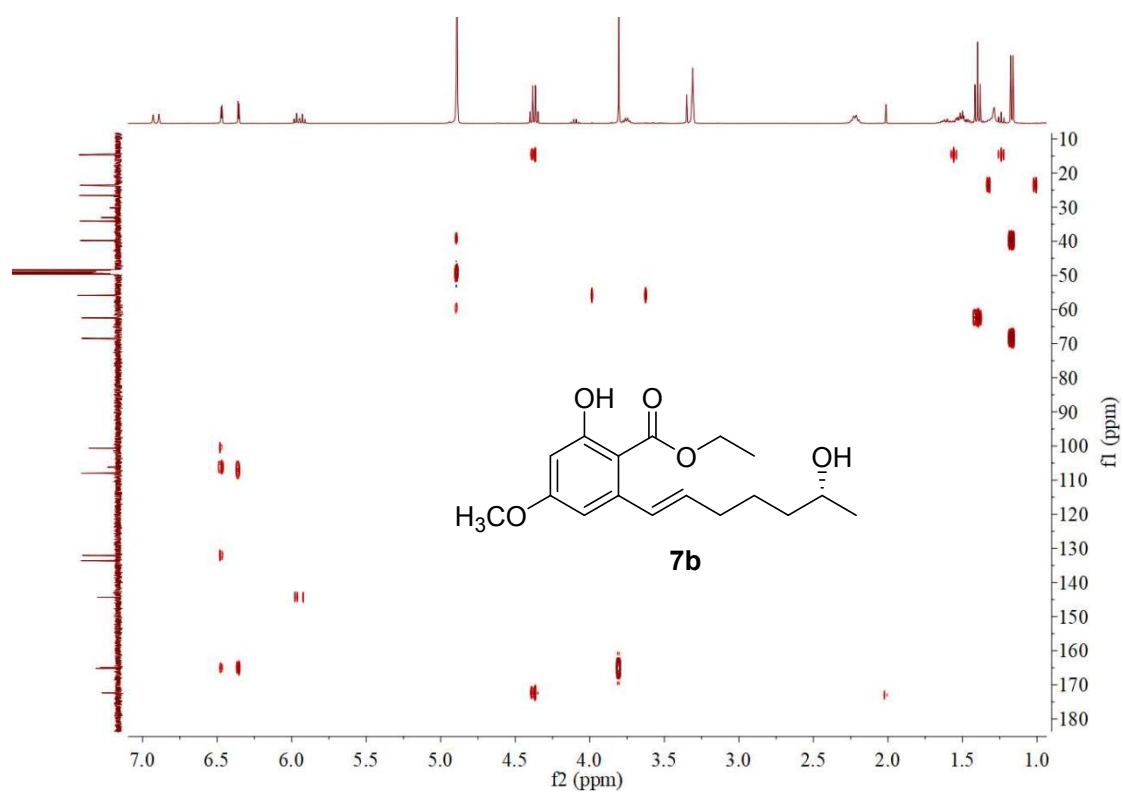


Figure S7.67. HMBC spectrum of compound **7b** in methanol-*d*₄

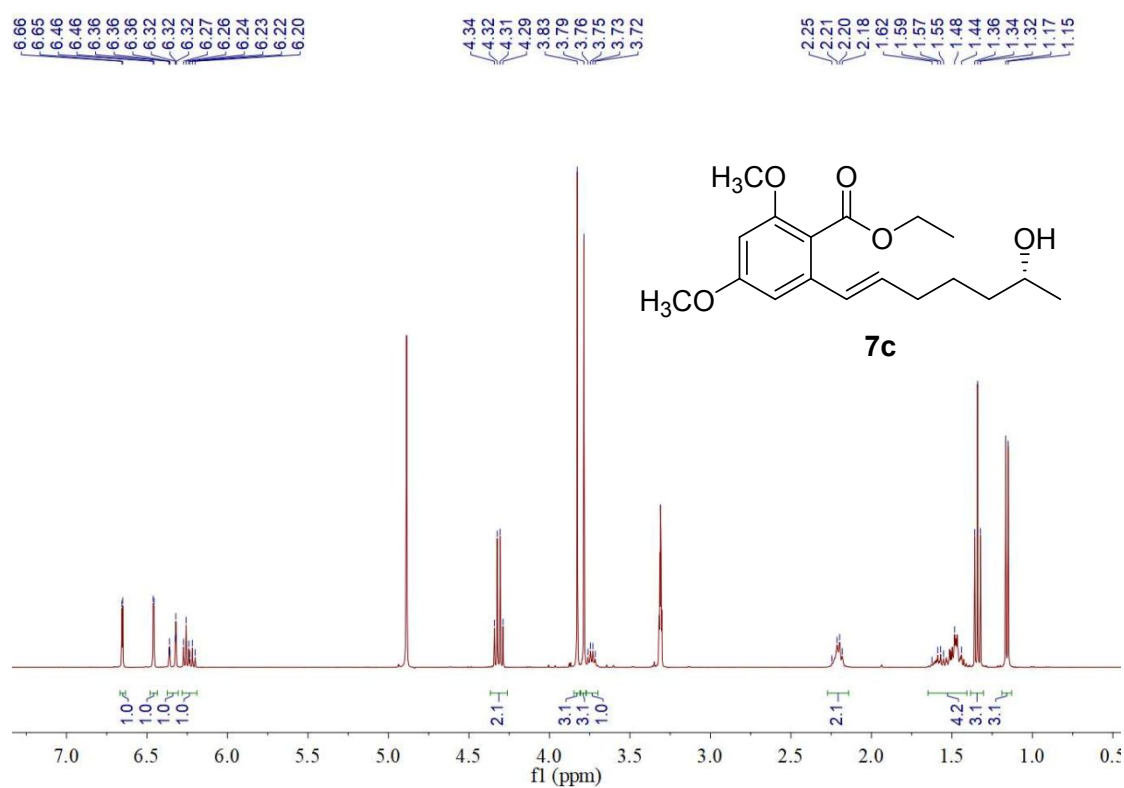


Figure S7.68. ^1H NMR spectrum of compound **7c** in methanol- d_4

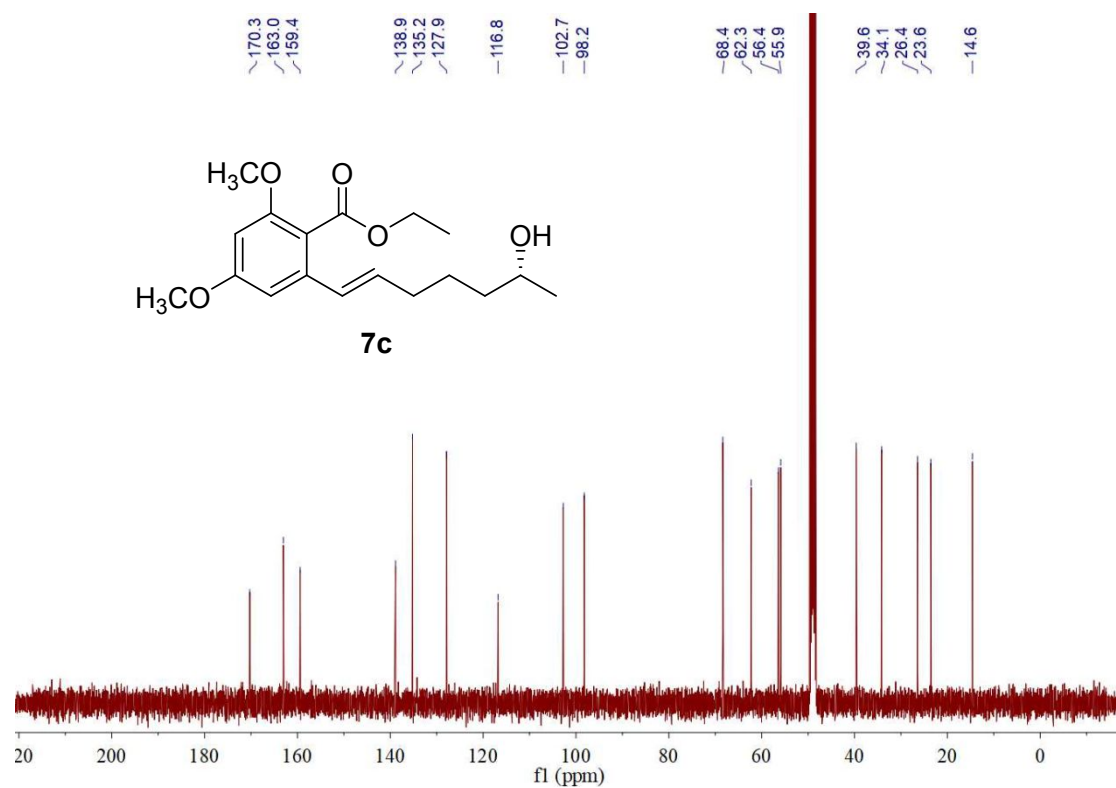


Figure S7.69. ^{13}C NMR spectrum of compound **7c** in methanol- d_4

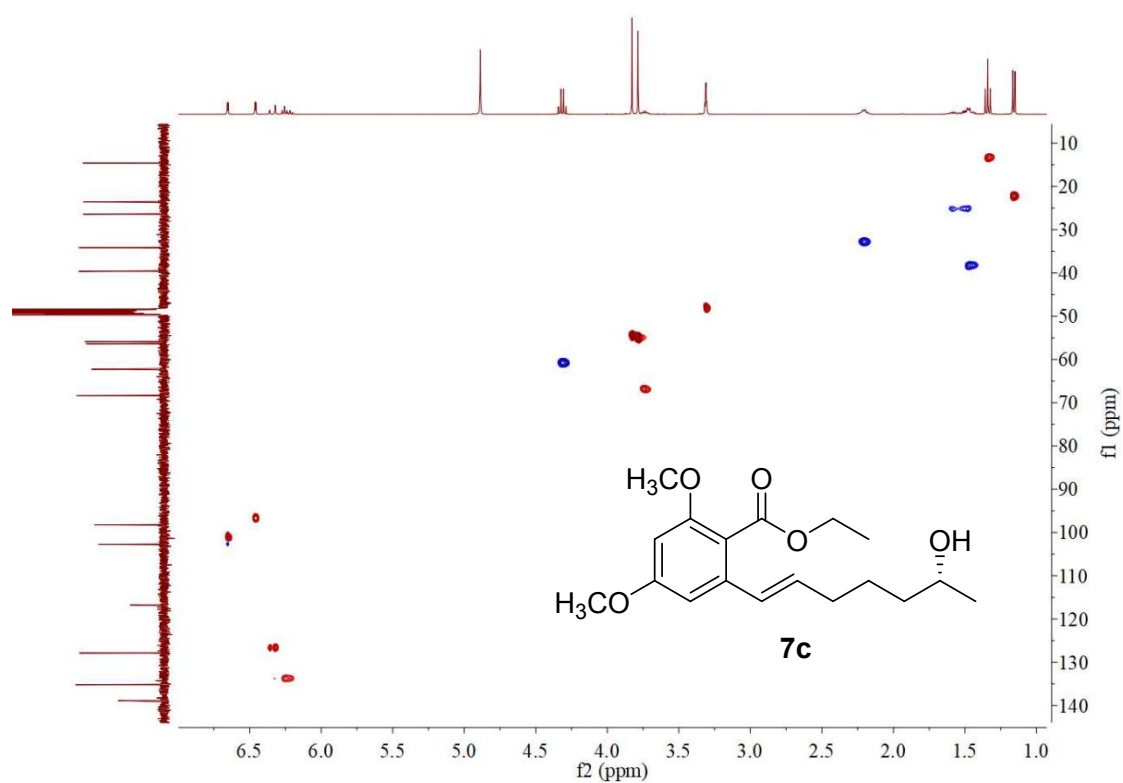


Figure S7.70. HSQC spectrum of compound **7c** in methanol-*d*₄

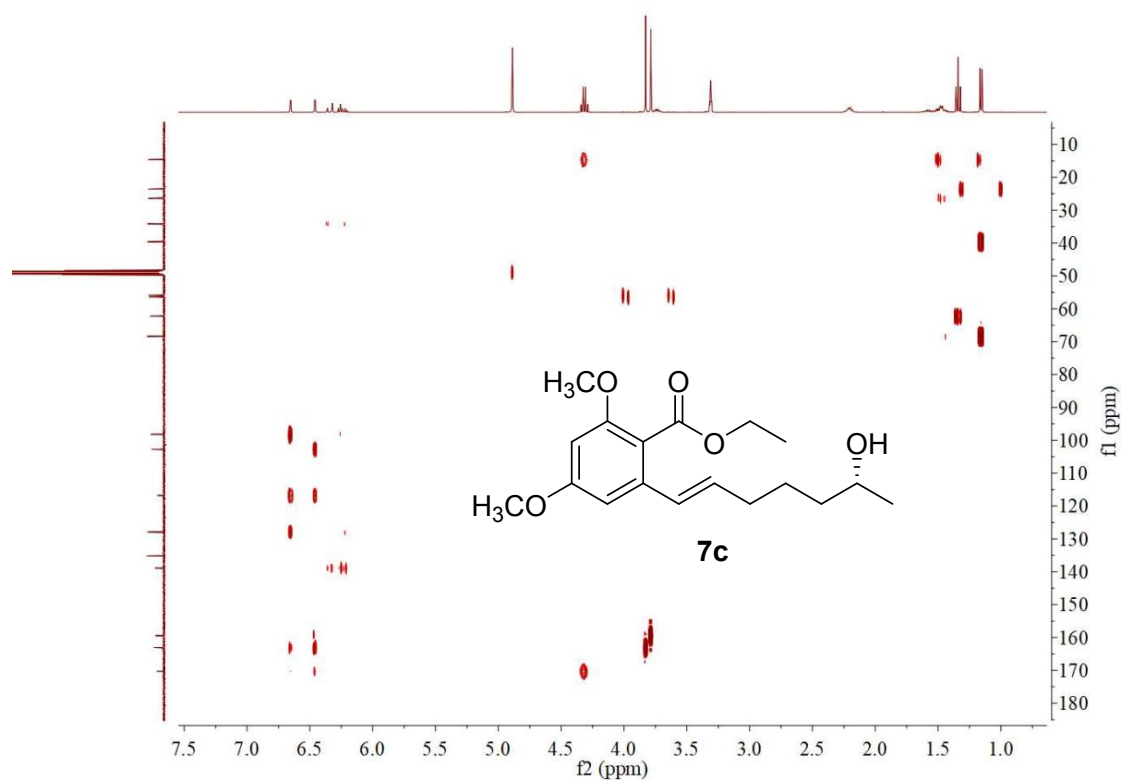


Figure S7.71. HMBC spectrum of compound **7c** in methanol- d_4

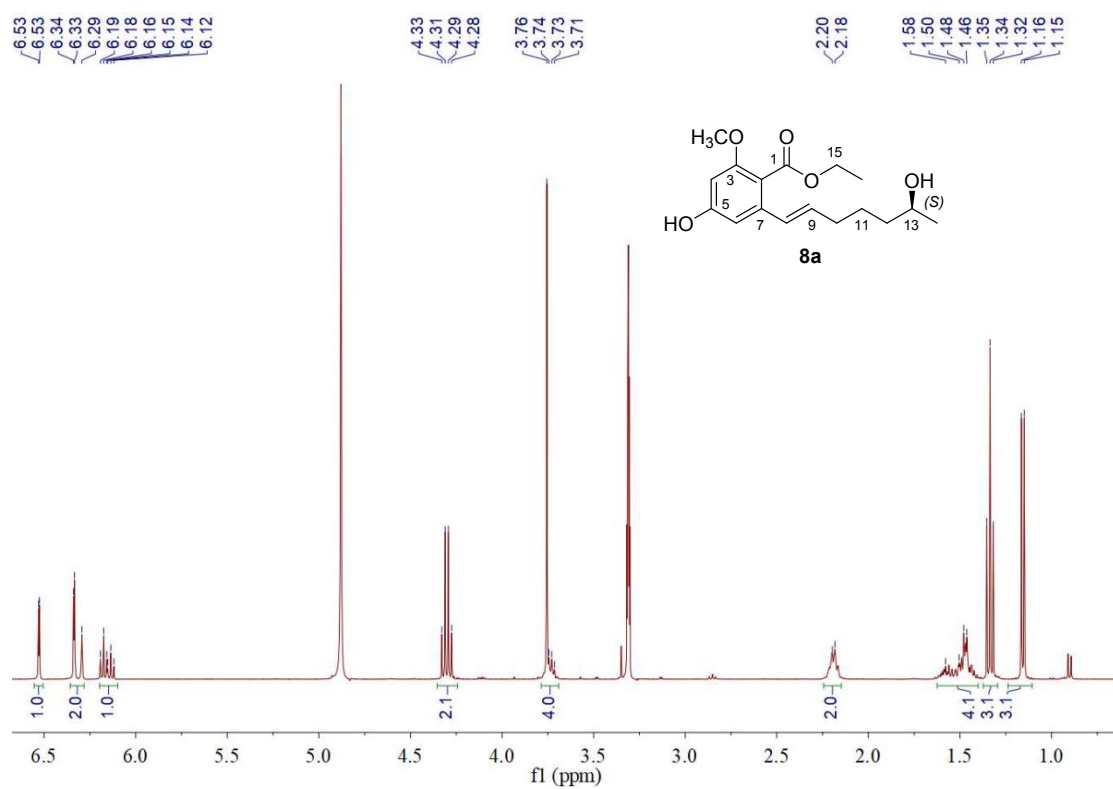


Figure S7.72. ¹H NMR spectrum of compound **8a** in methanol-*d*₄

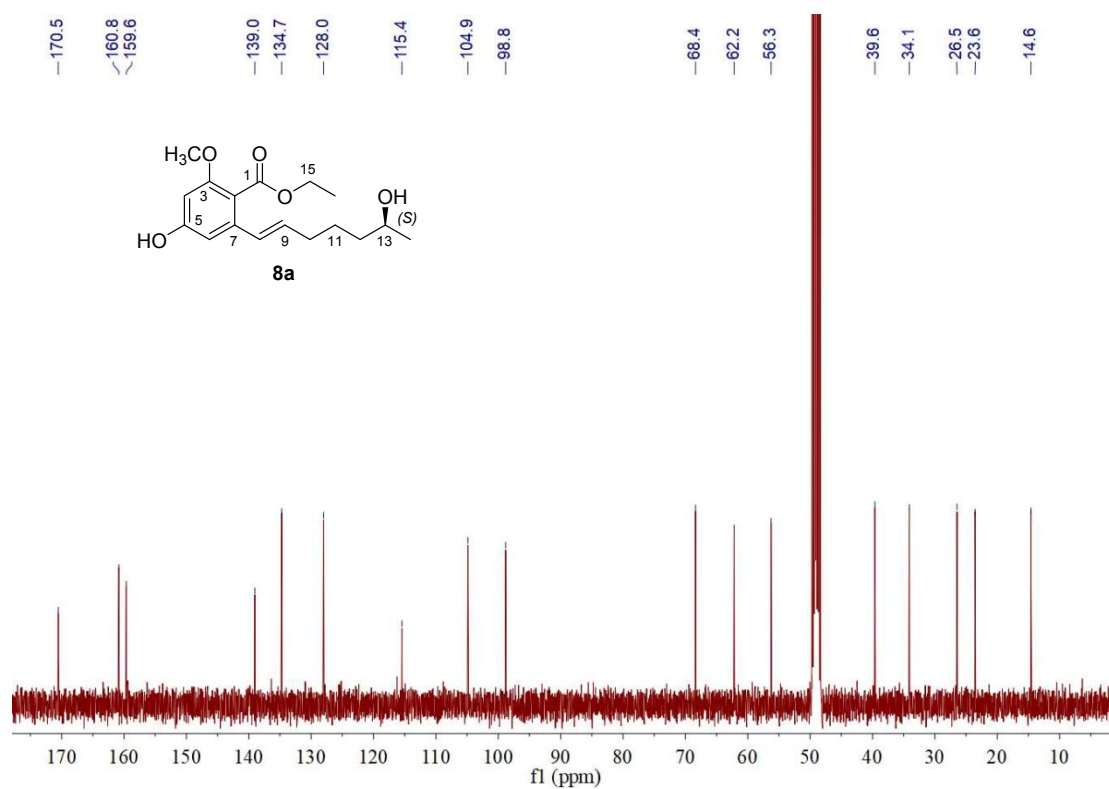


Figure S7.73. ^{13}C NMR spectrum of compound **8a** in methanol- d_4

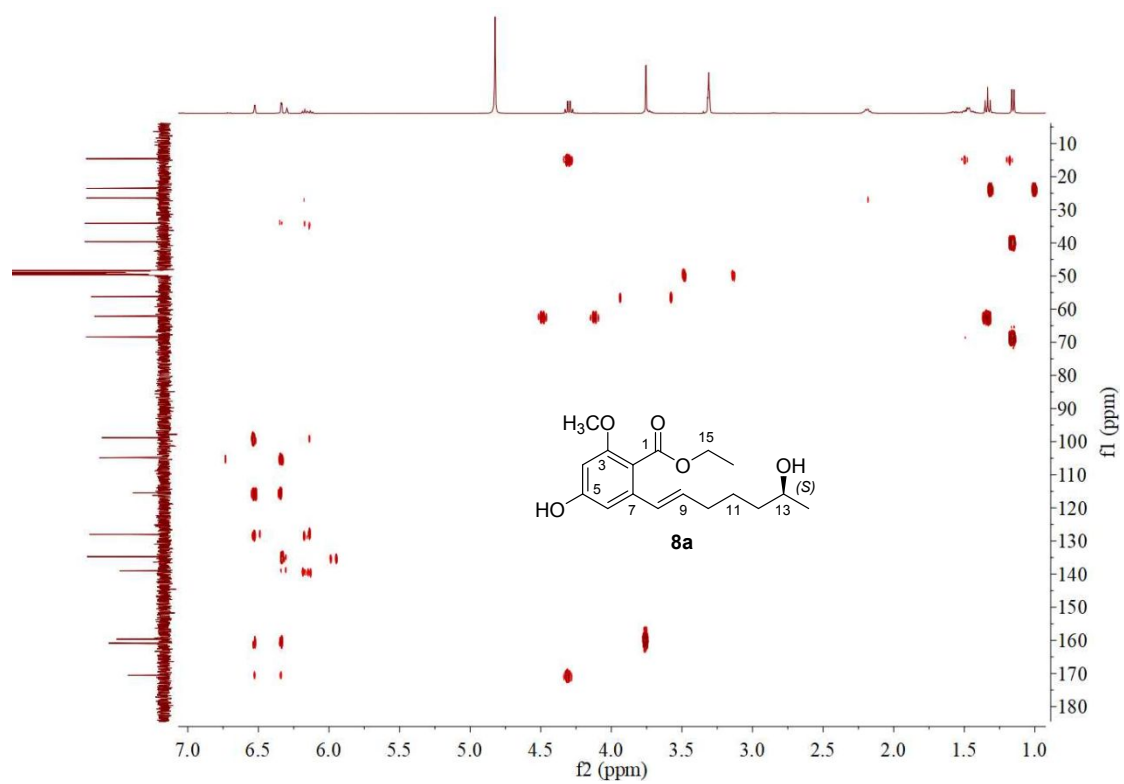


Figure S7.74. HMBC NMR spectrum of compound **8a** in methanol- d_4

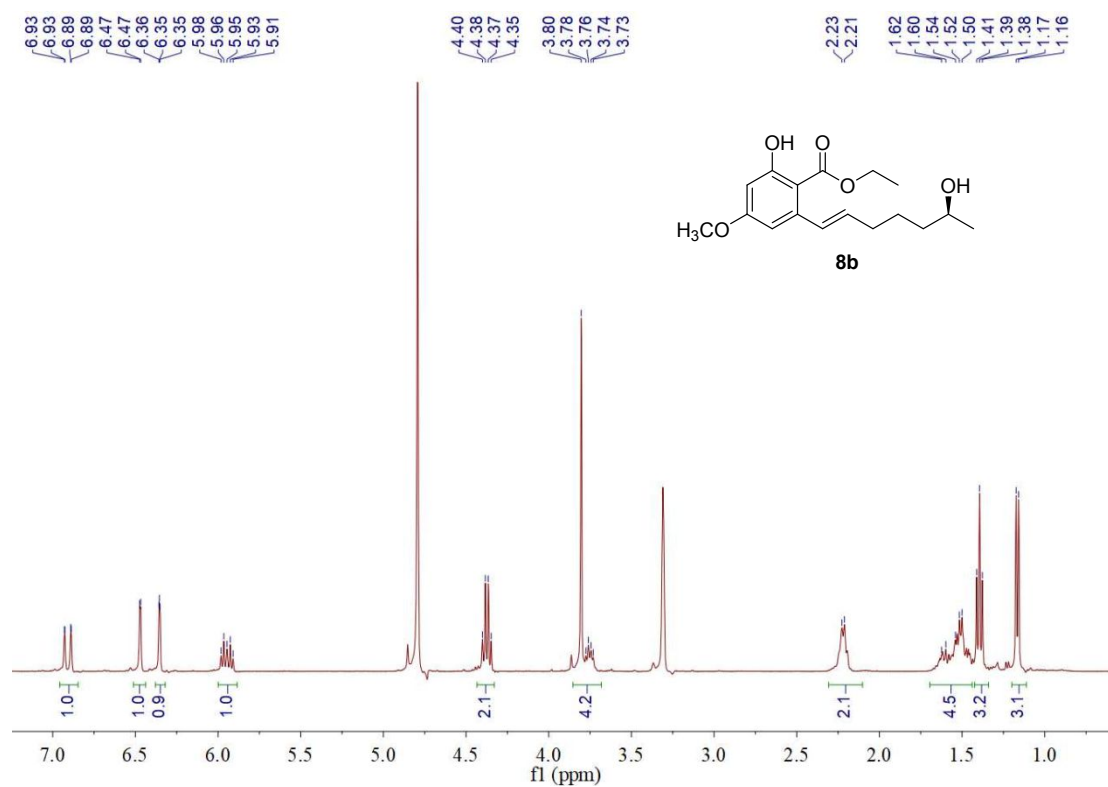


Figure S7.75. ¹H NMR spectrum of compound **8b** in methanol-*d*₄

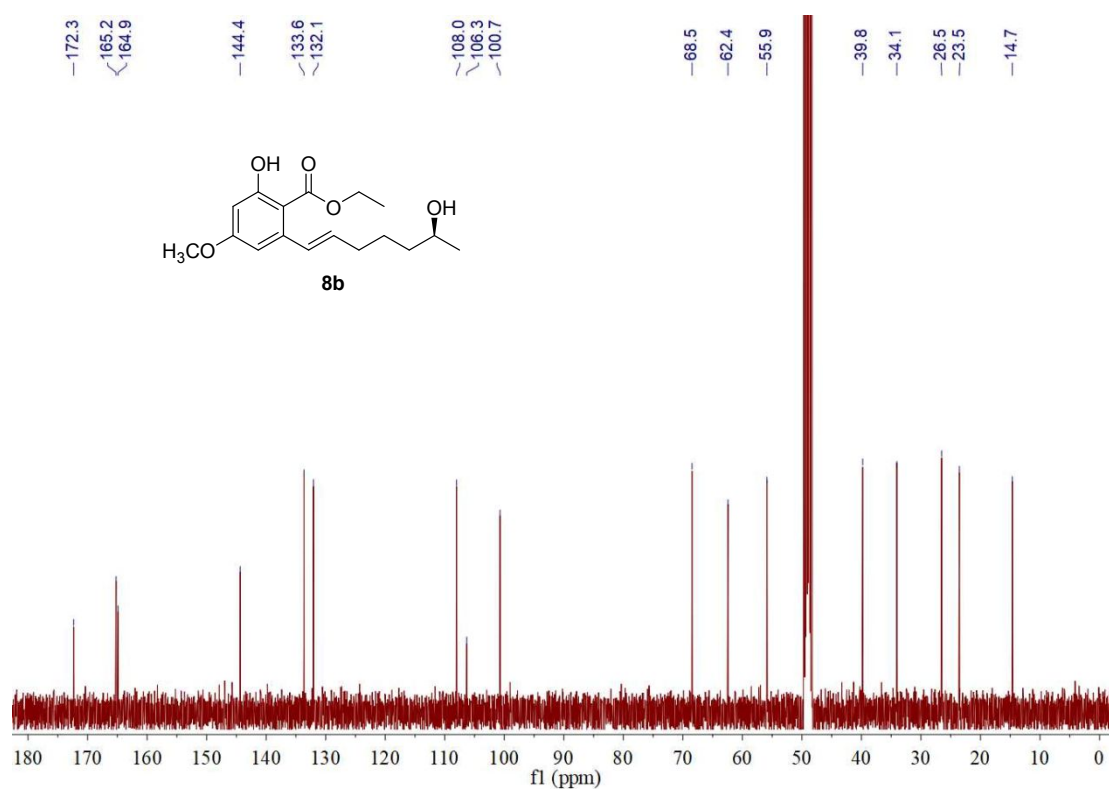


Figure S7.76. ¹³C NMR spectrum of compound **8b** in methanol-*d*₄

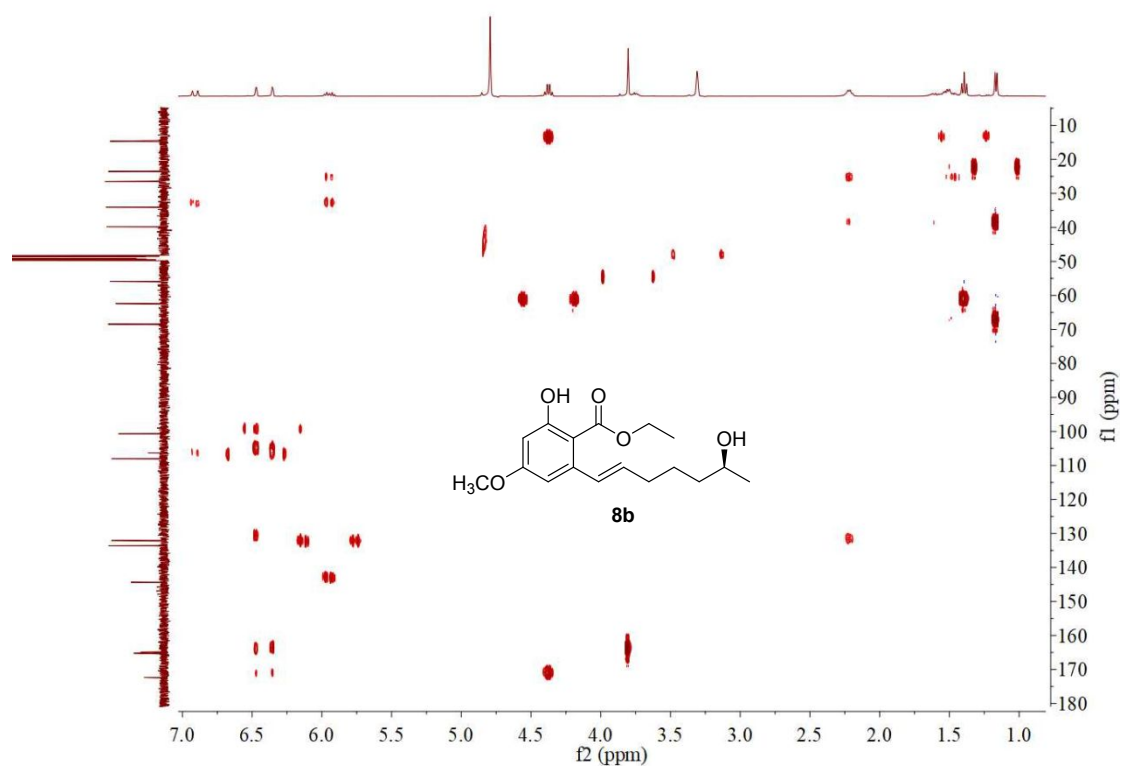


Figure S7.77. HMBC spectrum of compound 8b in methanol- d_4

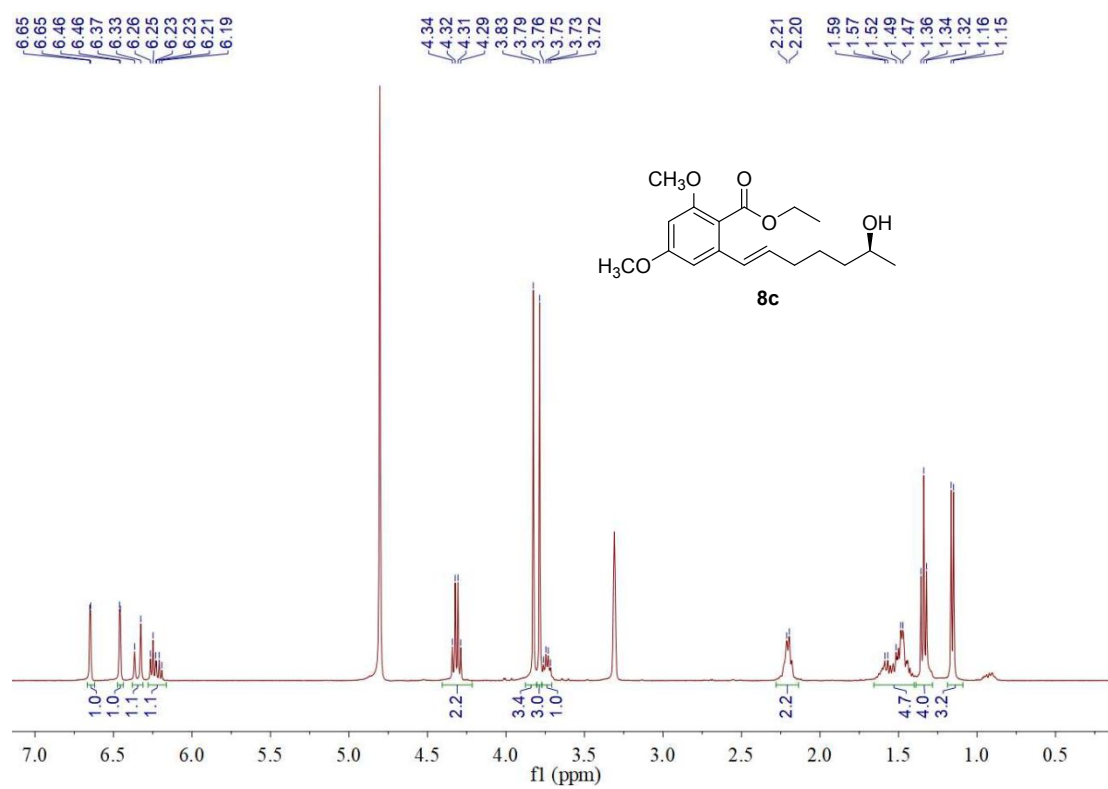


Figure S7.78. ^1H NMR spectrum of compound **8c** in methanol- d_4

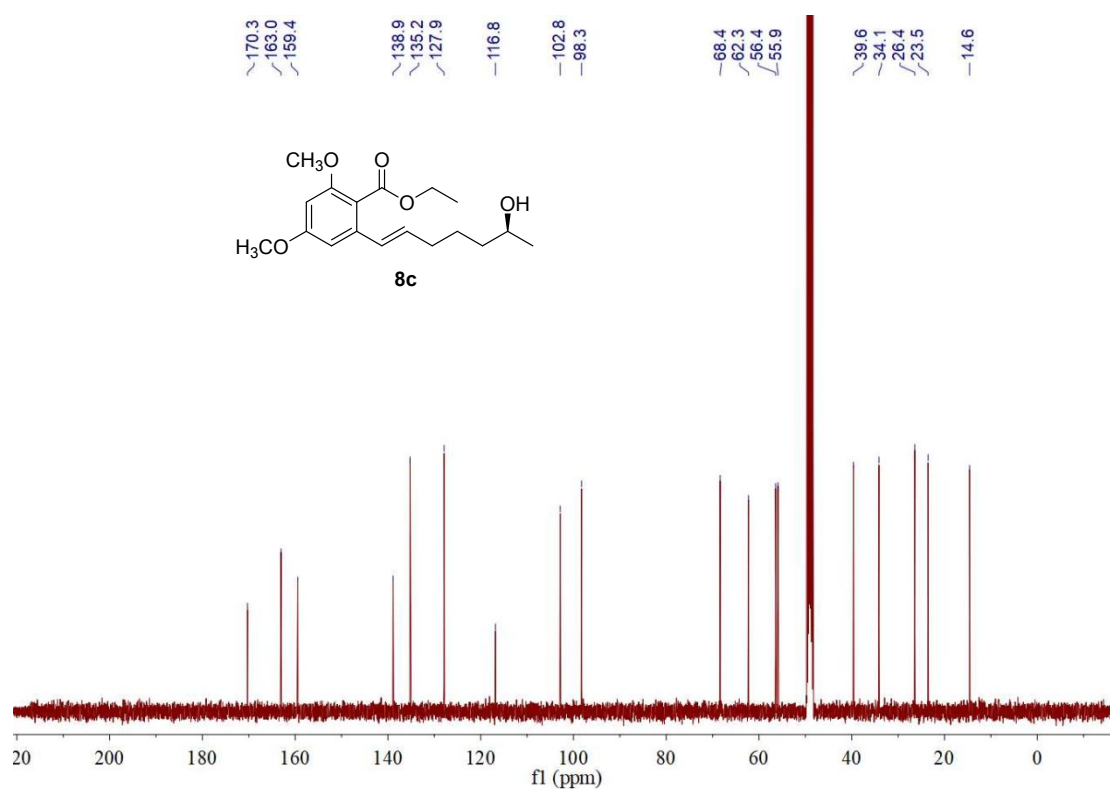


Figure S7.79. ^{13}C NMR spectrum of compound **8c** in methanol- d_4

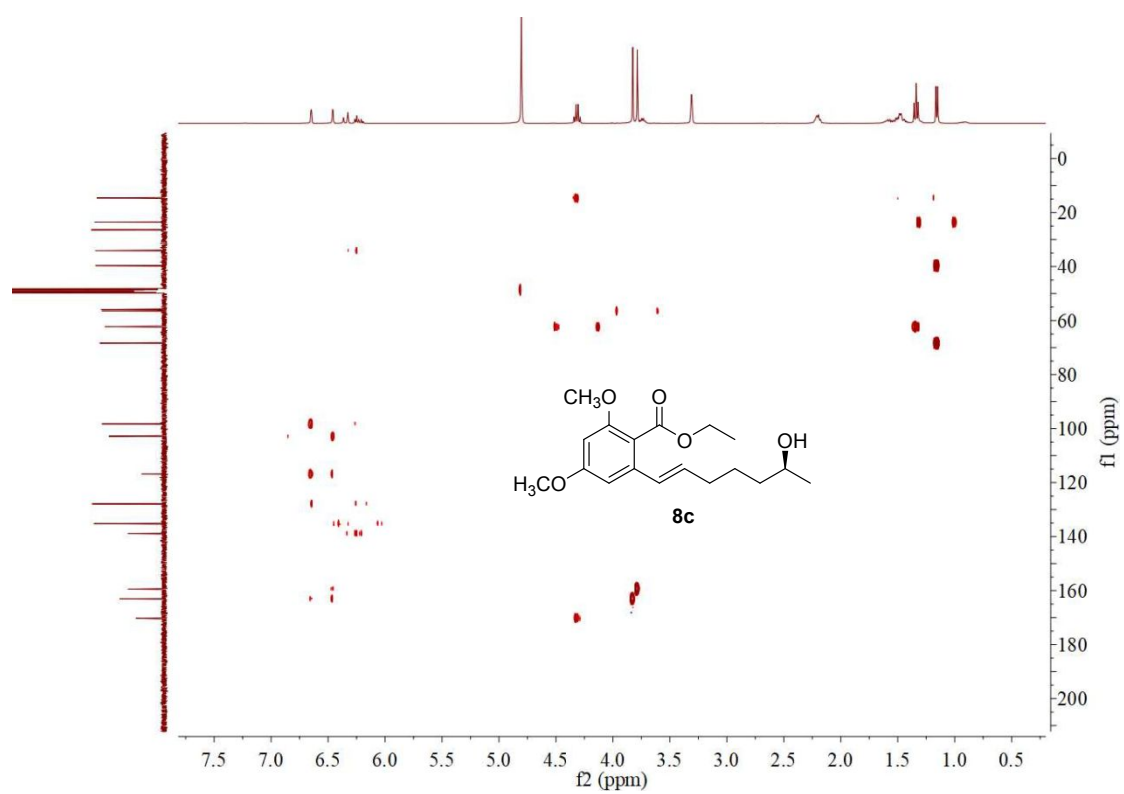
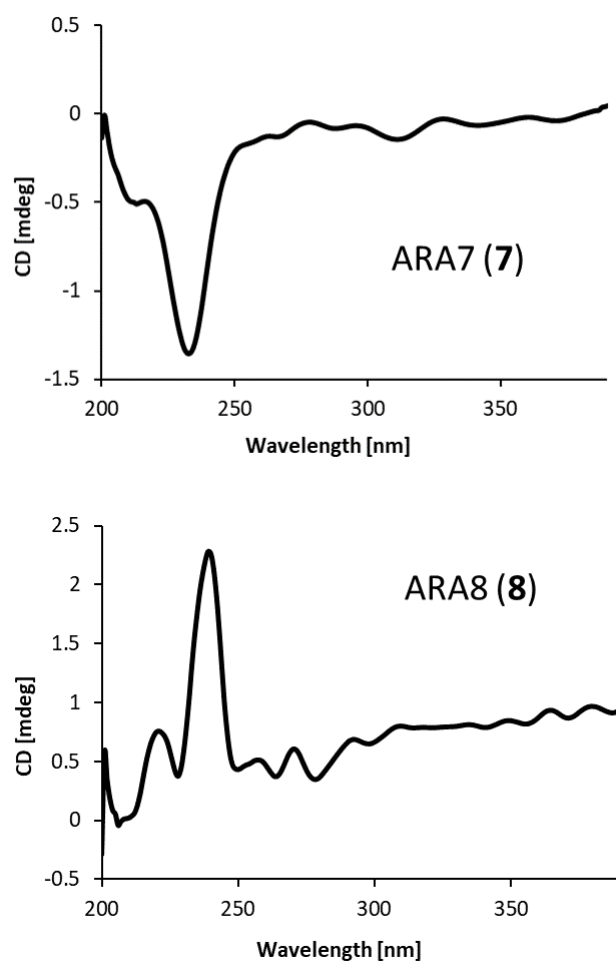


Figure S7.80. HMBC spectrum of compound 8c in methanol- d_4

Figure S8. CD spectra of ARA7 and ARA8.



4 SI References.

1. Xu, Y.; Zhou, T.; Espinosa-Artiles, P.; Tang, Y.; Zhan, J.; Molnár, I. Insights into the biosynthesis of 12-membered resorcylic acid lactones from heterologous production in *Saccharomyces cerevisiae*. *ACS Chem. Biol.* **2014**, *9*, 1119–1127.
2. Reeves, C. D.; Hu, Z.; Reid, R.; Kealey, J. T. Genes for biosynthesis of the fungal polyketides hypothemycin from *Hypomyces subiculosus* and radicicol from *Pochonia chlamydosporia*. *Appl. Environ. Microbiol.* **2008**, *74*, 5121–5129.
3. Xie, L.; Zhang, L.; Wang, C.; Wang, X.; Xu, Y.-M.; Yu, H.; Wu, P.; Li, S.; Han, L.; Gunatilaka, A. L.; Wei, X.; Lin, M.; Molnár, I.; Xu, Y. Methylglucosylation of aromatic amino and phenolic moieties of drug-like biosynthons by combinatorial biosynthesis. *Proc. Natl. Acad. Sci. U.S.A.* **2018**, *115*, E4980–E4989.
4. Bai, J.; Lu, Y.; Xu, Y.-M.; Zhang, W.; Chen, M.; Lin, M.; Gunatilaka, A. L.; Xu, Y.; Molnár, I. Diversity-oriented combinatorial biosynthesis of hybrid polyketide scaffolds from azaphilone and benzenediol lactone biosynthons. *Org. Lett.* **2016**, *18*, 1262–1265.
5. Xu, Y.; Zhou, T.; Zhang, S.; Espinosa-Artiles, P.; Wang, L.; Zhang, W.; Lin, M.; Gunatilaka, A. L.; Zhan, J.; Molnár, I. Diversity-oriented combinatorial biosynthesis of benzenediol lactone scaffolds by subunit shuffling of fungal polyketide synthases. *Proc. Natl. Acad. Sci. U.S.A.* **2014**, *111*, 12354–12359.
6. Xu, Y.; Zhou, T.; Zhou, Z.; Su, S.; Roberts, S. A.; Montfort, W. R.; Zeng, J.; Chen, M.; Zhang, W.; Lin, M.; Zhan, J.; Molnár, I. Rational reprogramming of fungal polyketide first-ring cyclization. *Proc. Natl. Acad. Sci. U.S.A.* **2013**, *110*, 5398–5403.
7. Xu, Y.; Zhou, T.; Zhang, S.; Xuan, L. J.; Zhan, J.; Molnár, I. Thioesterase domains of fungal nonreducing polyketide synthases act as decision gates during combinatorial biosynthesis. *J. Am. Chem. Soc.* **2013**, *135*, 10783–10791.
8. Wang, S.; Xu, Y.; Maine, E. A.; Wijeratne, E. K.; Espinosa-Artiles, P.; Gunatilaka, A. L.; Molnár, I. Functional characterization of the biosynthesis of radicicol, an Hsp90 inhibitor resorcylic acid lactone from *Chaetomium chiversii*. *Chem. Biol.* **2008**, *15*, 1328–1338.
9. Ma, S. M.; Li, J. W.-H.; Choi, J. W.; Zhou, H.; Lee, K. M.; Moorthie, V. A.; Xie, X.; Kealey, J. T.; Silva, N. A. D.; Vederas, J. C.; Tang, Y. Complete reconstitution of a highly reducing iterative polyketide synthase. *Science*. **2009**, *326*, 589–592.
10. Gietz, R. D.; Woods, R. A. Genetic transformation of yeast. *Biotechniques*. **2001**, *30*, 816–+.
11. Biasini, M.; Bienert, S.; Waterhouse, A.; Arnold, K.; Studer, G.; Schmidt, T.; Kiefer, F.; Cassarino, T. G.; Bertoni, M.; Bordoli, L.; Schwede, T. SWISS-MODEL: modelling protein tertiary and quaternary structure using evolutionary information. *Nucleic. Acids Res.* **2014**, *42*, W252–258.
12. Singh, S.; Chang, A.; Goff, R. D.; Bingman, C. A.; Grünschow, S.; Sherman, D. H.; Phillips, G. N., Jr.; Thorson, J. S. Structural characterization of the mitomycin 7-O-methyltransferase. *Proteins*. **2011**, *79*, 2181–2188.
13. Holm, L.; Laakso, L. M. Dali server update. *Nucleic. Acids Res.* **2016**, *44*, W351–355.
14. Gaffoor, I.; Brown, D. W.; Plattner, R.; Proctor, R. H.; Qi, W.; Trail, F. Functional analysis of the polyketide synthase genes in the filamentous fungus *Gibberella zeae* (anamorph *Fusarium graminearum*). *Eukaryot Cell*. **2005**, *4*, 1926–1933.

15. Kim, Y. T.; Lee, Y. R.; Jin, J.; Han, K. H.; Kim, H.; Kim, J. C.; Lee, T.; Yun, S. H.; Lee, Y. W. Two different polyketide synthase genes are required for synthesis of zearalenone in *Gibberella zeae*. *Mol Microbiol.* **2005**, *58*, 1102-1113.